Development of polymerase chain reaction enzyme linked immunosorbent assay for

detection of human papillomavirus 16 L1 gene methylation

Miss Sasiprapa Liewchalermwong

จุฬาลงกรณ์มหาวิทยาลัย

CHULALONGKORN UNIVERSITY

A Thesis Submitted in Partial Fulfillment of the Requirements

for the Degree of Master of Science in Medical Microbiology

Medical Microbiology,Interdisciplinary Program

GRADUATE SCHOOL

Chulalongkorn University

Academic Year 2019

การพัฒนาวิธีพีซีอาร์เอนไซม์ลิงค์อิมมูโนซอบเบนเพื่อตรวจภาวะเมธิลเลชั่นของยีนแอลวันของเชื้อ
ไวรัสแปปิโลมาชนิด 16

น.ส.ศศิประภา ลิ่วเฉลิมวงศ์

วิทยานิพนธ์นี้เป็นส่วนหนึ่งของการศึกษาตามหลักสูตรปริญญาวิทยาศาสตรมหาบัณฑิต
สาขาวิชาจุลชีววิทยาทางการแพทย์ สหสาขาวิชาจุลชีววิทยาทางการแพทย์
บัณฑิตวิทยาลัย จุฬาลงกรณ์มหาวิทยาลัย
ปีการศึกษา 2562

Thesis Title   Development of polymerase chain reaction enzyme
                      linked immunosorbent assay for detection of human
                      papillomavirus 16 L1 gene methylation
By   Miss Sasiprapa Liewchalermwong
Field of Study   Medical Microbiology
Thesis Advisor   ARKOM CHAIWONGKOT, Ph.D.
Thesis Co Advisor   Associate Professor PARVAPAN BHATTARAKOSOL, Ph.D.

Accepted by the GRADUATE SCHOOL, Chulalongkorn University in Partial Fulfillment of the Requirement for the Master of Science

.... Dean of the GRADUATE SCHOOL
(Associate Professor THUMNOON NHUJAK, Ph.D.)

THESIS COMMITTEE

.... Chairman
(Professor NATTIYA HIRANKARN, Ph.D.)

.... Thesis Advisor
(ARKOM CHAIWONGKOT, Ph.D.)

.... Thesis Co-Advisor
(Associate Professor PARVAPAN BHATTARAKOSOL, Ph.D.)

.... Examiner
(Navapon Techakriengkrai, DVM, Ph.D.)

.... External Examiner
(Associate Professor Nakarin Kitkumthorn, Ph.D.)

ศศิประภา ลิ่วเฉลิมวงศ์ : การพัฒนาวิธีพีซีอาร์เอนไซม์ลิงค์อิมมูโนซอบเบนเพื่อตรวจภาวะเมธิเลชั่นของยีนแอลวันของเชื้อไวรัสแปปิโลมาชนิด 16. (Development of polymerase chain reaction enzyme linked immunosorbent assay for detection of human papillomavirus 16 L1 gene methylation) อ.ที่ปรึกษาหลัก : ดร.อาคม ไชยวงศ์คต, อ.ที่ปรึกษาร่วม : รศ. ดร.ภาวพันธ์ ภัทรโกศล

       ไวรัสฮิวแมนแปปิลโลมาเป็นเชื้อไวรัสไม่มีเปลือกหุ้มชั้นนอก มีเปลือกหุ้มชั้นในเป็นลักษณะแบบเหลี่ยมลูกบาศก์เรียงตัวแบบสมมาตรกัน ห่อหุ้มสาร พันธุกรรมที่เป็นดีเอ็นเอสายคู่ขดเป็นวงกลม เป็นที่รู้อย่างกว้างขวางว่ามะเร็งปากมดลูกนั้น มีสาเหตุหลักเกิดจากไวรัสฮิวแมนแปปิลโลมาชนิดความเสี่ยงสูง โดยส่วนใหญ่เกิดจาก ชนิด 16 และ 18 อย่างไรก็ตาม มีผู้หญิงจำนวนน้อยที่ติดเชื้อไวรัสชนิดความเสี่ยงสูงแล้วพัฒนาไปเป็นมะเร็ง การคัดกรองจึงมีความสำคัญมากในการคัดแยกผู้ที่ติดเชื้อไวรัสชนิด ความเสี่ยงสูงและมีความเสี่ยงในการเป็นมะเร็ง เพื่อที่จะตรวจด้วยวิธีการส่องกล้องต่อไป ปัจจุบันมีรายงานหลายฉบับบันทึกว่าการเกิดภาวะเมธิเลชั่นสูงตรงยีนแอลหนึ่งของ เชื้อไวรัสแปปิโลมาชนิด 16 มีความสัมพันธ์กับการพบเซลล์ปากมดลูกผิดปกติและเซลล์มะเร็ง การศึกษานี้จึงมีจุดประสงค์ในการพัฒนาวิธีพีซีอาร์อีไลซ่า เพื่อที่จะตรวจภาวะ เมธิเลชั่นตรงยีนแอลหนึ่งของเชื้อไวรัสแปปิโลมาชนิด 16 โดยผู้วิจัยได้เก็บตัวอย่างเซลล์ปากมดลูกจากผู้ที่เข้ารับการส่องกล้องในโรงพยาบาลจุฬาลงกรณ์ และทำการ ตรวจหาชนิดของไวรัสฮิวแมนแปปิโลมาโดยใช้วิธีของ Cobas4800 และ Reba-ID จากนั้นเลือกเฉพาะไวรัสชนิด 16 มาทำการทดสอบต่อไป โดยในตัวอย่าง 207 ราย มี ตัวอย่าง 70 ราย ที่มีผลเป็นไวรัสชนิด 16 และมีความผิดปกติของเนื้อเยื่อแบบต่างๆ และผู้วิจัยได้นำตัวอย่างทั้ง 70 รายมาทำ bisulfite conversion และพีซีอาร์ที่จำเพาะต่อ ยีนแอลหนึ่งของเชื้อไวรัสแปปิโลมาชนิด 16 เพื่อที่จะตรวจหาการเกิดภาวะเมธิเลชั่นที่ CpG ตำแหน่ง 5600, 5606, 5609 และ 5615 ผู้วิจัยพบว่าตัวอย่างจำนวน 26 ราย เท่านั้นที่ให้ผลเป็นบวก (130 bps) จึงได้นำตัวอย่างกลุ่มนี้มาทำไพโรซีเควนซิ่งซึ่งเป็นการตรวจหาร้อยละของภาวะเมธิเลชั่นที่เป็นที่ยอมรับในปัจจุบัน และผลที่ได้จะถูกใช้เป็น ค่าอ้างอิงร้อยละการเกิดภาวะเมธิเลชั่นในการพัฒนาเทคนิคพีซีอาร์อีไลซ่า เมื่อตรวจหาร้อยละของภาวะเมธิเลชั่นด้วยวิธีไพโรซีเควนซิ่ง พบว่าที่ CpG ตำแหน่ง 5600 และ 5609 ของตัวอย่างที่มีผลเนื้อเยื่อเป็น CIN2/3 มีภาวะเมธิเลชั่นมากกว่าร้อยละ 20 ในขณะที่ตัวอย่างที่มีผลเนื้อเยื่อเป็น CIN1 มีภาวะเมธิเลชั่นน้อยกว่าร้อยละ 10 ในการ พัฒนาเทคนิคพีซีอาร์อีไลซ่าผู้วิจัยได้หาสภาวะที่เหมาะสม โดยทดสอบกับความเข้มข้นที่ต่างกันในสารจำกัดๆ และถึงแม้จะได้สภาวะที่เหมาะสมแล้ว แต่เมื่อทำการทดสอบกับ ตัวอย่างที่ไม่มีภาวะเมธิเลชั่น พบว่าเกิดการจับแบบไม่จำเพาะระหว่างดีเอ็นเอในตัวอย่างกับ DIG-labelled probe ผู้วิจัยจึงปรับอุณหภูมิในขั้นตอนการจับระหว่าง amplicons-probe hybrids กับ streptavidin จาก 37 องศาเซลเซียส เป็น 60 องศาเซลเซียส เพื่อที่จะลดการจับแบบไม่จำเพาะ พบว่าที่ 60 องศาเซลเซียส ค่าการดูดกลืน แสงลดลงเมื่อใช้ดีเอ็นเอที่มีความเข้มข้น 10 ถึง 100 นาโนกรัม แต่ที่ 1,000 นาโนกรัม ยังคงให้ค่าการดูดกลืนแสงที่สูง โดยสุดท้ายได้ผลการพัฒนา ดังนี้ อุณหภูมิในการทำ ปฏิกิริยา hybridization ที่ 60 องศาเซลเซียส, streptavidin 2 ไมโครกรัมต่อหลุม, DIG-labelled probe 294 นาโนกรัมต่อหลุม, antibody dilution 1:3200 และอุณหภูมิ ในการอินคูเบท DNA-probe กับ streptavidin คือ 60 องศาเซลเซียส ผู้วิจัยยังได้ทำการตรวจวัดขีดจำกัดของการตรวจตัวอย่างที่มีการเกิดภาวะเมธิเลชั่นร้อยละหนึ่งร้อย พบว่าตัวอย่างดีเอ็นเอที่มีความเข้มข้น 10 นาโนกรัมเป็นขีดจำกัดของการตรวจ แต่เพื่อที่จะลดการจับแบบไม่จำเพาะ จึงควรใช้ตัวอย่างที่มีความเข้มข้นน้อยกว่า 1000 นาโน กรัม เพื่อที่จะแยกตัวอย่างที่ไม่เกิดภาวะเมธิเลชั่นออกจากตัวอย่างที่มีการเกิดภาวะเมธิเลชั่น และความเข้มข้นของตัวอย่างมาตรฐานกับความเข้มข้นของตัวอย่าง ควรเป็นความ เข้มข้นที่ใกล้เคียงกัน เพื่อให้ได้ค่าการดูดกลืนแสงและผลการคำนวณร้อยละการเกิดภาวะเมธิเลชั่นที่น่าเชื่อถือ ในการทดสอบความไว ผู้วิจัยพบว่าตัวอย่างที่มีการเกิดภาวะ เมธิเลชั่นร้อยละ 20 มีค่าการดูดกลืนแสงสูงกว่าตัวอย่างที่ไม่มีการเกิดภาวะเมธิเลชัน และมีค่าใกล้เคียงกับผลที่ได้จากวิธีไพโรซีเควนซิ่ง (ร้อยละ 21) ซึ่งตัวอย่างที่มีการเกิดภาวะ เมธิเลชั่นร้อยละ 20 ที่ตรวจวัดด้วยวิธีไพโรซีเควนซิ่ง ให้ผลการเกิดภาวะเมธิเลชั่นร้อยละ 9.5 เมื่อตรวจด้วยวิธีพีซีอาร์อีไลซ่า ดังนั้นตัวอย่างที่มีผลการเกิดภาวะเมธิเลชั่นที่ได้จากวิธี พีซีอาร์อีไลซ่าเท่ากับหรือมากกว่าร้อยละ 10 จึงน่าจะสัมพันธ์กับตัวอย่างที่มีรอยโรคตั้งแต่ CIN2 ขึ้นไป ซึ่งมีการเกิดภาวะเมธิเลชั่นที่สูง (มากกว่าร้อยละ 20) ในการทดสอบกับ ตัวอย่าง ผู้วิจัยได้ใช้ตัวอย่างมาตรฐานที่มีความเข้มข้น 600 นาโนกรัม ซึ่งเป็นความเข้มข้นที่ใกล้เคียงกับตัวอย่างพีซีอาร์ส่วนมาก (500-600 นาโนกรัม) สุดท้ายผู้วิจัยได้ทำการ ตรวจวัดการเกิดภาวะเมธิเลชั่นด้วยวิธีพีซีอาร์อีไลซ่ากับตัวอย่างจำนวน 26 ตัวอย่าง ซึ่งมีผลร้อยละการเกิดภาวะเมธิเลชั่นจากวิธีไพโรซีเควนซิ่งก่อนหน้านี้ พบว่าจำนวน ตัวอย่างที่มีผลการเกิดภาวะเมธิเลชั่นที่คำนวณได้จากการทำพีซีอาร์อีไลซ่าใกล้เคียงกับวิธีไพโรซีเควนซิ่ง ในตัวอย่างที่มีรอยโรคแบบ CIN1 และ CIN2/3 คิดเป็นร้อยละ 71.43 (10/14) และ 80 (8/10) ตามลำดับ และเมื่อพิจารณาให้การเกิดภาวะเมธิเลชั่นร้อยละ 10 เป็นเกณฑ์แยกระหว่าง CIN1 และ CIN2/3 ในการศึกษานี้ พบว่ามีความไวร้อยละ 50 และความจำเพาะสูงถึงร้อยละ 80 อย่างไรก็ตามการศึกษานี้มีประชากรที่ใช้ศึกษาจำนวนน้อย ดังนั้นในอนาคตจึงควรเพิ่มขนาดประชากรให้มากกว่านี้ เพื่อให้ได้ความไวและ ความจำเพาะของวิธีพีซีอาร์อีไลซ่าที่น่าเชื่อถือ

สาขาวิชา	จุลชีววิทยาทางการแพทย์	ลายมือชื่อนิสิต	....
ปีการศึกษา	2562	ลายมือชื่อ อ.ที่ปรึกษาหลัก	....
		ลายมือชื่อ อ.ที่ปรึกษาร่วม	....

6187227320 : MAJOR MEDICAL MICROBIOLOGY

KEYWORD: Human Papillomavirus, L1 Methylation, Cervical intraepithelial neoplasia, Pyrosequencing, Polymerase chain reaction Enzyme-Linked-Immunosorbent Assay

Sasiprapa Liewchalermwong : Development of polymerase chain reaction enzyme linked immunosorbent assay for detection of human papillomavirus 16 L1 gene methylation. Advisor: ARKOM CHAIWONGKOT, Ph.D. Co-advisor: Assoc. Prof. PARVAPAN BHATTARAKOSOL, Ph.D.

It has been well known that cervical cancer is caused by persistent infections with the high risk human papillomavirus (HR-HPV) especially HPV16 and 18. However, a minority of HR-HPV infected women developed cancer, therefore, triage test is necessary to particularly select some HR-HPV infected women who are at higher risk to progress to cervical cancer quickly for colposcopy examination. Since HPV16 L1 gene hypermethylation has been reported to be correlated well with high grade cervical lesions and cancer, the present study aims to develop PCR-ELISA for detection of HPV16 L1 gene methylation. Cervical cells were collected from women who referred for colposcopy in Chulalongkorn memorial hospital. Cobas4800 and REBA-ID assays were used to discriminate HPV 16 positive samples from other types. Of 207 samples, seventy samples resulted in HPV16 positive with histology confirmed as CIN1-3 and other abnormality. All seventy samples were used to perform bisulfite conversion and HPV16 L1 PCR to detect methylation at CpGs5600, 5606, 5609 and 5615. Twenty-six PCR positive samples (130 bps) were used in pyrosequencing assay to evaluate methylation profile which were then used as reference data for PCR-ELISA development. Methylation level >20% was detected at CpGs 5600 and 5609 of CIN2/3, while <10% methylation was mostly found in CIN1 samples. For PCR-ELISA assay optimization, different concentration of reagents was performed. Although final protocol was successfully optimized, but non-specific binding was observed when testing with 0% methylated DNA. Thus, the protocol at streptavidin and amplicons-probe hybrids binding step was changed from 37 °C to 60 °C as the same as hybridization temperature to prevent non-specific binding. We found that at adjusted protocol, the absorbance was lower in DNA concentration 10-100 ng, but still high in 1,000 ng. The final optimized protocol for further experiments was as followed: the hybridization temperature was 60°C, 2 microgram/well of streptavidin, 294 ng/well of DIG-labelled probe and 1:3200 of antibody dilution, the binding step temperature was 60 °C. The detection limitation of CaSki DNA (approximately 100% methylation) was as low as 10 ng, however, to reduce the non-specific binding, the amplicons concentration must be lower than 1000 ng to efficiently differentiate between unmethylated and methylated CpG. It was noted that the concentrations used in standard curve controls and samples should be the same to obtain reliable absorbance for calculation of methylation percentage. The sensitivity of PCR-ELISA was as low as 20% methylation that absorbance value was higher than value obtained from 0% methylated amplicons and was consistent with pyrosequencing result (21%). Samples with 20% methylation detected by pyrosequencing assay showed methylation value 9.5% when detected by developed PCR-ELISA assay, thus, it can be indicated that clinical sample which represents methylation percentage equal or more than 10% by PCR-ELISA assay, might consider as hypermethylation sample (>20%) with CIN2+. All clinical samples' DNA concentration was approximately 600 ng. Thus, standard DNA controls concentration 600 ng/microliter were used to set standard curves. Twenty-six samples which were previously analysed for methylation profile by pyrosequencing assay, were used to perform PCR-ELISA. Number of CIN1 and CIN2/3 samples that showed calculated PCR-ELISA methylation percentage similar to pyrosequencing assay was 71.43% (10/14) and 80% (8/10), respectively. When, percentage of methylation at 10% was used as cut-off in the present developed PCR-ELISA method, the sensitivity and the specificity would account for 50% and 71.43%, respectively. However, clinical samples used in present study is limited. Thus, the larger sample size is needed to achieve more accurate specificity and sensitivity.

Field of Study:	Medical Microbiology	Student's Signature ....
Academic Year:	2019	Advisor's Signature ....
		Co-advisor's Signature ....

ACKNOWLEDGEMENTS

TABLE OF CONTENTS

LIST OF TABLES

LIST OF FIGURES

LIST OF ABBREVIATIONS

A	Adenine
ASC	Atypical squamous cells
ASC-H	Atypical squamous cells, cannot exclude HSIL
ASC-US	Atypical squamous cells of undetermined significance
β	Beta
BCIP	5-bromo-4-chloro-3-indolyl-phosphate
bp	Base pair
BSA	Bovine serum albumin
C	Cytosine
°C	Degree Celsius
CIN	Cervical intraepithelial neoplasia
CV	Coefficients of variation
DDW	Deionized distilled water
DIG	Digoxigenin
DNA	Deoxyribonucleic acid
dNTP	Deoxynucleoside triphosphate
DW	Distilled water
E	Early
EDTA	Ethylenediaminetetraacetic acid
EGFRs	Epidermal growth factor receptors

ELISA	Enzyme linked immunosorbent assay
EV	Epidermodysplasia verruciformis
G	Guanine
HCl	Hydrochloric acid
HPV	Human Papillomavirus
HR	High-risk
HRP	Horseradish peroxidase
HSIL	High-grade squamous intraepithelial lesions
HSPGs	Heparin sulfate proteoglycans
IRB	Institutional Review Board
L	Late
LCR	Long control region
LR	Low-risk
LSIL	Low-grade squamous intraepithelial lesions
M	Molar
$MgCl_2$	Magnesium chloride
ml	Milliliter
mM	Millimolar
mΩ	Milliohm
mRNA	Messenger ribonucleic acid
MSP	Methylation-specific polymerase chain reaction

Na$_2$HPO$_4$	Sodium phosphate, dibasic
NaH$_2$PO$_4$	Sodium phosphate, monobasic
NASBA	Nucleic acid sequence-based amplification
NBT	4-nitro blue tetrazolium chloride
NCR	Non-coding region
nm	Nanometer
NMSC	Nonmelanoma skin cancer
OD	Optical density
ORF	Open reading frame
%	Percentage
Pap	Papanicolaou-stained
PBS	Phosphate-buffered saline
PCR	Polymerase Chain Reaction
pRb	Retinoblastoma protein
RNA	Ribonucleic acid
ROC	Receiver operating characteristic
rpm	Revolutions per minute
RPP	Recurrent laryngeal papillomatosis
RRP	Recurrent respiratory papillomatosis
SSC	Saline Sodium Citrate
SCC	Squamous cell carcinoma

SD	Standard deviation
SDS	Sodium dodecyl sulfate
T	Thymine
TBS	Tris Buffered saline
TGN	Trans-Golgi network
TMB	3′,5,5′-Tetramethylbenzidine
μg	Microgram
μL	Microliter
μM	Micromolar
URR	Upstream regulatory region
VAIN	Vaginal intraepithelial neoplasia
VIA	Visual Inspection with Acetic acid
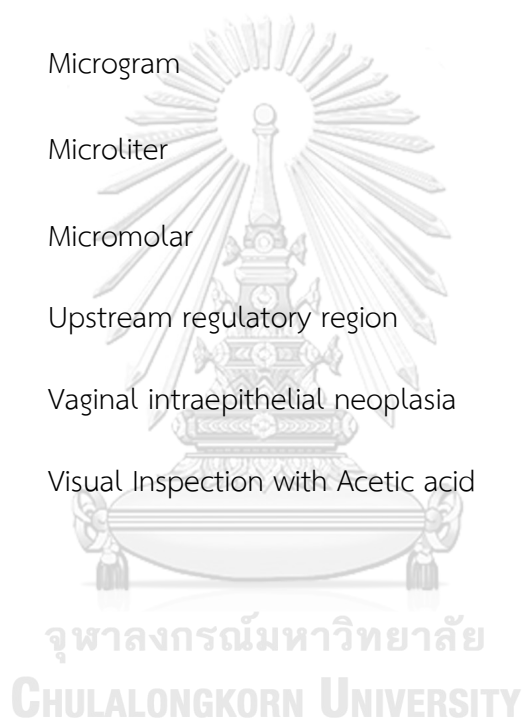
CHAPTER I

INTRODUCTION

Human Papillomaviruses (HPVs) are non-enveloped, dsDNA viruses (1, 2). The HPV genome can be divided into three regions according to their functions: the early (E) region that contains early genes E1, E2, E4, E5, E6 and E7. Late (L) region that encodes L1 and L2 capsid proteins (3). Long control region (LCR) or Upstream regulatory region (URR), a non-coding region (NCR) (4, 5).

More than 200 HPV genotypes have already been identified. Some types infect cutaneous epithelial cells, while the other types infect mucosal epithelial cells (1, 2). Mucosal HPV genotypes can be subdivided into 2 groups according to their abilities to cause cervical cell transformation including high risk and low risk types.

Cervical cancer is the 3rd most common cancer among women worldwide, with an estimated over 500,000 new cases and approximately 311,365 deaths in 2018 (GLOBOCAN). It has been reported that HR-HPV types were found nearly 100% of cervical cancer cases worldwide, in which HPV-16 and 18 were found in 55% and 15% of all cervical cancer cases, respectively. The other HR-HPV types detected in cervical cancers worldwide were 31, 33, 35, 45, 52 and 58 (6).

Papanicolaou stained (Pap) smear, a cervical cytology test invented by pathologist George Papanicolaou, has been used for cervical cancer screening for more than 50 years. However, Pap smear is found to have 20 to 30% of false-negative results (7). HR-HPV DNA testing has been introduced as additional test with cytology test to screen women who need further colposcopy examination. However, HR-HPV testing lacks of specificity because minority of HR-HPV infected women develop cervical cancer after a decade of persistent infection (8). Moreover, the study from the National Cancer Institute reported that 50% of HPV positive women referred to colposcopy showed normal cervical lesion (9). Thus, we aim to improve the sensitivity and specificity of screening test. HPV16 L1 gene methylation has been reported to be correlated well with high grade cervical lesions and cancer. So far, L1 gene methylation

can be detected by several molecular techniques such as pyrosequencing, methylation-specific PCR (MSP) and next-generation sequencing technique (10). However, molecular techniques are high cost technique and required professional technician, so these techniques may be hard to perform in developing country. Thus, low cost and easy to perform assay is needed using equipment available in routine laboratory such as PCR cycler, incubator, shaker and spectrophotometer, therefore we need to develop Polymerase Chain Reaction Enzyme-Linked-Immunosorbent Assay (PCR-ELISA) for detection of HPV16 L1 Gene methylation. So far, ELISA technique for methylation detection was developed to detect host gene, but HPV16 L1 Gene methylation ELISA method has not been developed. Since, L1 is viral capsid gene, L1 hypermethylation indicate cancer caused by viral infection. Whereas, host gene hypomethylation only indicate cancer development.

CHAPTER II
OBJECTIVE

Objective

1. To develop PCR-ELISA assay for detection of HPV16 L1 gene methylation.

2. To compare HPV typing results between the REBA® HPV Test and the Cobas® HPV Test

Hypothesis

1. HPV16 L1 gene methylation can be detected by developed PCR-ELISA assay.

2. HPV typing results obtained from the REBA® HPV Test is in concordance with the results obtained from the Cobas® HPV Test.

จุฬาลงกรณ์มหาวิทยาลัย
CHULALONGKORN UNIVERSITY

CHAPTER III

REVIEW OF LITERATURE

Virology of Human papillomaviruses

Human Papillomaviruses (HPVs) are small, double-stranded, circular DNA viruses (〜7,000-8,000 bp) which belongs to the *Papillomaviridae* Family. HPVs are an icosahedral symmetric virus with approximately 55 nm in size (1, 2). The HPV genome can be divided into three different regions including the early region, late region and Long control region (Figure 1): 1. Early (E) region, a coding region comprises of six early genes E1, E2, E4, E5, E6 and E7 which is responsible for viral protein synthesis. E1 and E2 proteins involve in viral replication and transcription. E5, E6 and E7 proteins are oncoproteins. 2. Late (L) region, a coding region containing the major (L1) and minor (L2) capsid proteins which are responsible for capsid protein synthesis (3). 3. Long control region (LCR) or Upstream regulatory region (URR), a non-coding region (NCR) located between ORFs L1 and E6. LCR contains short DNA sequence motifs called regulatory elements that are recognized and bound by regulatory host proteins such as SP-1, NF, TBP and AP1, and viral E1/E2 proteins binding site. Regulatory elements modulate viral replication, transcription and post-transcriptional control (4, 5). HPV genes are transcribed from one stranded. The function of all HPV genes are listed in Table 1 (11).

There are over 200 HPV genotypes that have been discovered so far (1, 2) The characterization of novel papillomaviruses is based on nucleotide similarity. Therefore, HPVs are classified into genotypes. Each genotype is grouped by similarity of the highly conserve L1 sequence of less than 90% (12). HPVs can also be classified based on tissue tropism. Therefore, HPVs are divided into two large groups. The largest group mainly infects mucosal epithelia of the genital and oral tract (1, 2). This group comprises of approximately 64 HPV genotypes. Moreover, the mucosal HPV types are subdivided into two groups based on their oncogenic potential. First, non-oncogenic type called low-risk (LR) HPV types such as 6, 11, 40, 42, 43, 44, 54, 61, 70, 72, 81, these

LR types can cause low-grade lesion of anogenital tract called genital warts, a disease of respiratory tract called recurrent respiratory papillomatosis (RRP), laryngeal papillomatosis. Second, an oncogenic type called high-risk (HR) HPV types including fifteen HPV types (16, 18, 31, 33, 35, 39, 45, 51, 52, 56, 58, 59, 68, 73, and 82). High-risk HPV types can cause disease of an anogenital tract called intraepithelial neoplasia (cervical, vaginal, penile and anal cancers). HPV 16 is mostly found approximately 55% of cervical cancer, while the second type, HPV 18 is detected approximately 15% in cervical cancer (6).

HPV can be transmitted by direct contact with the virus, sexual contact and micro abrasion of the cervical epithelium (13). HR-HPVs infect cells of the basal layer between the endo- and ectocervix, where it is presented at a relatively low copy number (14). HPV L1 capsid protein binds cellular receptors called heparin sulfate proteoglycans (HSPGs) (15). When L1 binds HSPGs, there is a conformational change in N-terminus of L2 (16) which then cleaved by furin and/or PC5/6. This N-terminus can bind secondary receptors on the cell membrane (17) such as epidermal growth factor receptors (EGFRs), integrin-α6 (18). HPVs internalize into the cytoplasm by endocytosis mechanism. Then, papillomavirus is uncoated by the acidity of the late endosome. L1 protein is separated from L2 and vDNA complex (L2/vDNA), followed by degradation of L1 in the lysosome. L2/vDNA with a small amount of L1 travels through the trans-Golgi network (TGN) (Figure 2) (19). Then viral genome detaches from TGN and enters the nucleus via nuclear pores by the microtubules during mitosis of the host cell (20). E6 and E7 are expressed from the p97 promoter and control the cell cycle by stimulating the S phase entry (21). E1 and E2 are expressed to maintain an episomal form of viral DNA in the lower epithelial layers (22). E1/E2 complexes involved in the initiation of HPV genome replication (23). After HPV infection into basal cells, the viral genome is presented at a low copy number (50–100 copies per cell) in the basal layer of the epithelium but in the productive phase, the HPV genome is amplified to more than a thousand copies per cell (24).E6 and E7 oncogenes are expressed under the

control of E2 protein, E6 degrades p53 and E7 disrupts retinoblastoma protein (pRb) to maintain viral genome replication and as a consequence, HPV infected cells do not exit the cell cycle (25). When host basal cells proliferate and differentiate to cells at the upper layer of the epithelium, L1 and L2 capsid proteins are produced, the viral genomes are encapsidated to form viral particles. finally, human papillomaviruses exit the cells by cell lysis (13). The HPV life cycle is shown in Figure 3.
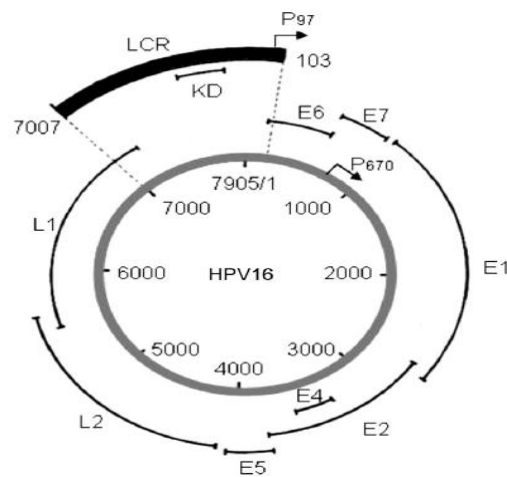
Figure 1 The double-stranded DNA HPV 16 genome is represented by the gray circle labeled with the nucleotide number. The position of the long control region (LCR) and the early genes (E1-E7) and late genes (L1 and L2) are shown (3).

Table 1 Human papillomavirus genes functions (11)

Viral Protein	Functions and Features
E1	Initiates replication of viral genome. Activates helicase, keeps viral DNA episomal
E2	Viral transcription and DNA replication. Segregation of viral genomes
E4	Facilitates packing of viral genome. Maturation of viral particles. Interaction with RNA helicase
E5	Interaction with EGF-receptor, activates PDGF receptor. Oncoprotein allows continuous proliferation of the host cell and delays differentiation
E6	Blocks the normal regulation of the host cell division. Degrades p53 in the presence of E6-AP. Interaction with several host proteins. Major oncoprotein.
E7	Blocks the normal regulation of the host cell division. Binds to pRB-105. Interaction with several host proteins. Major oncoprotein
L1	Major capsid protein
L2	Minor capsid protein. Contributes to viral localization into nucleus
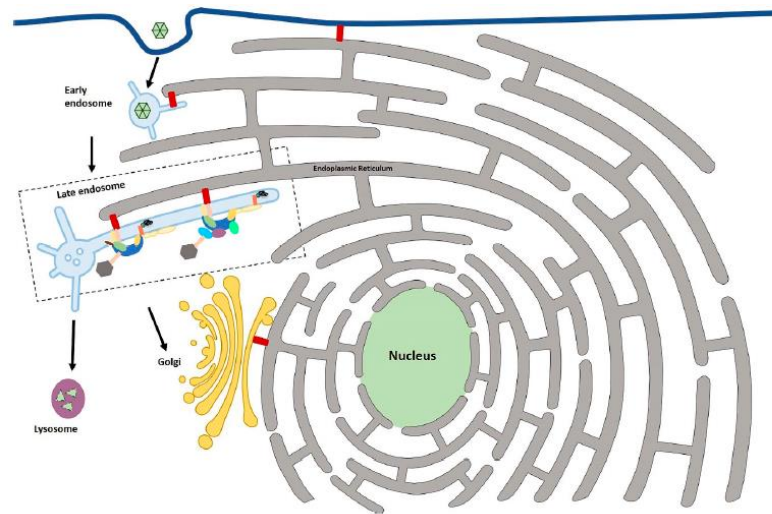
Figure 2 HPV intracellular trafficking to the TGN (26)
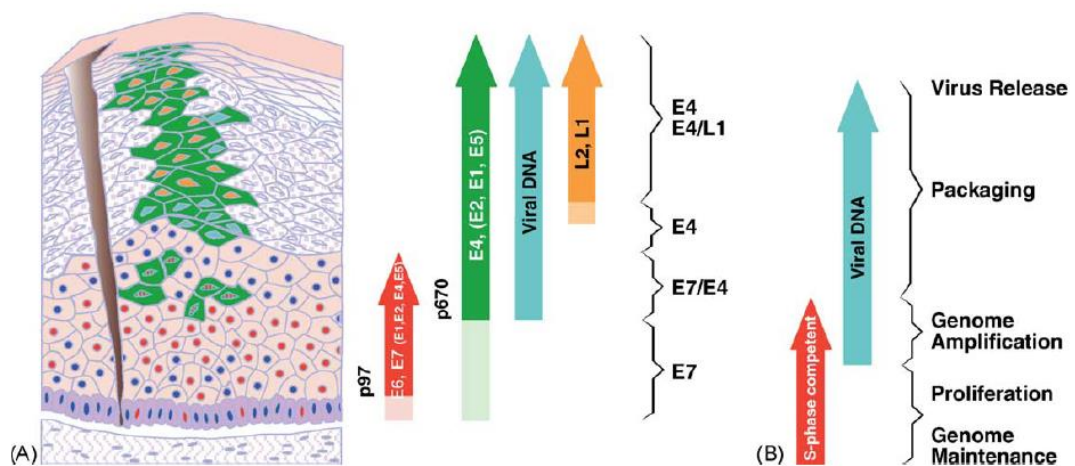
Figure 3 The life cycle of Human papillomavirus during the productive phase (A) HPV infects basal cell of the epithelium through micro abrasion, the viral genome is maintained as a low copy number. After the differentiation of epithelium cell, the p97 promoter is activated to express E6 and E7 genes which drive the host cell to entry S-phase (red). At the upper part of the epithelial layer, the p670 promoter is activated to expresses several HPV genes including E1, E2 E4 and E5 (green) that help to support amplification of viral genomes (blue). Finally, L1 and L2 capsid proteins are produced in differentiated cells and finally assemble to form viral particle (yellow). (B) Summarize the life cycle of HPV starting from genome maintenance in basal cells to viral genome amplification phase in the upper epithelial layers. Virion packaging and virus release during terminal differentiation of host cell (13).

Clinical manifestations of HPV infections

Spontaneous regression occurs in most of HPV infected healthy women, however, minor of them progress to cancer, it takes several years to develop malignant transformation. HPVs are associated with many diseases, from benign verrucae vulgares and condylomata acuminata to the malignancies of the cervix, vulva, anus, and penis Diseases related to HPV can be divided into two categories, including anogenital (mucosal) and nongenital (cutaneous) (27).

Anogenital HPV infection occurs in the genital area. Genital HPV can present in three different manifestations: clinical, subclinical, and latent infection. The clinical manifestation such as Genital wart, precancerous and cancerous lesions (28). Genital warts (condyloma acuminata) usually be found on moist surfaces of the genital area, they present as small papules, soft, pink, or white cauliflower-like sessile (29), genital warts are mainly caused by HPV 6 and 11 with approximately 90% (30). Moreover, the most prevalent of anogenital HPV infection are cervical intraepithelial neoplasia (CIN) and cervical cancer. It has been known that HPV infections are related to cervical cancer lesions, HPV-16 and 18 are detected in more than 90% of all cervical cancer cases (31). Condylomata plana or flat warts are subclinical lesions that can be seen only with the use of enhancing technique. Latent infections are defined by the presence of HPV DNA in areas with no clinical or histological evidence of HPV infection (27).

Nongenital HPV infection is divided into two categories based on tissue tropism. First, the mucosal lesions usually occur in the oral and respiratory tract such as an oral wart, oropharyngeal cancer, and recurrent laryngeal papillomatosis (RPP). Oral warts (verruca vulgaris) are usually asymptomatic, they are associated with HPV 2 and 4. Oropharyngeal cancer can be divided into two groups, HPV-positive, which are associated with HPV infection, and HPV-negative cancers, which are mostly linked to alcohol or tobacco use. HPV, remarkably type 16, is caused about 25% of oropharyngeal cancers (27). Recurrent laryngeal papillomatosis is a rare disease caused by HPV 6 and HPV 11 (32). Second, cutaneous (skin) lesions such as a common wart, Epidermodysplasia verruciformis (EV) and Nonmelanoma skin cancer (NMSC). Common wart or verruca vulgaris can be caused by several low-risk HPV types and can occur

anywhere on the skin surface (27). Epidermodysplasia verruciformis (EV) is an autosomal-recessive genetic disorder characterized by impaired cellular immunity to HPV infection (33). Nonmelanoma skin cancer (NMSC) usually occurs in fair-skinned populations (34).

Table 2 Human papilloma virus (HPV) types in various clinical lesions (27)

Manifestation	HPV types
Anogenital lesions	
Genital wart (condylomata acuminata)	6, 11, 30, 42, 43, 44, 45, 51, 52, 54
Bowenoid papulosis	16, 18, 34, 39, 42, 45
Bowen disease	16, 18, 31, 34
Gigantski kondilom (Buschke-Löwenstein)	6, 11
Low-grade intraepithelial neoplasias	6, 11, 43
High-grade intraepithelial neoplasias	16, 18, 31, 33, 35, 39,
Bowenoid papulosis	42, 44, 45, 51, 52, 53,
Erythroplasia Queyrat	56, 58, 59, 62, 66
Invasive cancer	
Nongenital mucous lesions	
Recurrent laryngeal papillomatosis	6, 11
Squamous cell lung cancer	6, 11, 16, 18
Laryngeal cancer	16, 18
Focal epithelial hyperplasia (Heck disease)	13, 32
Conjuctival papillomas	6, 11
Oral warts	2, 4
Oral condyloma	6, 11
Florid oral papillomatosis	6, 11
Nongenital skin lesions	
Common wart (verrucae vulgaris)	1, 2, 4, 26, 27, 29, 41, 57, 60, 63, 65
Plantar wart	1, 2, 4, 63
Flat wart (verrucae plana)	3, 10, 27, 28, 29, 38, 41, 49
Butcher's wart	1, 2, 3, 4, 7, 10, 28
Epidermodysplasia verruciformis	3, 4, 5a, 5b, 8, 9, 12, 14, 15, 17, 19-25, 36-38, 47, 49, 50, etc.
Skin tag	6, 11
Nonmelanoma skin cancer (basal cell carcinoma, squamous cell carcinomas, Bowen's disease)	8, 15, 20, 23, 36, 38

Screening of cervical cancer

Various methods have been developed, evaluated, and implemented in many laboratories for screening of cervical cancer. Cytology was first performed over 50 years ago. HPV DNA testing assays both target and signal amplifications have been implemented to help selecting women referred for colposcopy. Methods for cervical cancer screening are discussed as follows.

1. Conventional cytology

Papanicolaou stained (Pap) smear was introduced by a pathologist, George Papanicolaou in 1949. It is a screening test for observing abnormal cells of the transformation zone of the cervix, however, inadequate samples and clumping of cells are found to cause false-negative approximately 20 to 30% (7). For this reason, monolayer cytology was developed to reduce false negative of the pap smear test. the specimen is collected in a preservative solution in order to fix and preserve the cellular structure (42). This technique is significantly better at predicting the presence of dysplasia than pap smear when compared to a gold standard, Colposcopically-directed biopsies (43).

2. HPV DNA testing

2.1 Signal amplification

Signal amplification is based on the hybridization of the target HPV-DNA with RNA probe in clinical specimen without amplifying of the HPV genome. The HPV DNA-RNA hybrid is captured by anti-DNA-RNA hybrid antibody. This technique has lower false-positive rate (8). Currently, FDA (Food and Drug Administration) has been approved only two methods for diagnostic testing in the United States: The Hybrid Capture II (hc2) technique, and the CareHPV test (44).

2.2 Nucleic acids amplification assays

Nucleic acids amplification assays are based on amplification of HPV genomes in order to improve sensitivity. Currently, many techniques are used to detect a multiple HPV genotypes in a single tube. For example, the FDA approved COBAS 4800

HPV test which detects HPV genotypes by Real-time PCR technique. It can detect 14 hrHPV types including HPV16, HPV18, and 12 other high-risk HPVs (hrHPVs) (HPV31, -33, -35, -39, -45, -51, -52, -56, -58, -59, -66, and -68, as a pooled result). The reaction contains a primer of β-globin to be used as a genomic DNA control to confirm the sufficient quantity and quality of samples. However, HPV DNA testing has low specificity for detection of abnormal cervical cells (8).

3. HPV mRNA target amplification

E6 and E7 oncogenes that are expressed from HR-HPV types can induce cervical cells transformation, and they also play an important role in cell cycle modulation such as E6 causes p53 degradation (45). Thus, screening tests for diagnosing precancerous lesions based on the presence of E6/E7 transcripts were developed (46).

The main techniques used to detect E6/E7 oncogenes mRNA are two commercial assays: PreTect Proofer and APTIMA HPV Assay (47). The principle is based on nucleic acid sequence-based amplification (NASBA) of full-length E6/E7. The PreTect HPV-Proofer assay (NorChip AS, Klokkarstua, Norway) is an assay based on Real-Time multiplex PCR which detects E6/E7 mRNA from five HR-HPV (-16, -18, -31, -33, and -45) (44). APTIMA HPV assay (Gen-Probe, San Diego, CA, USA) detects HPV E6/E7 mRNA of the 14 HR-HPV (-16, -18, -31, -33, -35, -39, -45, -51, -52, -56, -58, -59, -66, and -68) (48). Detection of HR-HPV E6/E7 mRNA is more specific to detect abnormal cervical cells than HPV DNA testing, however, expensive equipment and high cost is of concerned.

4. Visual Inspection with Acetic acid (VIA)

Visual inspection acetic acid (VIA) is currently a popular method for screening of cervical cancer in low resource countries. VIA is performed by applying freshly prepared 4% acetic acid to the cervix. The test results are observed after 1-minute, the positive result is interpreted if an acetowhite area is seen in the transformation zone that due to numerous proteins and other components clumping inside abnormal

cells, and normal cells with less protein content are negative that no acetowhite is observed (49).

5. p16/Ki-67 Dual Immunostaining

p16^{INK4a} (p16) and Ki-67 immunostaining are used as prognosis tests for screening of cervical lesions. p16 is a cellular protein correlated to the increased expression of oncogenic E7 protein, p16 is a cyclin dependent kinase inhibitor. The mechanism is that cell cycle controlling protein retinoblastoma protein (pRb) is bound by E7 protein and cause the release of E2F protein that drive cell cycle into S-phase, as a consequence of deregulated cellular proliferation, a negative feedback mechanism is activated and caused p16 overexpression (50). Sano T. and colleagues reported that p16 overexpression is found in most cases of cervical precancers and cancers while in normal tissue, p16 expression is rarely found (51). Moreover, the expression of Ki-67, a proliferation marker, within the same cervical cell may be used as a marker of cell-cycle disruption. These two independent biomarkers have been reported to be an efficient triage test for screening of cervical lesions (52).

6. Human papillomavirus L1 (Cytoactive)

L1 is a major capsid protein of HPV which can be detected only at a productive phase (53). L1 capsid proteins are mostly expressed in patient with LSIL but rarely expressed inpatient with HSIL (54). According to this knowledge, several studies have been confirmed that a loss of viral L1 capsid protein, could be a prognostic marker for the development of CIN lesions. (55-57). Currently, Cytoactiv is an objective standard to identify transient HPV infections and precancerous lesions (mild and moderate dysplasia) caused by high-risk HPV. This assay is based on a nuclear immunochemical staining reaction. Limitations of L1 detection are low sensitivity of L1 antibodies and false-negative results are due to point mutation of L1 epitopes as a result of immune evasion (53).

7. HPV genome methylation in HPV 16

DNA methylation is facilitated by DNA methyltransferases. The methyl group can regulate transcription and expression of coding gene (58, 59). Methylation occurs on CpG Islands where are often located at gene promotor (60). There has been reported that promoter methylation of tumor suppressor genes related to malignant cellular transformation (61). Methylation of HPV DNA may serve as a host defense mechanism for silencing viral replication and transcription. L1 genes of HPV16 were found to be hypermethylated in cervical carcinomas, whereas in low-grade CIN or normal samples were reduced (62, 63). Similar results were found in L1/L2 and E2/L2/L1 regions (10, 64). Nowadays, there are several assays to detect DNA methylation such as pyrosequencing, methylation-specific PCR (MSP) and next-generation sequencing techniques (10).

HPV genome methylation and its significance

DNA methylation is an epigenetic mechanism that occurs by the addition of a methyl (CH3) group to DNA at the 5-carbon of the cytosine ring resulting in 5-methylcytosine (5-mC). 98% of DNA methylation occurs at a CpG site, in which a cytosine nucleotide is located next to a guanidine nucleotide. DNA methylation is controlled by a family of DNA methyltransferases (DNMTs): DNMT1, DNMT2, DNMT3A, DNMT3B, and DNMT3L. DNMT1 is responsible for the maintenance of methyltransferase during DNA synthesis, while DNMT3A and 3B is responsible for *de novo* DNA methylation (65). *De novo* DNA methylation is essential for the reprogramming of genetic information in early embryogenesis (66). DNA methylases DNMT3A and 3B can also target viral DNA during tumorigenesis. Methylation of the promoters of tumor suppressor genes is found in cancer (67). The Epstein–Barr Virus (EBV) was thought to be the only virus targeted by *de novo* methylation, as methylation may repress the EBNA promoters, thereby immune escaping occurs during EBV-induced carcinogenesis (68). HPV-16 genome was also found to be methylated in cell lines and in clinical samples (69). Moreover, HPV-16 DNA is mostly methylated in undifferentiated cells , but becomes demethylated in differentiated cells (70).

HPV E6 and E7 protein are oncoprotein which can be suppressed by E2 protein. The E2 binds proximal E2BSs and prevents the binding of host transcription factors and RNA polymerase. Viral integration into the host genome can cause the loss of E2 genes, thereby loss the ability to suppress E6 and E7 genes. Thus, E6 and E7 protein are overexpressed, suggesting that viral integration is an essential event during malignant transformation. However, it has been shown that episomal HPV16 genome with intact E2 gene was found approximately 50% in cervical cancer samples (71). It has been reported that *de novo* methylation of episomal HPV16 E2BSs can also upregulate E6 and E7 oncogene expression by interfering E2 binding to its specific binding sites (72). Methylation state of integrated HPV16 E2BSs was copy number dependent, in which high methylated E2BSs was found in high copy number of integrated HPV16, while no methylation at E2BSs was found in single copy of integrated HPV 16 genome (72). It has been shown that HPV16 E7 protein could bind and activate DNA methyltransferase DNMT1 that resulting in self E2BSs methylation of multi-copies of integrated HPV16, however, there was a few transcriptionally active E2BSs for E6/E7 oncogene expressions (73). It can be speculate that HPV self-methylation of multi-copies E6/E7 oncogenes promoter could regulate the promoter activity and levels of E6/E7 oncoproteins to help the survival of cancer cells (74).

During productive infection, HPV infects undifferentiated basal cells where viral early proteins are expressed. Viral late proteins, L1 and L2 are expressed in differentiated cells to form the capsid (75). Viral self-methylations are caused the loss of the L1 capsid protein production in undifferentiated basal cells by adding methyl (CH3) group at CpG site of L1 gene, in order to regulate the expression L1 protein which is highly immunogenic protein (5, 76). Thus, hypermethylation in L1 gene are caused loss of L1 capsid protein expression that could help virus to survive inside the cells and develop high grade cervical lesions (77). Moreover, It has been reported that HPV16 was found approximately 40-50% episomal form and 50-60% integration form in cervical cancer cases, hence, it is speculated that both episomal and integration form contain hypermethylated L1 (71, 78). Previously, the study in Thailand demonstrated that means of methylation of the HPV16 5′ L1 at CpGs 5600, 5606, 5609, 5615 in squamous cell carcinoma (SCC) was higher than the HPV16 3′ L1 at CpGs 7136,

7145 (63). Moreover, hypermethylation at CpGs 5600 and 5609 has been reported to differentiate between normal and cervical neoplasia (79, 80).

Bisulfite based assay for HPV genome methylation detection

Sodium bisulfite deaminates unmethylated cytosine residues and converts them to uracils, while methylated cytosines remain intact. When bisulfite-modified DNA is subjected to PCR, the uracil residues are converted to thymidines by DNA polymerase (81). Methylation status of bisulfite-treated DNA can be determined by several methods.

1. Methylation specific PCR (MSP)

Methylation specific PCR (MSP) was first introduced by Herman et al. in 1996 who developed a selective amplification of methylated and unmethylated genes. Taking advantage of the sequence differences obtained from bisulfite modification, two different primers were designed, one specific to methylated sequence and another specific to unmethylated sequence (81, 82). A two-round of MSP has been introduced (83). Real-time PCR also uses in methylation detection, for example, MethylQuant, a real-time PCR technique using SYBR Green I as fluorescence (84). Methylation detection can be measured by adding a melting step to distinguish the methylation status of individual alleles by comparison with standards of known methylation status (85).

2. Pyrosequencing

Pyrosequencing is based on synthesis method; the result is presented in real-time through the enzymatic conversion of released pyrophosphate into a proportional light signal. The synthesis process relies on sequential addition, deoxynucleoside triphosphate (dNTP) including adenine (dATP), cytosine (dCTP), guanine (dGTP), and thymine (dTTP), is added to the template strand one by one (86). Pyrosequencing can quantitate methylation status at multiple CpG sites within short fragment of DNA (～30 nucleotides) and represents an average of methylation levels at a specific site by percentage (87).

ELISA assay for detection of genome methylation

    1. Principle of PCR-ELISA for detection of genomic sequences

    ELISA assay is a pathobiological technique which is mostly used for detection of antibody and antigen, based on reaction between antibody-antigen complex. ELISA assay can also be applied to detect DNA sequences, PCR-ELISA was developed to detect nucleic acid instead of protein that combines PCR and ELISA techniques.(88). PCR technique can amplify a piece of DNA to a large number of amplicons. Thus, development of specific probe is necessary for detection of PCR products (89). PCR-ELISA technique is an immunological method which can directly quantify the PCR product. The principle of PCR-ELISA was as followed, first, PCR amplification is performed and mostly carried out by using digoxigenin-11-dUTP (DIG-dUTP) nucleotide. DIG labelled PCR product is hybridized with biotin-labelled probe. Frist, streptavidin which has high binding affinity to biotin is coated on microplate. DIG labelled PCR product is hybridized with biotin-labelled probe. Then, biotinylated probe-PCR amplicons are added on microplate. Microplate is washed with washing buffer. Finally, enzyme conjugated anti-DIG antibody is added, follow by addition of substrate and absorbance is measured by spectrophotometry (90). This technique is sensitive, easy to perform and can be achieved the result at maximum 4 hours, without needed to advance laboratory equipments and professional person (91). Moreover, it is a semi-quantitative technique (92). Although the result is not as accurate as real-time PCR, PCR-ELISA is much cheaper. Thus, PCR-ELISA is a suitable alternative (Figure 4). PCR-ELISA is used for clinical and food industry. Microorganisms that detected by PCR-ELISA were reported such as trypanosomes (93), Hepatitis A virus and E (94), human papillomavirus (95), Human immunodeficiency virus type I (HIV-1) (96), and Respiratory tract pathogens (97).
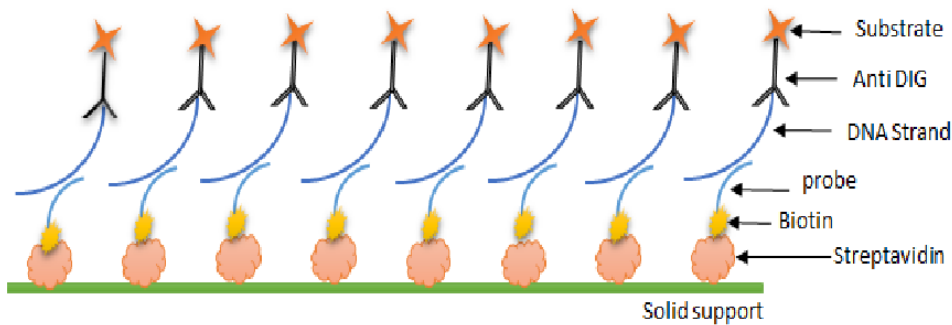
Figure 4 Detection of biotinylated DNA using an anti-DIG peroxidase conjugated with substrate (98).

2. Commercial kits for detection of genome methylation

Recently, there are few ELISA commercial kits which were developed in order to detect global DNA methylation. All of them used to detect host gene methylation without amplification of target DNA by either immobilizing total DNA on ELISA plate or hybridizing LINE-1 gene with biotin labelled probe specific for LINE-1 DNA. After that, methylated CpGs can be detected by using anti-5'methylcytosine mAb and anti-HRP-conjugated secondary antibody. The ELISA commercial kits are for example, MethylFlash Global DNA Methylation (5-mC) ELISA Easy Kit (EpiGentek, USA), DNA Methylation ELISA Kit (Cayman Chemical, USA), Global DNA Methylation Assay Kit (abcam, UK), Global DNA Methylation ELISA (Cell biolabs, USA), and Global DNA Methylation Assay–LINE-1 (Active Motif, USA). However, so far ELISA assay for detection of HPV genome methylation is not yet developed.

CHAPTER IV

MATERIALS AND METHODS

Conceptual frameworks

```
┌─────────────────────────────────────────────────────────────┐
│  Cervical samples are collected from women who are refered    │
│  for colposcopy                                               │
└─────────────────────────────────────────────────────────────┘
                              ↓
┌─────────────────────────────────────────────────────────────┐
│  HPV DNA detection and genotyping  using Roche Cobas 4800     │
│  and REBA HPV-ID                                              │
└─────────────────────────────────────────────────────────────┘
                              ↓
        ┌───────────────────────────────────────┐
        │  HPV16 positive samples are selected  for │
        │  Bisulfite modification                │
        └───────────────────────────────────────┘
                              ↓
              ┌──────────┐         ┌──────────┐
              │   PCR    │  →      │  ELISA   │
              └──────────┘         └──────────┘
                              ↓
        ┌───────────────────────────────────────┐
        │  Methylation analysis using Pyrosequencing │
        └───────────────────────────────────────┘
                              ↓
        ┌───────────────────────────────────────┐
        │  Statistical analysis using SPSS       │      ┌──────────────┐
        │  Comparison HPV types and Methylation  │  ←   │ Histological │
        │  status with histology results         │      │   results    │
        └───────────────────────────────────────┘      └──────────────┘
```

Part I   Cervical samples collection and HPV genotyping

1. Clinical specimens

The leftover of cervical cell lysate specimens collected from 207 women from Department of Gynecology, Faculty of medicine, Chulalongkorn University, Bangkok, Thailand were recruited. The study was approved by the Institutional Review Board (IRB) of Faculty of Medicine, Chulalongkorn University, IRB No. 042/60 COA No. 278/2019. Among 207 samples, 168 samples have histological examination as cervical

intraepithelial neoplasia 1-3 (131 CIN1, 11 CIN2, 26 CIN3) and 39 samples were non-CIN (vaginal intraepithelial neoplasia (VAIN), chronic cervicitis, benign squamous epithelium, condyloma acuminate and squamous metaplasia). Cervical samples were stored in lysis buffer (see Appendix B) and kept at -20 °C. They were used to analyse for HPV DNA detection and genotyping using the REBA® HPV Test and the Cobas® HPV Test. HPV16 positive samples tested by the Cobas® HPV Test were used for methylation analysis and Polymerase Chain Reaction-Enzyme-Linked-Immunosorbent Assay (PCR-ELISA) development.

2. HPV DNA detection and genotyping

HPV detection and genotyping were kindly performed by Dr. Arkom Chaiwongkot, Faculty of Medicine, Chulalongkorn University using the Cobas® HPV Test based on real-time PCR (RT-PCR) with a fully automated system (Roche, Switzerland). Cobas can detect HPV16, HPV18, and 12 other high-risk HPVs (HR-HPVs) (HPV31, -33, -35, -39, -45, -51, -52, -56, -58, -59, -66, and -68, as a pooled result). Moreover, the reaction contains a primer set specific to β-globin, as a genomic DNA control, to confirm the sufficient quantity and quality of samples. Extracted DNA was collected after the end of the process.

In addition, HPV type distribution was also performed using REBA® HPV Test based on reverse blot hybridization assay system (Molecules and Diagnostics, Korea). REBA can identify 32 types including the 18 high-risk HPVs (HPV genotypes 16, 26, 18, 31, 33, 35, 39, 45, 51, 52, 53, 56, 58, 59, 66, 68, 69, 73), 1 probable high-risk HPVs (HPV genotype 34), and the 13 low-risk HPVs (HPV genotypes 6, 11, 40 42, 43, 44, 54, 70, 72, 81, 84, 87). Genetic target of the kit is a L1 gene which is expressed at the late stage of infection cycles in host cells. In order to validate the correct test and good reagent, the membrane strip contains Hybridization control line to check the chromogenic reaction and the related reagents, Negative control line for contamination checking and positive control line (β-globin) to check a successful PCR amplification reaction. The procedure of HPV genotyping was followed by manufacturer's instruction. In brief,

extracted DNA was amplified. All PCR reactions were performed in a 50 μL volume. The protocol is as follows: 25 μL of 2X PCR premix, 16 μL of DNase/RNase-free water, 4 μL of primer mix and 5 μL of DNA. Provided positive control (HPV33 positive) and negative control were used. The PCR conditions were initial denaturing at 94 ℃ for 5 minutes, followed by 15 cycles of 94 ℃ for 30 seconds, 55 ℃ for 30 seconds, followed by 45 cycles of 94 ℃ for 30 seconds, 52 ℃ for 30 seconds and a cycle of 72 ℃ for 10 minutes. Amplified DNA, membrane strip and reagents including denaturation solution, hybridization solution, wash solution, alkaline phosphatase conjugated, conjugate dilution solution, NBT/BCIP solution, Distilled water were placed in the machine. HPV genotyping was processed by automated machine (REBA HPV-ID).

Part II HPV16 L1 gene methylation analysis

  1. Control cell lines and culture

CaSki and SiHa, human cervical carcinoma cell lines with about 600 copies and 1-2 copies of HPV 16 DNA were used as positive control cells for L1 gene methylation analysis using pyrosequencing and PCR-ELISA. Both cells were obtained from Virology Unit, Department of Microbiology, Chulalongkorn University. All cells were grown in growth medium: Dulbecco's Modified Eagle Medium (GIBCO, USA) supplemented with 10% fetal bovine serum (see Appendix B), 10^5 units/ml penicillin G (see Appendix B), 10^5 units/ml streptomycin (see Appendix B). When the cells were growing in monolayer nearly 80-90% confluent, subculturing was done. The culture media was removed, and monolayer cell was washed two times by 1X phosphate buffered saline (PBS; see Appendix B). Then, pre-warmed 0.25% trypsin Ethylenediaminetetraacetic acid (trypsin-EDTA; see Appendix B) were added and incubated for 1-5 minutes at 37 ℃ until most of the cells were separated under microscope followed by discarding of trypsin. Cells were detached by gently tapping and growth medium (see Appendix B) was added. The monolayer cell was subcultured at 2-3 days intervals with split ratio of 1:3. The cells were cultured at 37 ℃ in 5% CO_2 air atmosphere. The discarded cells were

collected in 15 ml centrifuge tube. Then, the tube was centrifuged for 5 minutes at 1,500 rpm, room temperature. Next, the media was discarded. Finally, the cell pellet was stored at -20℃.

2. DNA extraction

CaSki and SiHa cell pellets were extracted using QIAamp® genomic DNA kits (Qiagen, Germany). This technique based on solid phase extraction using the QIAamp silica-gel membrane. The procedure of DNA extraction was followed by manufacturer's instruction. In brief, 180 μl of lysis buffer and 20 μl of Proteinase K was added into 15 ml centrifuge tube containing cell pellet. The suspensions were mixed by vortexing and were moved into 1.5 ml microcentrifuge tube. Then, the mixture was incubated at 56℃ for 30 minutes to lyse cells. Next, 200 μl of binding buffer was added to the tube. The mixture was mixed by vortexing for 15 seconds and was incubated at 70℃ for 10 minutes. After incubation, 200 μl absolute ethanol (Merck, Germany) was added to the tube. The mixture was mixed by vortexing for 15 seconds and was moved into the QIAamp Mini spin column. Then, the column was centrifuged at 8000 rpm for 1 minute. The flow-through was discarded. Next, 500 μl of Buffer AW1 (washing buffer) was added to the column and the column was centrifuged at 8000 rpm for 1 minute. The flow-through was discarded. After first washing step, 500 μl of Buffer AW2 (washing buffer) was added to the column and the column was centrifuged at 14,000 rpm for 3 minutes. The flow-through was discarded. Next, the column was placed into a 1.5 ml microcentrifuge tube and 200 μl of elution buffer was directly added to the column matrix. The column was incubated at room temperature for 1 minute and was centrifuged for 1 minute at 8,000 rpm to elute the DNA. After elution, the extracted DNA was stored at -20℃.

3. Bisulfite conversion of HPV16 positive cervical samples

All HPV16 DNA positive samples, CaSki DNA and SiHa DNA were converted using the EZ DNA Methylation-Gold™ Kit (Zymo Research, USA). This technique involves treating methylated DNA with bisulfite, which converts unmethylated cytosines into

uracil. Methylated cytosines remain unchanged during the treatment. The procedure of bisulfite modification was followed by manufacturer's instruction. In brief, CT conversion reagent was prepared by adding 900 μl of water, 300 μl of dilution buffer, and 50 μl of dissolving buffer to a tube of CT conversion reagent (containing bisulfite) and mixed at room temperature with vortex for 10 minutes. Then, 130 μl of the CT Conversion Reagent and 20 μl of DNA were placed in PCR tube. Next, the sample tube was placed in a thermal cycler. The DNA was denatured by incubating at 98°C for 10 minutes. After denaturing, the DNA was incubated at 64°C for 2.5 hours to deaminate cytosine residues and was storage at 4°C. Then, a Zymo-Spin™ IC Column was placed into a Collection Tube and 600 μl of binding buffer was added into the column. Next, the incubated DNA was added into the Zymo-Spin™ IC Column containing the binding buffer. The column was inverted several times and was centrifuged for 30 seconds at 12,000 x g. After centrifugation, the flow-through was discarded and 100 μl of washing buffer was added to the column. Then, the column was centrifuged for 30 seconds at 12,000 x g. Next, 200 μl of desulphonation buffer was added to the column and was incubated at room temperature for 15 minutes to remove the bisulfite moiety and generate uracil. After incubating, the column was centrifuged for 30 seconds at 12,000 x g. Then, 200 μl of washing buffer was added to the column and the column was centrifuged for 30 seconds at 12,000 x g. The washing process was repeated. Next, the column was placed into a 1.5 ml microcentrifuge tube and 20 μl of elution buffer was directly added to the column matrix. The column was incubated at room temperature for 1 minute and was centrifuged for 30 seconds at 12,000 x g to elute the DNA. After elution, the DNA was stored at -20°C.

4. Methylation analysis by pyrosequencing

The sequences of the L1 forward and reverse primers for CpG positions 5600, 5606, 5609 and 5615 were as followed, FW biotin 5'-TAATATATAATTATTGTTGATGTAGGTGAT-3' and RV 5′-AACAATAACCTCACTAAACAACCAAAA-3′ (130 bps). Bisulfite modified HPV16 DNA positive

samples were used for PCR amplification, all PCR reactions were performed in a 50 μL volume using TaKaRa EpiTaq HS for bisulfite-treated DNA (Takara Bio, USA). The protocol is as follows: DNase/RNase-free water, 1× PCR buffer, 2.5 mM $MgCl_2$, 0.25 mM dNTP, 0.5 μM of each forward and reverse primers, 2 Units TaKaRa EpiTaq HS and 8 μL of DNA. The PCR conditions were initial denaturing at 95 °C for 10 minutes, followed by 40 cycles of 98 °C for 10 seconds, 53 °C for 30 seconds, and 72 °C for 30 seconds and a cycle of final extension at 72 °C for 5 minutes. CaSki and SiHa cells were used as positive control. The PCR products were detected by 1.5% agarose gel electrophoresis. PCR positive samples (130 bps) were used for L1 methylation analysis. The nucleotide sequence of methylated PCR product was shown in Figure 5.
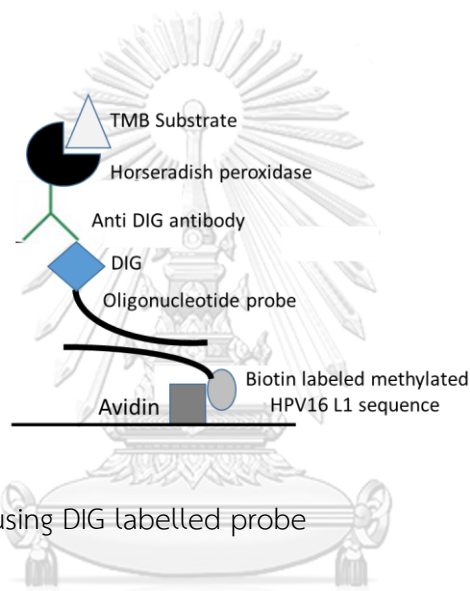
Next, pyrosequencing was performed using the PyroMark™ Q96 machine (Qiagen, Germany). Sequencing primer was 5600 5'-CCAAAAAAACATCTAAAAAAAAATATA ATA-3'. The procedure of pyrosequencing was followed by manufacturer's instruction. In brief, biotinylated DNA was immobilized on streptavidin coated Sepharose beads (GE Healthcare, USA). For each sample, the final immobilization volume was 80 μl. The protocol is as followed: 23 μL of Milli-Q 18.2 MΩ water, 40 μL of binding buffer, 2 μL of streptavidin sepharose beads and 15 μL of biotinylated DNA. The mixture was added to 96-well PCR plate. Then, the plate was mixed for at least 10 minutes at 1,400 rpm, room temperature. Next, 40 μl of 0.4 μM sequencing primer in annealing buffer was added to each well of the PyroMark Q96 Plate Low. Then, working station was prepared by adding approximately 120 ml of each reagent to each tray placing on PyroMark Q96 Vacuum Workstation. The reagents are as followed: Milli-Q 18.2 MΩ water, 70% ethanol, denaturation solution and 1X washing buffer. The beads containing immobilized DNA was captured using PyroMark Q96 Vacuum which have 96-filter probes. The vacuum was opened and placed into denaturation solution for 5 seconds and 70% ethanol for 5 seconds to denature the DNA. The vacuum was transferred to washing buffer and placed for 10 seconds to wash the DNA. After washing step, the vacuum was closed and was immediately placed into PyroMark Q96 Plate
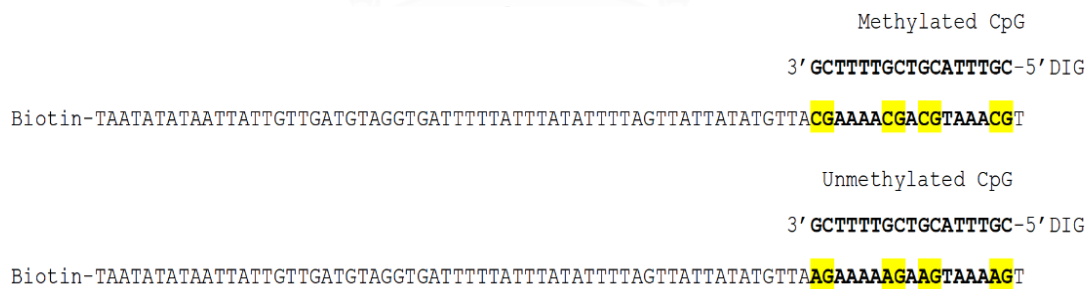
Low containing diluted primer. While holding the vacuum over the PyroMark Q96 Plate Low, the vacuum was gently shaken from side to side in the plate to remove the denatured DNA from the probe. Then, PyroMark Q96 Plate Low was incubated at 80℃ for exactly 2 minutes and was placed at room temperature to cool down. The reagents including enzyme, substrate, and dNTP (Thymine, Adenine, Guanine and Cytosine) were loaded separately in the reagent cartridge's compartment. The volume of each reagent is based on the number of samples. Finally, the PyroMark Q96 Plate Low and the cartridge were processed in the PyroMark Q96 ID.

```
  1 CAATATACAATTATTGCTGATGCAGGTGACTTTTATTTACATCCTAGTTATTACATGTTA

    :||||||:|||||||||:|||||:||||||:|||||||||:||::|||||||||:||||||

  1 TAATATATAATTATTGTTGATGTAGGTGATTTTTATTTATATTTTAGTTATTATATGTTA

Biotin-TAATATATAATTATTGTTGATGTAGGTGAT Forward

 61 CGAAAACGACGTAAACGTTTACCATATTTTTTTTCAGATGTCTCTTTGGCTGCCTAGTGAGGCCACTGTC

    ++||||++|++||||++||||::|||||||||||:||||||:|:|||||:||::|||||||||::|:|||:

 61 CGAAAACGACGTAAACGTTTATTATATTTTTTTTAGATGTTTTTTTGGTTGTTTAGTGAGGTTATTGTT

                                          AAAACCAACAAATCACTCCAATAACAA Reverse
```

Figure 5 Methylated PCR product 130 base pairs with forward and reverse primer used in this study

Part III Polymerase Chain Reaction-Enzyme-Linked-Immunosorbent Assay (PCR-ELISA) development

ELISA was developed based on the hybridization platforms using oligonucleotide probe specific to methylated CpGs 5600, 5606, 5609, 5615: 5'DIG-CGTTTACGTCGTTTTCG 3'. ELISA platforms are shown in Figure 6. Streptavidin was diluted with coating buffer. Then, 100 μl of diluted streptavidin was added to each well of ELISA plate. The plate was incubated at 37°C for 1 hour, after avidin incubation, the liquid was thoroughly aspirated and was tapped on thick paper towel. The plate was washed three times by adding 200 μl of washing buffer to the wells and shaking at 1,000 rpm for 5 minutes at room temperature. Then, 100 μl of blocking buffer (see Appendix B) was added to each well. The plate was incubated at 37°C for 1 hour. While incubating with blocking buffer, biotin labelled PCR product-DIG labelled probe hybrid was prepared in thermal cycler. The nucleotide sequence of methylated DNA and unmethylated DNA with DIG labelled probe was shown in Figure 7. Total volume was 100 μl per reaction, a volume (100 μl) of the DNA-probe hybrid was used to perform duplicate testing (50 μl/well). The protocol is as follows: mix DNA, DIG-labelled probe into hybridization buffer (see Appendix B), adjust Milli Q water to reach total volume of 100 μl. The hybridization conditions were initial denaturing at 95°C for 10 minutes, 60°C for 60 minutes. After incubation, the liquid was thoroughly aspirated and was tapped on thick paper towel. Next, A volume (50 μl) of Biotin labelled PCR product-DIG labelled probe hybrid was added into 50 μl of hybridization buffer in the wells. The plate was incubated at 37°C for 1 hour. After incubation, the liquid was thoroughly aspirated and was tapped on thick paper towel. Next, the plate was washed three times by adding 200 μl of post-hybridization washing buffer (see Appendix B) to the wells and shaking at 1,000 rpm for 5 minutes at room temperature. Meanwhile, horseradish peroxidase conjugated anti-Digoxigenin antibody was diluted with dilution buffer (see Appendix B). After washing step, 100 μl of diluted antibody was added to each well. The plate was incubated at 37°C for 1 hour. Then, the liquid was thoroughly

aspirated and was tapped on thick paper towel. Next, the plate was washed three times by adding 200 μl of washing buffer to the wells and shaking at 1,000 rpm for 5 minutes at room temperature. Then, 100 μl of 3′,5,5′-Tetramethylbenzidine substrate was added in to each well. The plate was incubated in the dark for 10 minutes for colour development. 100 μl of stop solution (see Appendix B) was then added into the wells. The absorbance was obtained from a spectrophotometer at 450 nm (Perkin Elmer, USA). Reagents used in PCR-ELISA optimization were listed in Table 3.

Figure 6 ELISA models using DIG labelled probe

```
                                          Methylated CpG
                             3'GCTTTTGCTGCATTTGC-5'DIG
Biotin-TAATATATAATTATTGTTGATGTAGGTGATTTTTATTTATATTTTAGTTATTATATGTTACGAAAACGACGTAAACGT

                                          Unmethylated CpG
                             3'GCTTTTGCTGCATTTGC-5'DIG
Biotin-TAATATATAATTATTGTTGATGTAGGTGATTTTTATTTATATTTTAGTTATTATATGTTAAGAAAAAGAAGTAAAAGT
```

Figure 7 The nucleotide sequence of methylated DNA and unmethylated DNA with DIG labelled probe

Table 3 List of reagents used in PCR-ELISA optimization

Reagents	Company
Phosphate-buffered saline 10X (PBS)	Apsalagen, Thailand
Tris Buffered saline 20X (TBS)	AMRESCO, USA
Saline Sodium Citrate Buffer 20X (SSC)	Invitrogen, USA
Sodium dodecyl sulfate (SDS)	Bio Basic, USA
Bovine Serum Albumin Fraction V	Bio Basic, USA
Formamide deionized	Life Sciences, USA
50X Denhardt's solution	Thermo Fisher Scientific, USA
ELISA Coating Buffer 1X	Abcam, UK
Native Streptavidin (5mg/ml)	Abcam, UK
Digoxigenin-labelled probe	Sigma Aldrich, USA
Mouse monoclonal antibody to Digoxigenin (HRP)	Abcam, UK
TMB ELISA substrate	Abcam, UK
Sulfuric acid 95-97%	Merck Millipore, Germany
MaxiSorp polystyrene 96 wells microplate	Nunc Thermo Scientific, USA

1. Standard preparation

    1.1 Plasmid

Plasmid used in this study named p1203 which is unmethylated HPV16 genome. The methylated plasmids were prepared using GpC Methylase kit (Zymo Research, USA). The procedure of GpC Methylase was followed by manufacturer's instruction. Reagents including 2 μl of 10X GpC Reaction Buffer, 1 μl of 20X SAM (S-adenosylmethionine) [12 mM], 6 μl of milli Q water, 10 μl of plasmid at 30 ng/μl and 1 μl of GpC Methylase (4 units/μl), were placed into 0.2 ml microcentrifuge tube. Then, the reaction tube was Incubated at 30 °C for 2 hours, followed by 65 °C for 20 minutes. Unmethylated plasmid was prepared by diluting the plasmid into the same

concentration as methylated plasmid. ELISA standard DNA was prepared by diluting methylated plasmids with unmethylated plasmid into the following ratio: 0:4, 1:3, 2:2, 3:1, 4:0 to obtain 0%, 25%, 50%, 75% and 100% methylation, respectively. Then, all mixed plasmids were used to perform bisulfite conversion, followed by PCR. All PCR reactions were performed in a 50 μL volume using TaKaRa EpiTaq HS for bisulfite-treated DNA (Takara Bio, USA). The protocol are as follows: DNase/RNase-free water, 1× PCR buffer, 2.5 mM MgCl$_2$, 0.25 mM dNTP, 0.5 μM of each forward and reverse primers, 2 Unit TaKaRa EpiTaq HS and 8 μL of DNA. The PCR conditions were initial denaturing at 95 °C for 10 minutes, followed by 40 cycles of 98 °C for 10 seconds, 53 °C for 30 seconds, and 72 °C for 30 seconds and a cycle of final extension at 72 °C for 5 minutes. All standard PRC products were used to perform pyrosequencing and PCR-ELISA.

        1.2 PCR product

ELISA standard was then prepared by diluting bisulfite modified CaSki PCR product with unmethylated plasmid PCR product (0% methylation) into the following ratio: 0:4, 1:3, 2:2, 3:1, 4:0 to obtain 0%, 25%, 50%, 75% and 100% methylation, respectively. The concentration of unmethylated plasmid PCR product was as same as CaSki PCR product. All standard PCR products were used to perform pyrosequencing to evaluate L1 methylation profile, followed by PCR-ELISA.

    2. Control DNA preparation

Bisulfite modified CaSki DNA was used as methylated control or positive control. CaSki was amplified using TaKaRa EpiTaq HS (Takara Bio, USA). PCR reagent control was prepared by using distilled water instead of CaSki DNA, in order to evaluate the cross-reaction causing by PCR reagents such as dNTP, and primer. All PCR reagent controls were pooled into one vial, as well as CaSki DNA. Both were measured for DNA concentration using nanodrop spectrophotometer (Eppendorf, Germany). CaSki DNA's concentration was 440 ng/μl, whereas PCR reagent control resulted in 59.9 ng/μl.

CaSki and reagent control were used to perform pyrosequencing to evaluate L1 methylation profile. Both were stored at -20°C.

3. PCR-ELISA Optimization

1. Washing buffer optimization

Two types of washing buffer for washing of enzyme conjugated antibody including TBST (Tris Buffered saline -Tween 20) and PBST (Phosphate Buffered saline - Tween 20) were prepared. TBST was prepared by diluting 20X TBS with Milli Q water into 1X TBS. Then, Tween 20 was added to obtain 0.05% Tween 20 in 1X TBS. PBST was prepared using the same protocol as TBST. TBST or PBST were used as washing buffer in post-coating step and post-antibody-capturing step. Bisulfite modified CaSki DNA was used as methylated control (440 ng/μl). The hybridization conditions were initial denaturing at 95°C for 10 minutes, 60°C for 60 minutes. Washing buffer was optimized. A streptavidin concentration, DNA concentration, DIG-labelled probe concentration and antibody dilution used for washing buffer optimization was listed in Table 4.

Table 4 Washing buffer optimization

Sample number	Washing buffer	Streptavidin (μg/well)	DNA (ng/well)	Probe (ng/well)	Antibody dilution
1	PBST	2.5	1,100	588	1:400
2		5	1,100	588	1:400
3		7.5	1,100	588	1:400
4		10	1,100	588	1:400
1	TBST	2.5	1,100	588	1:400
2		5	1,100	588	1:400
3		7.5	1,100	588	1:400
4		10	1,100	588	1:400

2. TBS and PBS based reagent optimization

    Reagents including blocking buffer and dilution buffer were prepared. Blocking buffer was composed of 3% BSA in 1X TBS or 1X PBS. Dilution buffer was composed of 0.05% tween20 and 0.5% BSA in 1X TBS or 1X PBS. Bisulfite modified CaSki DNA was used as methylated control (440 ng/μl). The hybridization conditions were initial denaturing at 95℃ for 10 minutes, 60℃ for 60 minutes. Reagents based PBS or TBS were optimized. A streptavidin concentration, DNA concentration, DIG-labelled probe concentration and antibody dilution used for the reagent optimization was listed in Table 5. Suitable reagents were chosen to use as buffer reagents in DNA optimization.

Table 5 TBS and PBS based reagent optimization

Sample number	Reagent	Streptavidin (μg/well)	DNA (ng/well)	Probe (ng/well)	Antibody dilution
1	PBS based	2.5	1,100	588	1:400
2		5	1,100	588	1:400
1	TBS based	2.5	1,100	588	1:400
2		5	1,100	588	1:400

3. DNA optimization

    Bisulfite modified CaSki DNA was used as methylated control (440 ng/μl). Reagent control was used to evaluate the cross-reaction causing by PCR reagents. Biotin labelled PCR product-DIG labelled probe hybrid was prepared. Total volume was 100 μl per reaction, A volume (100 μl) of DNA-probe hybrid was used to perform duplicate testing (50 μl/well). Different volume of DNA (2 μl, 4 μl, 5 μl, 6 μl, 8 μl) were placed in 0.2 ml microcentrifuge tube containing 20 μl of hybridization buffer and 4 μl of DIG-labelled probe. The hybridization conditions were initial denaturing at 95℃ for 10 minutes, 60℃ for 60 minutes. A streptavidin concentration, DIG-labelled probe concentration and antibody dilution used for DNA optimization was listed in

Table 6. Suitable concentration of DNA was chosen to use as fixed DNA concentration in DIG-labelled probe optimization. "W" letter in Table 7 indicates the fixed DNA concentration.

Table 6 DNA optimization

Sample number	Streptavidin (μg/well)	DNA (ng/well)	Probe (ng/well)	Antibody dilution
1	5	440	588	1:400
2	5	880	588	1:400
3	5	1,100	588	1:400
4	5	1,320	588	1:400
5	5	1,760	588	1:400

4. DIG-labelled probe optimization

DIG-labelled probe (Sigma Aldrich, USA) was optimized. Concentration of the probe was 294 ng/μl. Frist, DIG-labelled probe was diluted with DDW into four concentrations including 73.5, 147, 294, 588 nanogram per 20 μl of DDW using a two-fold serial dilution method. Then, biotin labelled PCR product-DIG labelled probe hybrid was prepared. Total volume was 100 μl per reaction. A volume (100 μl) of DNA-probe hybrid was used to perform duplicate testing (50 μl/well). A volume (40 μl) of different concentrations of probe was placed in 0.2 ml microcentrifuge tube containing 20 μl of hybridization buffer and CaSki DNA. The hybridization conditions were initial denaturing at 95℃ for 10 minutes, 60℃ for 60 minutes. Reagent control was used to evaluate the cross-reaction causing by PCR reagents. A streptavidin concentration, DNA concentration (represented by "W" letter) and antibody dilution used for DIG-labelled probe optimization was listed in Table 7. Suitable probe concentration was chosen to use as fixed probe concentration in antibody

optimization. "X" letter in Table 8 indicates the fixed DIG-labelled probe concentration.

Table 7. DIG-labelled probe optimization

Sample number	Streptavidin (μg/well)	DNA (ng/well)	Probe (ng/well)	Antibody dilution
1	5	W	73.5	1:400
2	5	W	147	1:400
3	5	W	294	1:400
4	5	W	588	1:400

5. Antibody optimization

Mouse monoclonal antibody to Digoxigenin conjugated HRP (Abcam, UK) was diluted with dilution buffer (see Appendix B) into 4 concentrations including 1:400, 1:800, 1:1600 and 1:3200 using a two-fold serial dilution method. Antibody dilution was optimized. Reagent control was used to evaluate the cross-reaction causing by PCR reagents. A streptavidin concentration, DNA concentration (represented by "W" letter) and DIG-labelled probe concentration (represented by "X" letter) used for antibody optimization was listed in Table 8. Suitable dilution of antibody was chosen to use as fixed dilution in streptavidin optimization. "Y" letter in Table 9 indicates the fixed dilution of antibody.

Table 8 Antibody optimization

Sample number	Streptavidin (μg/well)	DNA (ng/well)	Probe (ng/well)	Antibody dilution
1	5	W	X	1:400
2	5	W	X	1:800
3	5	W	X	1:1600
4	5	W	X	1:3200

6. Streptavidin optimization

Streptavidin (5 μg/μl) was diluted with coating buffer into 6 concentrations including 0.5, 1, 2, 2.5, 5, 7.5 μg per 100 μl coating buffers. First, 600 μl of coating buffer was added into six microcentrifuge tubes. Different volumes of streptavidin were added into each tube including 0.6 μl, 1.2 μl, 2.4 μl, 3 μl, 6 μl, 9 μl to obtain different concentration of 0.5, 1, 2, 2.5, 5, 7.5 μg per 100 μl coating buffers, respectively. Streptavidin concentration was optimized, DNA concentration (represented by "W" letter), DIG-labelled probe concentration (represented by "X" letter) and antibody dilution (represented by "Y" letter) used for streptavidin optimization was list in Table 9. Bisulfite modified CaSki DNA was used as methylated control, whereas, reagent control was used to evaluate the cross-reaction causing by PCR reagents. Suitable concentration of streptavidin was chosen to use as fixed streptavidin concentration in specificity test. "Z" letter in Table 11 indicates the fixed streptavidin concentration.

Table 9 Streptavidin optimization

Sample number	Streptavidin (μg/well)	DNA (ng/well)	Probe (ng/well)	Antibody dilution
1	0.5	W	X	Y
2	1	W	X	Y
3	2	W	X	Y
4	2.5	W	X	Y
5	5	W	X	Y
6	7.5	W	X	Y

7. Specificity of PCR-ELISA

Standard DNA controls with different methylation percentage including 0%, 25%, 50%, 75% and 100% (concentration 300 ng/μl) were used to set standard curves for determination of the methylation percentage in unmethylated plasmid PCR product. Absorbance (sample OD-blank OD) and pyrosequencing results of each standard DNAs were used to plot three types of standard curve including linear

regression with intercept, linear regression without intercept and logarithmic curve Table 10. R-squared which is a goodness-of-fit measure for linear regression models, achieved from linear line with intercept, linear line without intercept and logarithmic curve were calculated. Formula obtained from the curve that represented the highest R-squared were used to calculate percentage of methylation in samples.

To determine the specificity of the PCR-ELISA. A ten-fold serial dilution was performed. Unmethylated plasmid PCR product amplified from plasmid containing HPV16 genome were diluted into 1,000, 1000, 10, 1, 0.1 and 0.001 ng and used for specificity testing. All diluted samples were then used in hybridization step. DIG-labelled probe concentration (represented by "X" letter), antibody dilution (represented by "Y" letter) and streptavidin concentration (represented by "Z" letter) used for specificity testing was list in Table 11.

Table 10 The three formulas obtained from standard curves

Type of standard curve	Equation	Formula
Linear regression	y=ax+b	$x = \dfrac{y - b}{a}$
Linear regression without intercept	y=ax	$x = \dfrac{y}{a}$
Logarithmic curve	y = aln(x) + b	$x = e^{\frac{y-b}{a}}$

** y= absorbance (Sample OD-Blank OD), a = slope, b=y-intercept, x=percentage of methylation

Table 11 Specificity test

Sample number	0% methylation amplicons (ng)	Probe (ng/well)	Antibody dilution	Streptavidin (μg/well)
1	1,000	X	Y	Z
2	100	X	Y	Z
3	10	X	Y	Z
4	1	X	Y	Z
5	0.1	X	Y	Z
6	0.01	X	Y	Z

8. Adjusted PCR-ELISA to improve the specificity of the assay

The PCR-ELISA protocol was adjusted at step binding of biotin labelled PCR amplicons-Probe hybrid with streptavidin by changing the temperature from 37 °C to 60 °C. Moreover, the plate was shaking at 300 rpm while incubating.

9. Limit of detection

To determine the limit of detection. A ten-fold serial dilution was performed. PCR products amplified from CaSki DNA was diluted with Milli Q water into 1,000, 100, 10, 1, 0.1, 0.01, 0.001 ng. All diluted samples were then used in hybridization step. DIG-labelled probe concentration (represented by "X" letter), antibody dilution (represented by "Y" letter) and streptavidin concentration (represented by "Z" letter) used for limitation detection was list in Table 12. Standard DNA controls including 0%, 25%, 50%, 75% and 100% (concentration 300 ng/μl) were used to set standard curves according to absorbance and pyrosequencing results of standard control DNAs. The three formulas used to calculate percentage of methylation in CaSki DNA was shown in Table 10.

Table 12 Limit of detection

Sample number	CaSki (ng)	Probe (ng/well)	Antibody dilution	Streptavidin (μg/well)
1	1,000	X	Y	Z
2	100	X	Y	Z
3	10	X	Y	Z
4	1	X	Y	Z
5	0.1	X	Y	Z
6	0.01	X	Y	Z

10. Sensitivity of developed ELISA

To determine the sensitivity of the PCR-ELISA. Bisulfite modified CaSki PCR product was diluted with unmethylated plasmid PCR product (0% methylation) into percentage difference of methylation including 1.25%, 2.5%, 5%, 10%, 20%, 40%, 80% and 1.56%, 3.125%, 6.25%, 12.5%, 25%, 50%, 100% by using two-fold dilution method. The concentration of bisulfite modified CaSki PCR product was as same as unmethylated plasmid PCR product. All diluted samples were then used in hybridization step. DIG-labelled probe concentration (represented by "X" letter), antibody dilution (represented by "Y" letter) and streptavidin concentration (represented by "Z" letter) used for sensitivity test was list in Table 13. Standard DNA controls including 0%, 25%, 50%, 75% and 100% were used to set standard curves according to absorbance and pyrosequencing results of standard control DNAs. The three formulas used to calculate percentage of methylation in samples was shown in Table 10.

Table 13 Sensitivity test

Sample number	Percentage of methylation	Probe (ng/well)	Antibody dilution	Streptavidin (μg/well)
1	1.25	X	Y	Z
2	1.56	X	Y	Z
3	2.5	X	Y	Z
4	3.125	X	Y	Z
5	5	X	Y	Z
6	6.25	X	Y	Z
7	10	X	Y	Z
8	12.5	X	Y	Z
9	20	X	Y	Z
10	25	X	Y	Z
11	40	X	Y	Z
12	50	X	Y	Z
13	80	X	Y	Z
14	100	X	Y	Z

11. Methylation quantitation using PCR-ELISA

PCR-ELISA optimized condition was used to evaluate the percentage of methylation in PCR amplicons of HPV16 positive samples, which were already tested by pyrosequencing. Standard DNA controls including 0%, 25%, 50%, 75% and 100% were used to set the standard curve according to absorbance and pyrosequencing results of standard control DNAs. The three formulas used to calculate percentage of methylation in samples was shown in Table 10.

Part IV Statistical analysis

Statistical analysis was performed using the SPSS software package for Windows version 22.0 (SPSS Inc., Chicago, IL, USA). HPV genotyping concordance between Cobas® HPV Test and REBA® HPV Test was tested by Kappa. The Kappa statistics values range from 0 to 1 (<0.20=poor, 0.21-0.40=weak, 0.41-0.60=moderate, 0.61-0.80=good and 0.81-1.00=very good). 95% confidence intervals were calculated. Two-sided P values were calculated by McNemar's chi-square (p < 0.05).

Mean difference of HPV16 L1 gene methylation between CIN1 and CIN2/3 was analysed using Kruskal Wallis test. Receiver operating characteristic (ROC) curve was used to analyse sensitivity and specificity to differentiate between CIN1 and CIN2/3.

The reproducibility of PCR-ELISA optimization was evaluated by inter- and intra-variability. Duplicates of sample values within a single assay run for intra-variability were tested. The means absorbance (Sample O.D. - Blank O.D.) or the means ratio (Sample O.D./Blank O.D.) of duplicate samples were calculated. The means of absorbance or the means of ratio for three days was used for inter-variable calculation. Standard error of mean was shown in bar chart. Standard deviation and Coefficients of variation of intra-variability and inter-variability were calculated (%CV = S.D./mean X 100%). Mean difference of absorbance/ratio was analysed using Kruskal Wallis test.

HPV16 L1 gene methylation performed by PCR-ELISA and histology results were used for Receiver Operating Characteristic (ROC) curve analysis to evaluate sensitivity and specificity of PCR-ELISA. Moreover, Kappa analysis were used to analyse the correlation between pyrosequencing and PCR-ELISA. P-value less than 0.05 was considered statistically significant.

CHAPTER V

RESULTS

Part I. Comparison of HPV infection using the REBA® HPV Test and the Cobas® HPV Test

207 women, examined by colposcopy, cervical swabs and biopsy samples were collected for HPV genotyping and histological examination. 168 out of 207 samples had histological examinations revealing cervical intraepithelial neoplasia 1-3 (CIN1-3), which accounted for 81.15%, while 39 samples presented vaginal intraepithelial neoplasia (VAIN), chronic cervicitis, benign squamous epithelium, condyloma acuminate and squamous metaplasia. Most samples (131/207) presented CIN1 (63.28%), and some (37/207) were diagnosed as CIN2/3 (17.87%). The mean age of CIN1 was 40 and CIN2/3 were 42.21 years old. HPV detection and genotyping were performed using Roche Cobas 4800 HPV test and REBA HPV-ID. Cobas 4800 can detect HPV16, HPV18 and 12 other high-risk HPVs (HR-HPV types), while REBA HPV-ID can detect 18 HR-HPV types (including HPV16 and HPV18), 1 probable HR-HPV type and 13 low-risk HPVs (LR-HPV types).

In total, 207 samples were tested by Roche Cobas 4800 and REBA HPV-ID. The percentage of HR-HPV positive cases was 71.98% (149/207, Cobas) and 70.53% (146/207, REBA). The distributions of HR-HPV types tested by Cobas among each histological status were 93/131 (70.99%) for CIN1, 11/11 (100%) for CIN2, 22/26 (84.61%) for CIN3 and 23/39 (58.97%) for non-CIN. Similar results were observed in REBA among 146 HR-HPV, 92/131 (70.22%) was CIN1, 11/11 (100%) was CIN2, 21/26 (80.76%) was CIN3 and 22/39 (56.41%) was non-CIN. The percentage of HPV 16 infections per total cases was 33.81% (70/207, Cobas) and 30.91% (64/207, REBA). The distributions of HPV 16 infection among each histological status were 29.00% (38/131, Cobas) and 25.95% (34/131, REBA) for CIN1, 81.81% (9/11, Cobas) and 72.72% (8/11, REBA) for CIN2, 46.15% (12/26, Cobas) and 46.15% (12/26, REBA) for CIN3 and 28.20% (11/39, Cobas) and 25.64% (10/39, REBA) for non-CIN (Table 14). Within both HPV test

data, a similar result was observed in that the percentage of HPV type 16 infections was high in CIN2/3 when compared to CIN1 (Figure 8). Moreover, between the two HPV detection assays, there were no significant differences in the percentage of HR-HPV positive cases which accounted for CIN1 62.41% (93/149), CIN2/3 22.14% (33/149) for Cobas and CIN1 63.01% (92/146), CIN2/3 21.91% (32/146) for REBA (Figure 9). Moreover, 32 HPV16 positive samples detected by Roche Cobas 4800 represent 29 HPV16 positive, 1 other HR-HPV, 1 LR-HPV, 1 HPV negative when tested by REBA HPV-ID (Table 15). 30 HPV16 positive samples detected by REBA HPV-ID represent 24 HPV16 positive, 4 HPV16 and other HR-HPVs, 2 HPV negative when tested by Roche Cobas 4800 (Table 15). According to these results, some samples have different HPV typing results when tested by Roche Cobas 4800 and REBA HPV-ID.

จุฬาลงกรณ์มหาวิทยาลัย
CHULALONGKORN UNIVERSITY
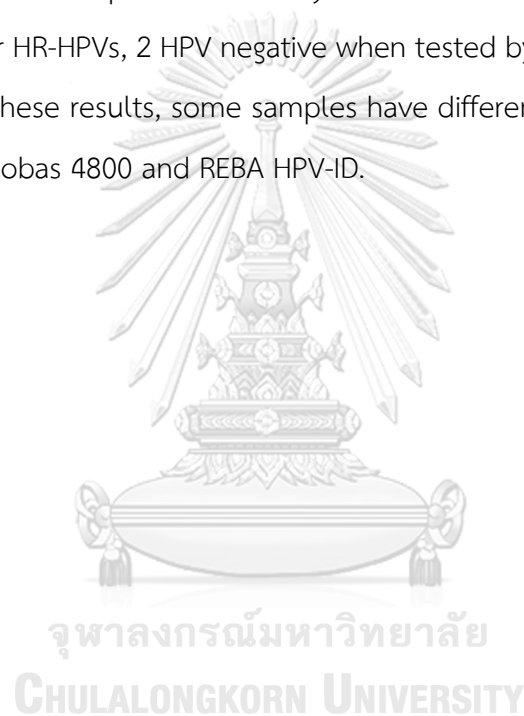
Table 14 Percentage of HR-HPV detected by Cobas4800 and REBA HPV-ID and histological classification

HPV results	Method	Histology				Total
		CIN1	CIN2	CIN3	Non-CIN	
Total number	Cobas4800/REBA HPV-ID	131	11	26	39	207
HPV negative	Cobas4800	38	0	4	16	58
	REBA HPV-ID	26	0	2	5	33
LR-HPV positive	Cobas4800	-	-	-	-	-
	REBA HPV-ID	13	0	3	12	28
HR-HPV positive	Cobas4800	93	11	22	23	149
	REBA HPV-ID	92	11	21	22	146
- HPV16+	Cobas4800	35	9	11	10	65
	REBA HPV-ID	33	8	12	9	62
- HPV18+	Cobas4800	3	0	1	1	5
	REBA HPV-ID	4	0	1	1	6
-Other HR-HPVs	Cobas4800	52	2	9	11	74
	REBA HPV-ID	54	3	8	11	76
- HPV16+ and HPV18+	Cobas4800	1	0	0	1	2
	REBA HPV-ID	1	0	0	1	2
- HPV16+, HPV18+ and Other HR-HPVs+	Cobas4800	2	0	1	0	3
	REBA HPV-ID	-	-	-	-	-
% HR-HPV (+) per all samples	Cobas4800	70.99 (93/131)	100 (11/11)	84.61 (22/26)	58.97 (23/39)	71.98 (149/207)
	REBA HPV-ID	70.22 (92/131)	100 (11/11)	80.76 (21/26)	56.41 (22/39)	70.53 (146/207)
Total HPV 16 positive	Cobas4800	38	9	12	11	70
	REBA HPV-ID	34	8	12	10	64
% HPV16+ per all samples	Cobas4800	29 (38/131)	81.81 (9/11)	46.15 (12/26)	28.2 (11/39)	33.81 (70/207)
	REBA HPV-ID	25.95 (34/131)	72.72 (8/11)	46.15 (12/26)	25.64 (10/39)	30.91 (64/207)
% HPV16+ per HR-HPV (+)	Cobas4800	40.86 (38/93)	81.81 (9/11)	54.54 (12/22)	47.82 (11/23)	46.97 (70/149)
	REBA HPV-ID	36.95 (34/92)	72.72 (8/11)	57.14 (12/21)	45.45 (10/22)	43.83 (64/146)
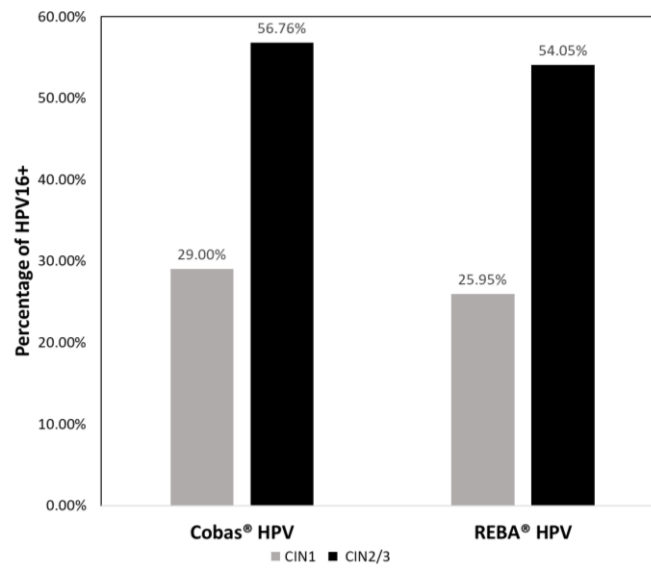
Figure 8 The distribution of HPV 16 infections per total cases among each histological status
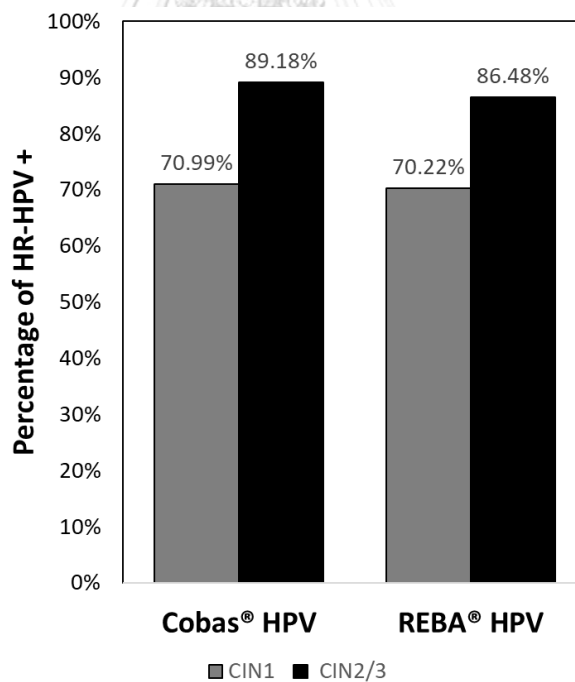
Figure 9 Percentage of HR-HPV positive cases among each histological status per total HR-HPV positive cases

Table 15 HPV typing results using Cobas4800 and REBA HPV-ID

		Cobas 4800								
		HPV 16	HPV 18	HPV 16 and HPV 18	HPV 16 and other hrHPVs	HPV 18 and other hrHPVs	HPV 16, HPV 18 and other hrHPVs	other hrHPVs	Negative	Total
REBA	HPV 16	24	0	0	4	0	0	0	2	30
	HPV 18	0	3	0	0	0	0	0	0	3
	HPV 16 and HPV 18	0	0	1	0	0	0	0	0	1
	HPV 16 and other hrHPVs	4	0	0	16	0	0	0	0	20
	HPV 18 and other hrHPVs	0	0	0	0	1	1	0	0	2
	HPV 16, HPV 18 and other hrHPVs	0	0	0	0	0	0	0	0	0
	other hrHPVs	1	0	0	3	0	0	44	3	51
	HPV 16 and lrHPVs	1	0	1	4	0	0	0	0	6
	HPV 18 and lrHPVs	0	1	0	0	0	0	0	0	1
	HPV 16, HPV 18 and lrHPVs	0	0	0	0	0	1	0	0	1
	HPV 16, other hrHPVs and lrHPVs	0	0	0	4	0	1	0	1	6
	other hrHPVs and lrHPVs	0	0	0	2	0	0	23	0	25
	LR-HPVs	1	0	0	0	0	0	5	22	28
	Negative	1	0	0	0	0	0	2	30	33
	Total	32	4	2	33	1	3	74	58	207

The results obtained from 207 samples were compared using the REBA® HPV Test and the Cobas® HPV Test to detect HPV positive samples (Table 16). The overall concordance rate was 85.02% (176/207), and the kappa value was 0.572 (95%CI, 0.400-0.701). Since the REBA® HPV Test and the Cobas® HPV Test both provide high-risk HPV detection, we also compared high-risk HPV positive rates between these tests as shown in Table 16. The concordance rate for high-risk HPV was 94.97% (170/179), and the kappa value was 0.838 (95% CI, 0.666-1.857). There were no significant differences for high-risk HPV detection between the REBA® HPV Test and the Cobas® HPV Test (McNemar's Test, P value = 0.508). However, HPV positive detection is significantly different between these two methods (McNemar's Test, P value = 0.0005). Moreover, we also compare high-risk HPV among each histology. The concordance rate for high-risk HPV detection in CIN2/3 was 100% (34/34), and the kappa value was 1.00 (Table 17).

Table 16 Comparison of HPV detection and high-risk HPV using the REBA® HPV Test and the Cobas® HPV Test					
		Cobas® HPV		Total	Kappa value (95% CI)	P-value
		HPV positive	HPV negative			
REBA® HPV	HPV+	146	28	174	0.572 (0.400 - 0.701)	0.0005
	Negative	3	30	33		
	Total	149	58	207		
		Cobas® HPV		Total	Kappa value (95% CI)	P-value
		High risk HPV	HPV negative			
REBA® HPV	High risk HPV	140	6	146	0.838 (0.666 - 1.857)	0.508
	Negative	3	30	33		
	Total	143	36	179		

** Kappa statistics values range from 0 to 1 (<0.20=poor, 0.21-0.40=weak, 0.41-0.60=moderate, 0.61-0.80=good and 0.81-1.00=very good)
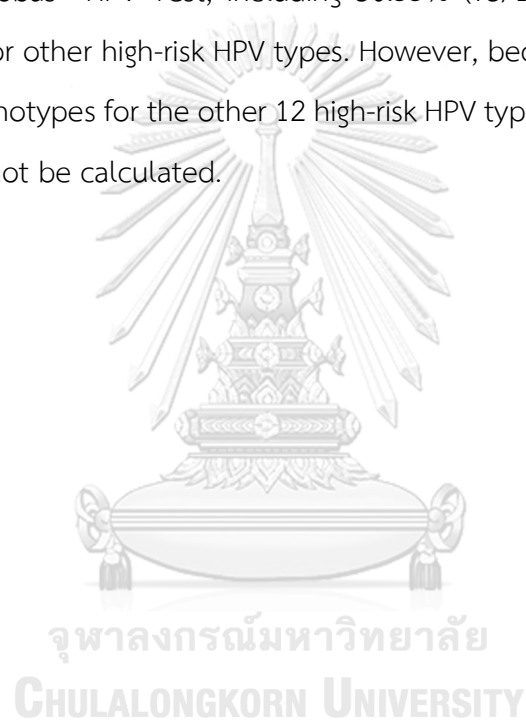
Table 17 Comparison of high-risk HPV detection among each histology using the REBA® HPV Test and the Cobas® HPV Test

Histology			Cobas		Total	Kappa value
			High risk HPV	HPV negative		
CIN1	REBA	High risk HPV	87	5	92	0.834
		HPV negative	2	24	26	
	Total		89	29	118	
CIN2/3	REBA	High risk HPV	32	0	32	1.000
		HPV negative	0	2	2	
	Total		32	2	34	
Other abnormality	REBA	High risk HPV	21	1	22	0.755
		HPV negative	1	4	5	
	Total		22	5	27	
Total	REBA	High risk HPV	140	6	146	0.838
		HPV negative	3	30	33	
	Total		143	36	179	

** Kappa statistics values range from 0 to 1 (<0.20=poor, 0.21-0.40=weak, 0.41-0.60=moderate, 0.61-0.80=good and 0.81-1.00=very good)

A visual comparison of the detection results and HPV types distribution obtained from the 207 samples using the REBA® HPV Test and the Cobas® HPV Test is shown in Figure 10. HPV16 infection was predominantly found to be either single infection or co-infection with other types by both assays, A total of 174 samples were identified as HPV positive by the REBA® HPV Test, including 40.22% (70/174) for HPV16/HPV18, 21.26% (37/174) for single HPV type and 24.13% (42/174) of multiple HPV type infections. By comparison, a total of 149 samples were identified as HPV positive by the Cobas® HPV Test, including 50.33% (75/149) for HPV16/HPV18 and 49.66% (74/149) for other high-risk HPV types. However, because the Cobas® HPV Test cannot identify genotypes for the other 12 high-risk HPV types, the number of multiple HPV types could not be calculated.

REBA® HPV

HPV Detection

HPV Genotyping

Cobas® HPV

HPV Detection

HPV Genotyping

Figure 10 Detection results for 207 samples using the REBA® HPV Test and the Cobas® HPV Test

Part II. Methylation levels of HPV16 5′L1 region of L1 gene
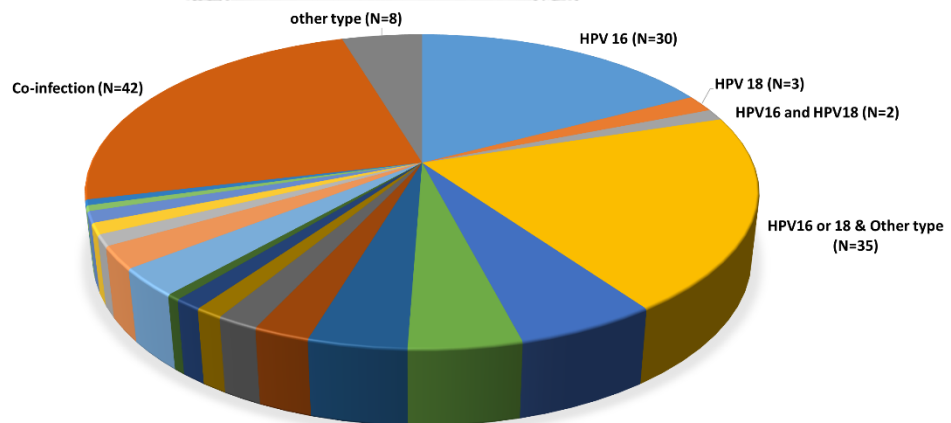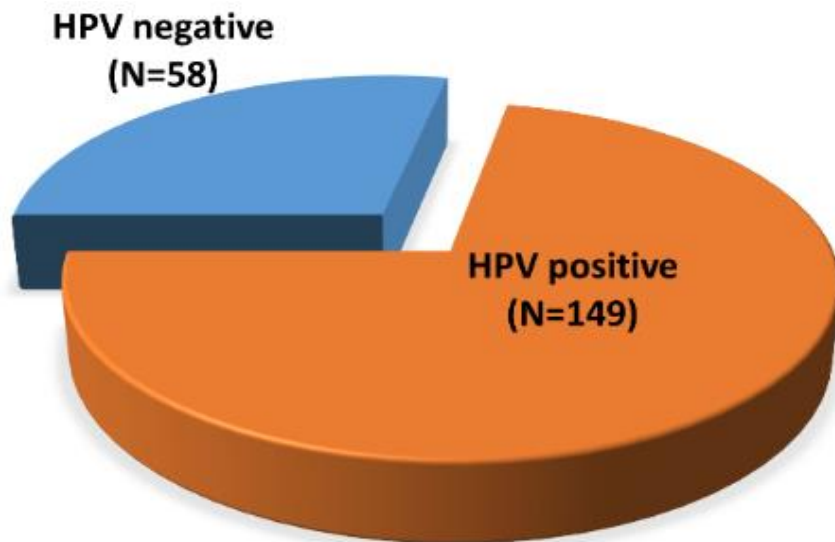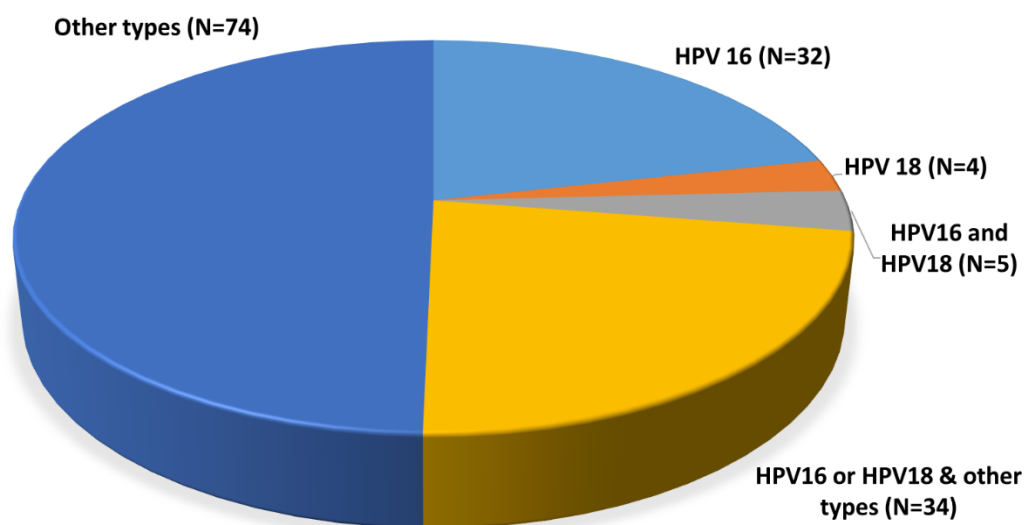
5′L1 region within HPV16 L1 gene including CpGs 5600, 5606, 5609, 5615 were selected for methylation analysis. CaSki and SiHa cancerous cell lines containing L1 gene hypermethylation were used as positive controls in pyrosequencing assay. All 70 HPV16 positive samples were used to perform bisulfite modification and polymerase chain reaction (PCR) using L1 primer, 26 samples showed L1 specific band. Therefore, methylation results were obtained from these 26 HPV16 samples. Among 26 samples, 14 samples were CIN1, 4 samples were CIN2, 6 samples were CIN3, 1 sample was benign squamous epithelium and 1 sample was VAIN3. Means of methylation of the HPV16 L1 gene was low in CIN1 (<10% of all CpGs), while high methylation was found in CIN2/3 especially at CpG 5600 (>20%) and 5609 (>20%). In addition, benign squamous epithelium was found to have high methylation (>20%) while VAIN3 has lower methylation. Means of methylation of the HPV16 5′ L1 at CpGs 5600, 5606, 5609, 5615 in samples with varying grades of cervical lesions were shown in Table 18.

Mean difference of HPV16 L1 gene methylation between CIN1 and CIN2/3 was analyzed using Kruskal Wallis test. Mean difference of HPV16 5′ L1 at CpGs 5600, 5606, 5609 and 5615 were significantly different between CIN1 and CIN2/3 with the *p*-value of 0.008, 0.029, 0.003 and 0.028, respectively (Figure 11). Receiver operating characteristic (ROC) curve of CpG 5600 and CpG 5609 also showed high value of area under curve (AUC) of 0.821 and 0.857, respectively (Figure 12). CpGs 5600 and 5609 showed high methylation in CIN2/3 samples, in which samples with >10% methylation in CIN1 and CIN2/3 at CpG5600 were 3/14 (21.43%) and 9/10 (90%), respectively. For CpG5609, there were 2/14 (14.29%) and 8/10 (80%) samples showed methylation level >10% in CIN1 and CIN2/3, respectively. When 9.5% methylation was used as cut off analyzed by ROC curve to differentiate between CIN2/3 and CIN1, the sensitivity of CpG5600 and 5609 was 90.0% and the specificity was 64.3% for both CpGs. When 19.50% methylation was used as cut off, the specificity and sensitivity of CpG5600 were

85.7% and 40%, respectively. When 19.00% methylation was used as cut off, the specificity and sensitivity of CpG5609 were 100% and 30%, respectively (Table 19). Methylation profile of low methylation sample, high methylation sample, CaSki and SiHa tested using pyrosequencing were shown in Figure 13. The nucleotide sequence of methylated DNA and unmethylated DNA with sequencing primer used in this study were shown in Figure 14.

Table 18 Means of methylation in 26 HPV16 positive samples and control cells (CaSki, SiHa) with varying grades of cervical lesions

Histology and cell lines	CpG positions in L1 gene			
	5600	5606	5609	5615
CIN1 (14 samples)	9.43%	4.29%	5.86%	3.57%
CIN2/3 (10 samples)	30.30%	18.20%	26.30%	17.40%
Benign squamous epithelium (1 sample)	48%	29%	38%	26%
VAIN3 (1 sample)	16%	10%	13%	7%
CaSki (Cervical cancer cell line)	89%	71%	90%	78%
SiHa (Cervical cancer cell line)	90%	91%	91%	87%
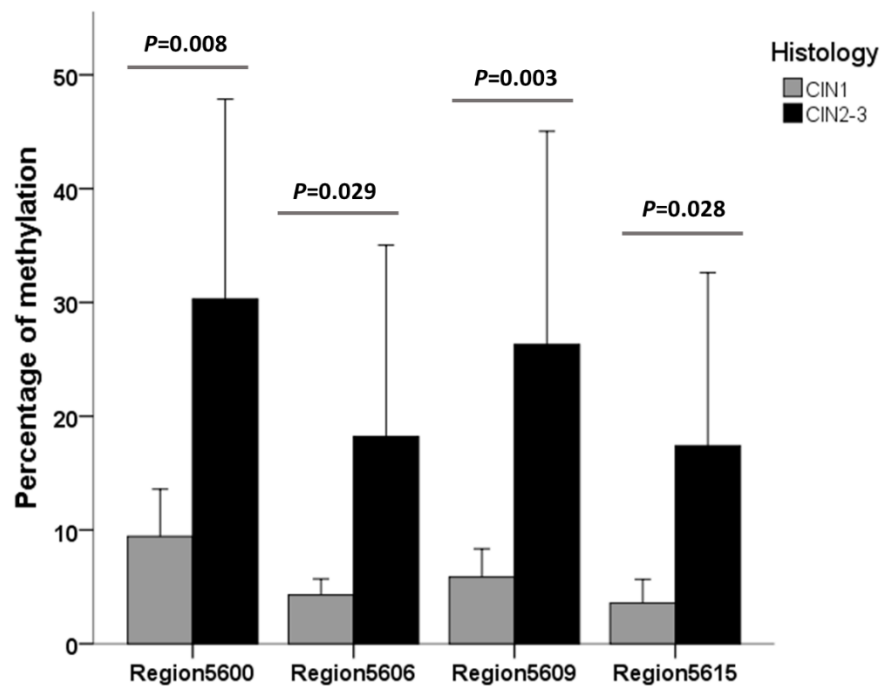
Figure 11 Methylation at CpGs 5600, 5606, 5609 and 5615 between CIN1 and CIN2/3 (mean percentage +/-2 SE). Significant difference between CIN1 and CIN2/3 at CpG5600 (p=0.008), 5606 (p=0.029), 5609 (p=0.003) and 5615 (p=0.028) was shown.
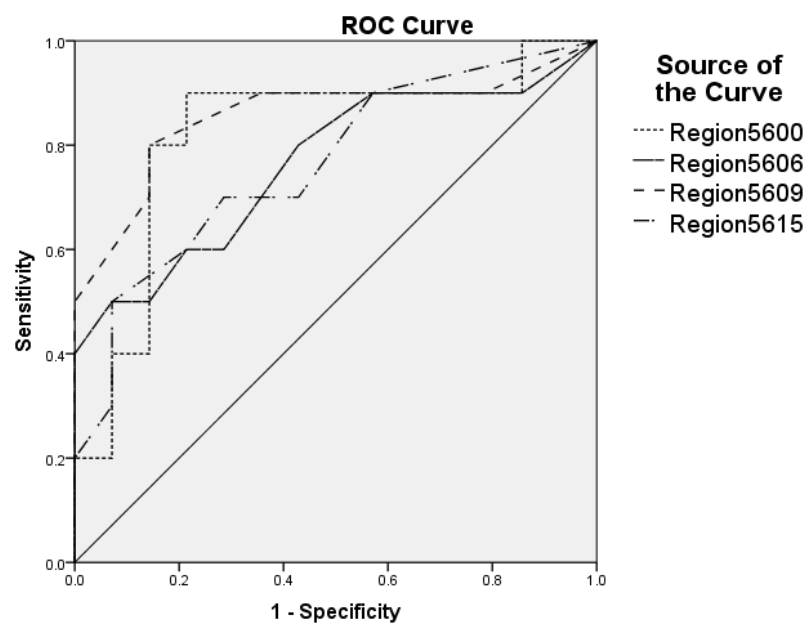
Figure 12 Receiver operating characteristic (ROC) curve for discrimination between CIN1 and CIN2/3. Area under curve (AUC) of CpGs 5600, 5606, 5609 and 5615 were 0.821, 0.764, 0.857, 0.764, respectively.

Table 19 Sensitivity and specificity of CpG5600 and 5609

CpG	Percentage of methylation	Sensitivity	1-Specificity	Sensitivity (%)	Specificity (%)
5600	1.50	1.000	0.857	100	14.3
	3.50	0.900	0.857	90	14.3
	8.50	0.900	0.429	90	57.1
	9.50	0.900	0.357	90	64.3
	11.00	0.900	0.214	90	78.6
	14.00	0.800	0.214	80	78.6
	16.50	0.800	0.143	80	85.7
	17.50	0.700	0.143	70	85.7
	18.50	0.500	0.143	50	85.7
	19.50	0.400	0.143	40	85.7
5609	1.50	0.900	0.786	90	21.4
	3.50	0.900	0.571	90	42.9
	7.00	0.900	0.429	90	57.1
	9.50	0.900	0.357	90	64.3
	11.50	0.700	0.143	70	85.7
	14.50	0.500	0.000	50	100
	17.00	0.400	0.000	40	100
	19.00	0.300	0.000	30	100
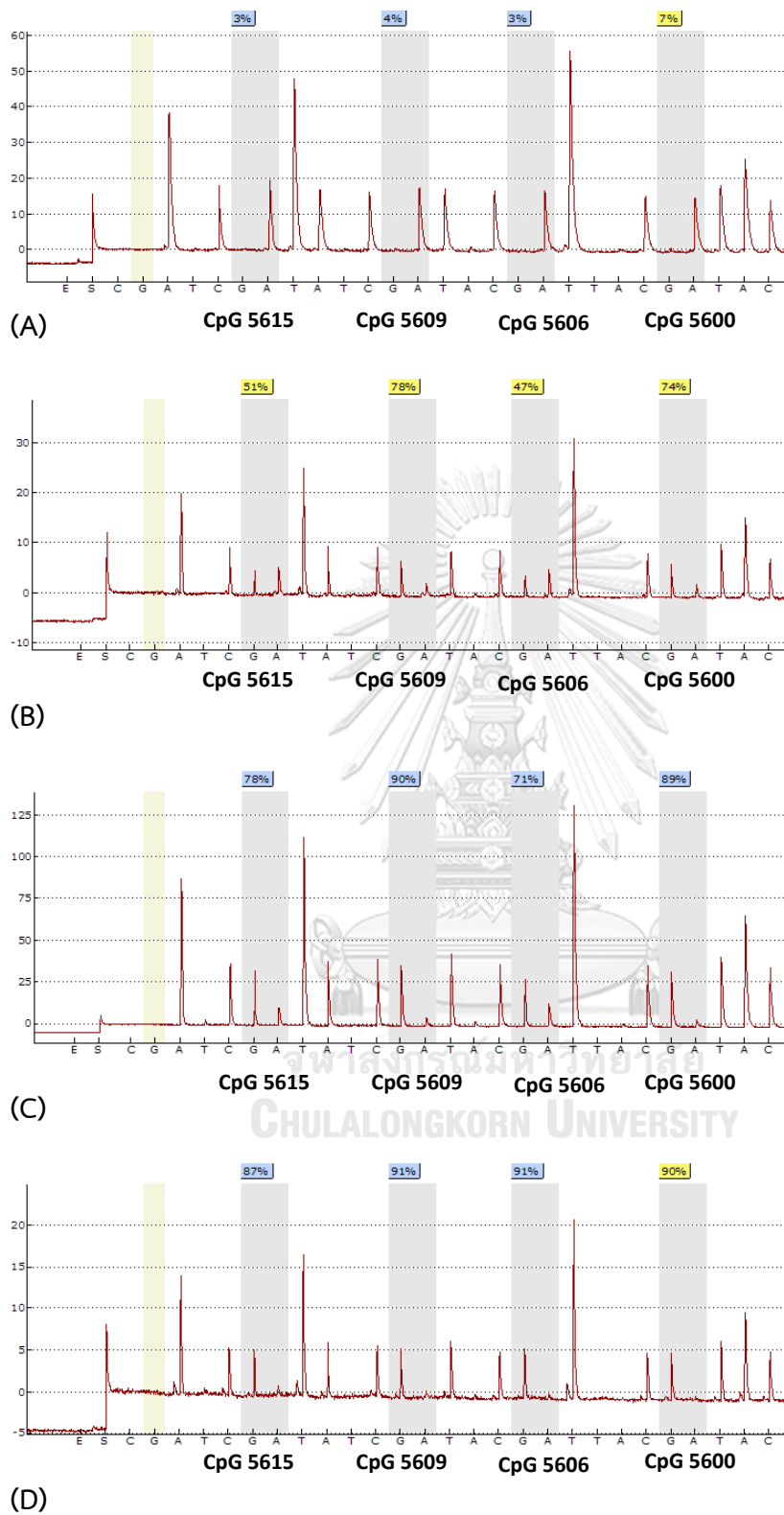
Figure 13 Methylation profile tested by pyrosequencing (A) Low methylation sample
(CIN 1). (B) High-methylation sample (CIN 2). (C) CaSki. (D) SiHa.

Sequencing primer for pyrosequencing

5'-CCAAAAAAACATCTAAAAAAAAATATA ATA-3'.

Methylated CpG
Sequencing primer
3'ATAATATAAAAAAAAATCTACAAAAAAACC-5'

Biotin-TAATAXXXXXXXXXXXXXAGTTATTATATGTTA**CGAAAACGACG**TAAA**CG**TTTATTATATTTTTTTTTAGATGTTTTTTTGG

5600 5606 5609 5615

Unmethylated CpG
Sequencing primer
3'ATAATATAAAAAAAAATCTACAAAAAAACC-5'

Biotin-TAATATAXXXXXXXXXXXXXXXAGTTATTATATGTTA**AGAAAAAGAAGTAAAAG**TTTATTATATTTTTTTTTAGATGTTTTTTTGG

5600 5606 5609 5615

Figure 14 The nucleotide sequence of methylated DNA and unmethylated DNA with sequencing primer

Part III. PCR-ELISA optimization

1. L1 methylation profile of standard DNA, CaSki and reagent control using pyrosequencing

ELISA standard DNAs were prepared by diluting either plasmid p1203 or bisulfite modified CaSki PCR product with unmethylated plasmid PCR product (0% methylation) into 0%, 25%, 50%, 75% and 100% methylation, then all standard controls were used to evaluate methylation percentage by pyrosequencing as shown in Table 20.

According to pyrosequencing results of these two standard curve preparation methods, the result of standard DNA prepared by mixing CaSki with unmethylated PCR product was better than the result obtained by diluting plasmid. Thus, standard DNAs prepared by mixing CaSki PCR product with unmethylated PCR product were used as standard control in PCR-ELISA method.

In PCR-ELISA optimization, CaSki DNA was used as methylated control or positive control, whereas, PCR master mix reagents without amplified products was used as reagent control to evaluate the cross-reaction caused by PCR reagents. All reagent controls were pooled into one vial, as well as methylated control. Both were used to perform pyrosequencing to evaluate L1 methylation profile as shown in Table 20. Methylation profiles of standard controls , pooled methylated control and pooled

reagent control used in this study were shown in Figure 15. The standard curve was plotted using the exact percentage of methylation obtained from pyrosequencing and the absorbance obtained from PCR-ELISA.

Table 20 L1 methylation profile of standard DNA and PCR reagent control using pyrosequencing

Standard curve preparation methods	Sample	CpG positions in L1 gene				
		5600	5606	5609	5615	Mean
Diluting plasmid p1203	0% standard control (Unmethylated plasmid)	10%	16%	7%	8%	10%
	25% standard control	23%	25%	22%	19%	22%
	50% standard control	40%	37%	38%	34%	37%
	75% standard control	61%	50%	58%	52%	55%
	100% standard control (methylated plasmid)	86%	68%	84%	73%	78%
Mixing bisulfite modified CaSki PCR product with unmethylated plasmid PCR product (0% methylation)	0% standard control (Unmethylated plasmid PCR product)	9%	14%	7%	7%	9%
	25% standard control	27%	27%	22%	21%	24%
	50% standard control	54%	47%	51%	44%	49%
	75% standard control	66%	54%	64%	57%	60%
	100% standard control (pooled CaSki control)	87%	69%	84%	75%	79%
	Pooled PCR reagent control	10%	16%	7%	8%	10.25%

(A1)

(A2)

(A3)

(A4)
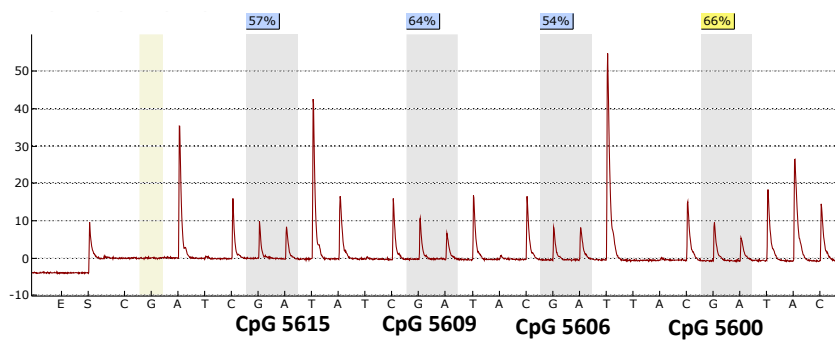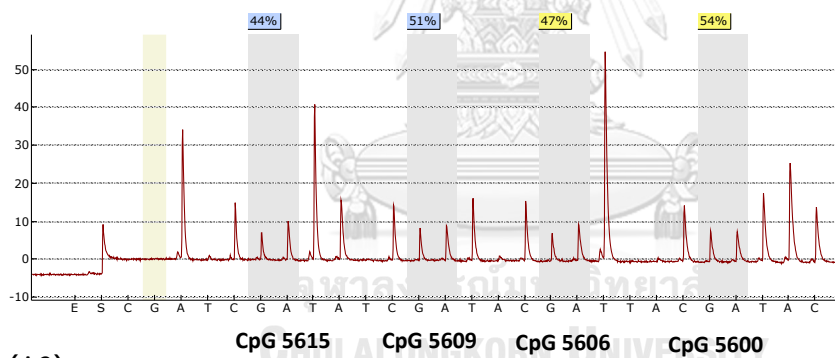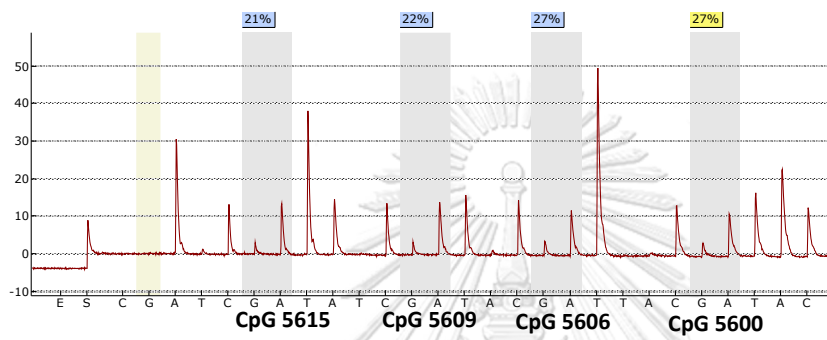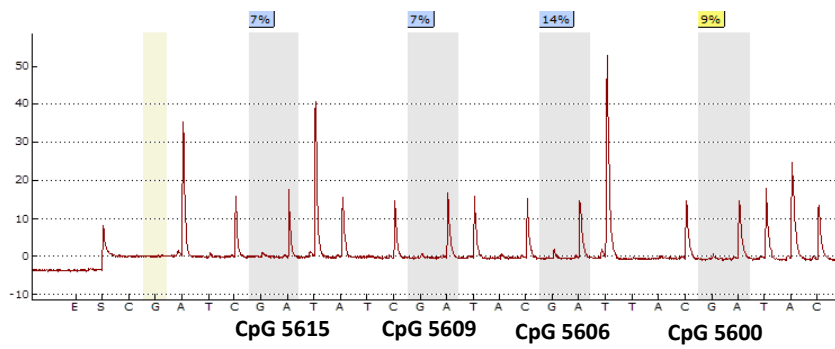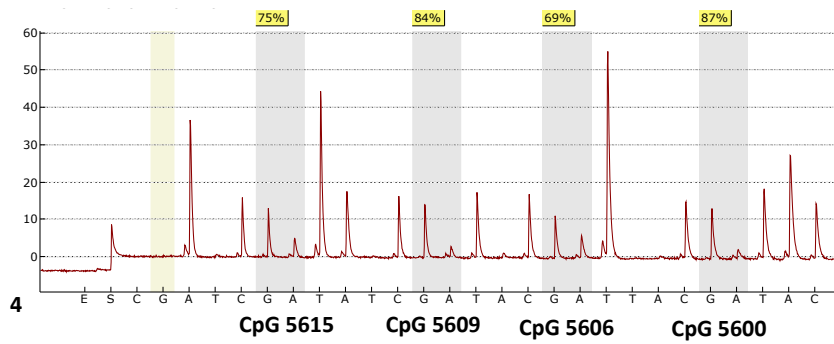
(A5)
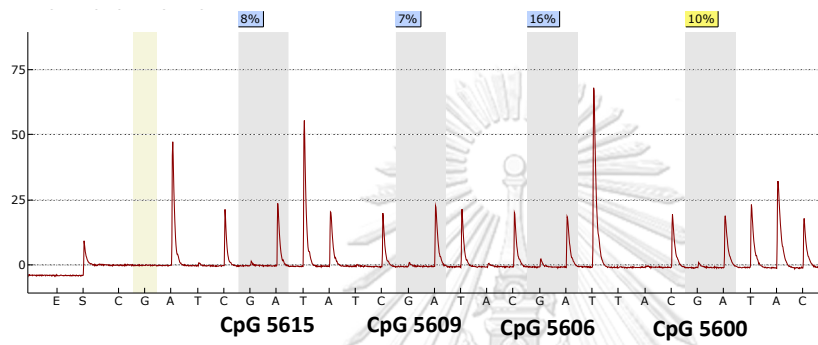
(B)

Figure 15 Methylation profile tested by pyrosequencing (A1-A5) Standard control 0%, 25%, 50%, 75%, 100%, respectively. (B) PCR reagent control.

2.   Washing buffer optimization

TBST or PBST were used as washing buffer in post-coating step and post-antibody-capturing step. Bisulfite modified CaSki DNA was used as methylated control (440 ng/μl). The mean absorbance (Sample O.D.-Blank O.D.) and the mean ratio (Sample O.D./Blank O.D.) of duplicate samples within single run were calculated. Although absorbance obtained from PBST was higher than TBST (Figure 16A). However, absorbance obtained from TBST are not significantly different when compare with PBST (p=0.208). Nevertheless, ratio obtained from TBST represented significantly higher than ratio obtained from PBST (p=0.001) due to high background of blank control when using PBST (Figure 16B). Thus, only ratio was used to determine the suitable washing buffer. In conclusion, TBST was chosen based on ratio.
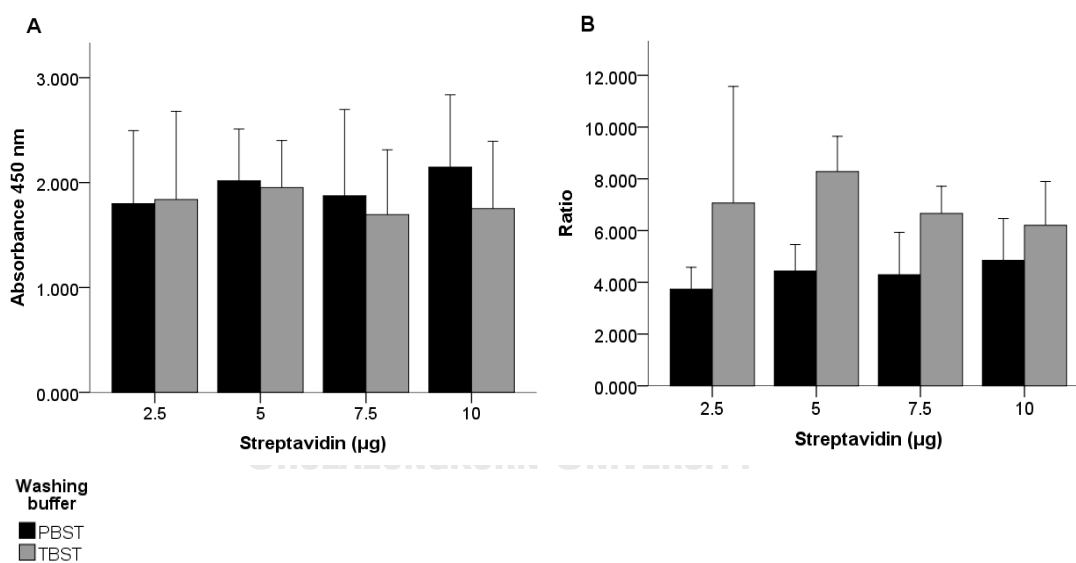
Figure 16 Washing buffer optimization represented by absorbance 450 nm (A) Ratio (B). Mean±2SE are shown.

3. TBS and PBS based reagent optimization

Reagents including blocking buffer and dilution buffer were prepared based on TBS or PBS. The mean absorbance (Sample O.D.-Blank O.D.) and the mean ratio (Sample O.D./Blank O.D.) of duplicate samples within single run were calculated. Absorbance obtained from PCR-ELISA using PBS based reagents were higher than TBS based reagent (P=0.021). In term of ratio, the same result was found (P=0.021) (Figure 17). Thus, PBS based reagents were chosen.
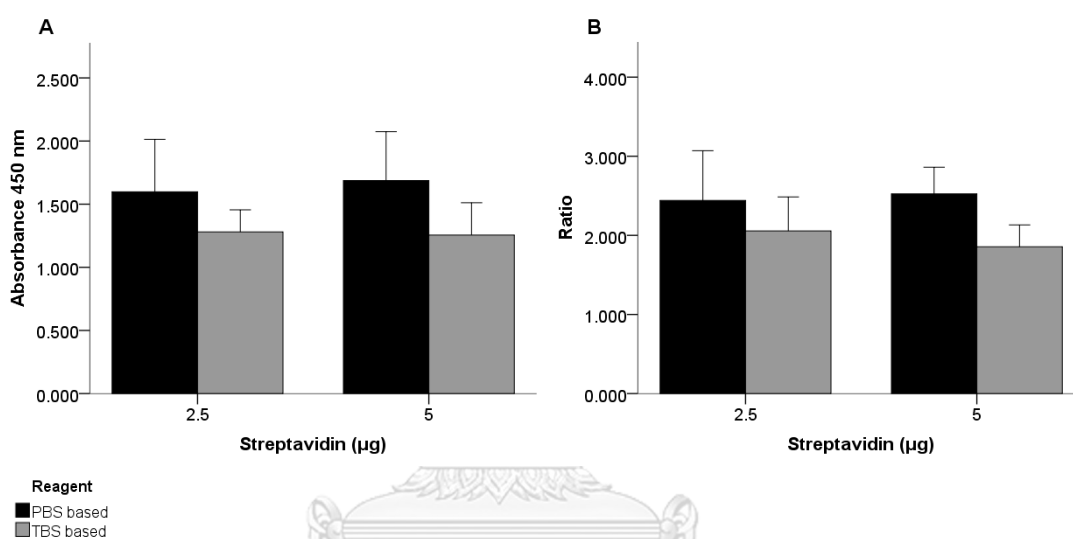
Figure 17 TBS and PBS based reagent optimization represented by absorbance 450 nm (A) Ratio (B). Mean±2SE are shown.
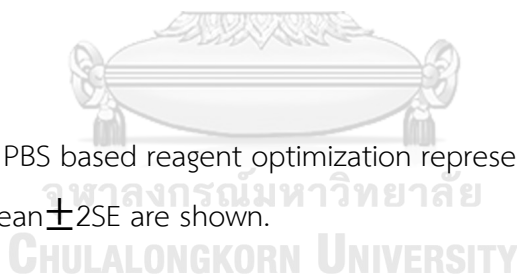
4.   DNA optimization

         To optimize the DNA concentration in PCR-ELISA, different concentration of
DNA including 440 ng, 880 ng, 1100 ng, 1320 ng, 1760 ng were tested. The concentration
of bisulfite modified CaSki DNA was 440 ng/μl. The mean absorbance of CaSki was not
significantly different across the DNA concentration for both Intra (Figure 18. A1-A3) and
inter (Figure 18. A4) variability. The mean ratio represents the same results.
Additionally, mean absorbance and mean ratio of reagent control was the same across
all DNA concentration. However, CaSki DNA concentration 440 ng represented the
highest absorbance at 450 nm for both Intra (Figure 18. A1-A3) and inter (Figure 18. A4)
variability of DNA optimization. In term of ratio, the same results were observed for
both Intra (Figure 19. B1-B3) and inter (Figure 19. B4) variability. Non-specific reaction
was not found when testing with reagent control. Intra-variability coefficient of
variations of absorbance and ratio was 0-9% (Table 21) and 1-15% (Table 22),
respectively, Whereas, Inter-variability resulted in 24-53% (Table 21)and 9-37% (Table
22). Interestingly, CaSki DNA concentration 440 ng represent the lowest inter-variability
for both absorbance and ratio, which accounting for 24% and 9%, respectively.
However, coefficient of variations more than 20% is not acceptable in this study. Thus,
only ratio was used to determine the suitable DNA concentration. In summary, CaSki
DNA concentration 440 ng was chosen based on ratio.
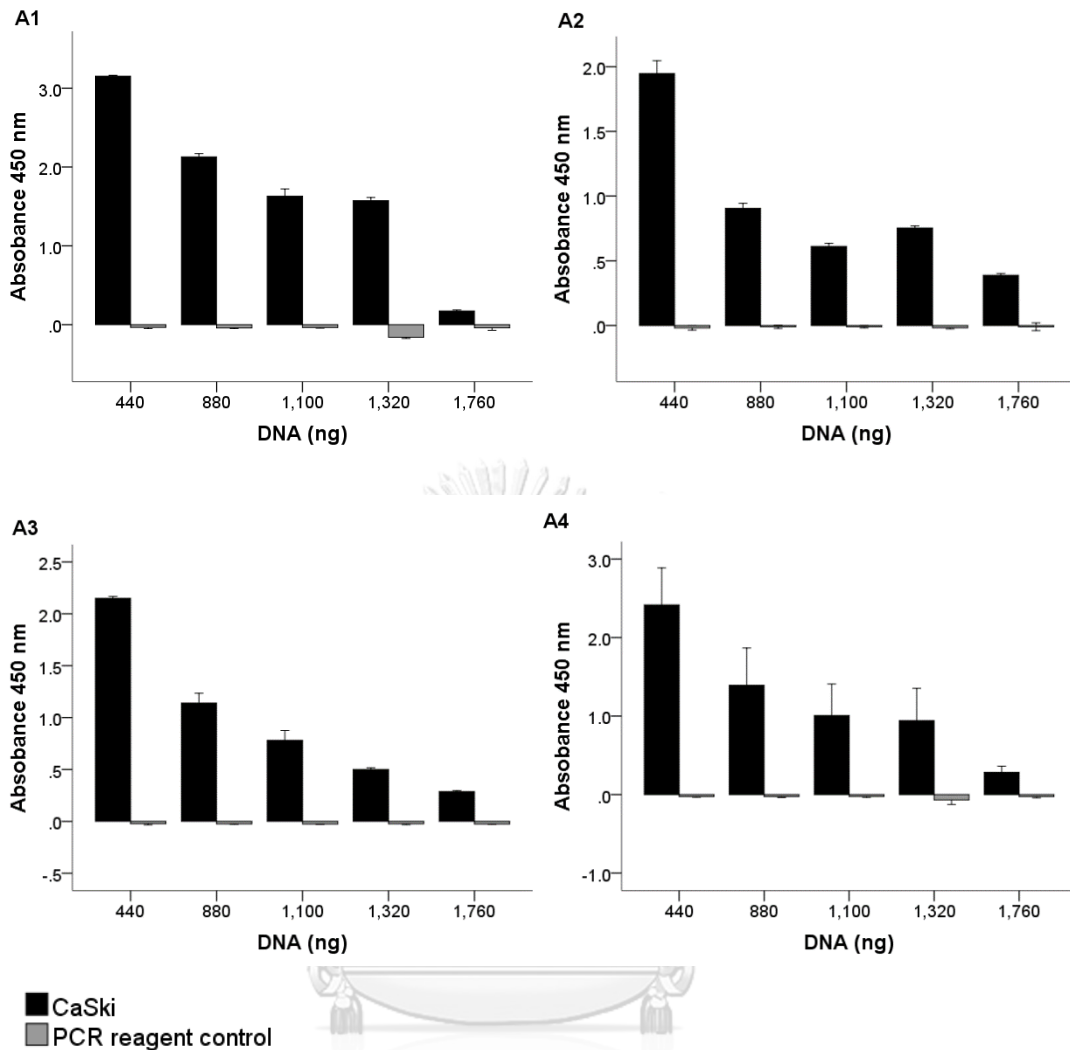
Figure 18 Intra and inter variability of DNA optimization represented by absorbance 450 nm. (A1-A3) Intra-variability obtained duplicate testing on day 1, day 2 and day 3, respectively. (A4) inter-variability tested using data of day 1 to day 3; mean±2SE are shown. The mean absorbance of CaSki was the same across the DNA concentration on day 1 (p=0.078, A1), day 2 (p=0.068, A2) and day 3 (p=0.068, A3); except for mean absorbance of day 1-3 (p=0.0005, A4). The mean absorbance of reagent control was the same across the DNA concentration on day 1 (p=0.321, A1), day 2 (p=0.835, A2), day 3 (p=0.976, A3) and day 1-3 (p=0.969, A4).
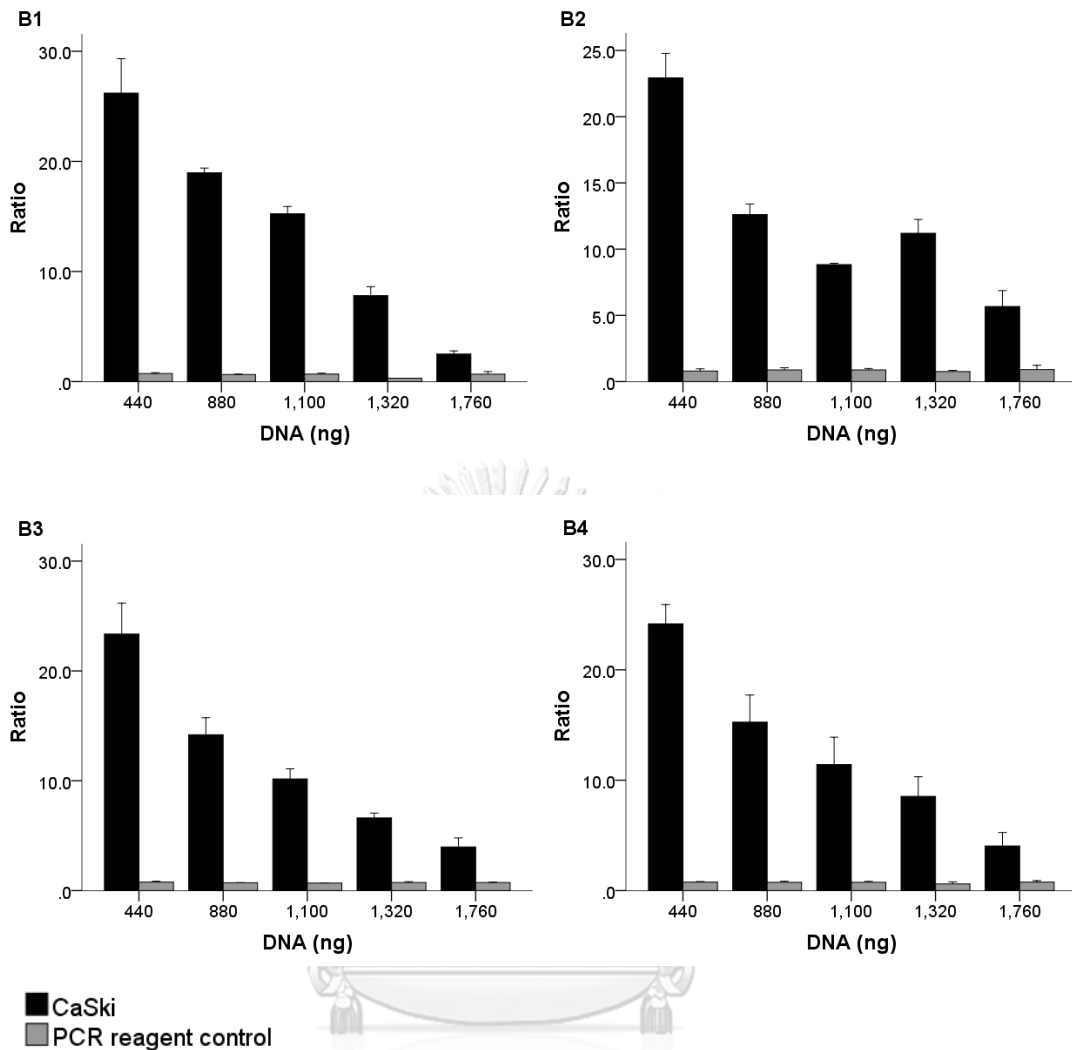
Figure 19 Intra and inter variability of DNA optimization represented by ratio. (B1-B3) Intra-variability obtained duplicate testing on day 1, day 2 and day 3, respectively. (B4) inter-variability tested using data of day 1 to day 3; mean±2SE are shown. The mean ratio of CaSki was the same across the DNA concentration on day 1 (p=0.068, B1), day 2 (p=0.068, B2) and day 3 (p=0.068, B3); except for mean ratio of day1-3 (p=0.0005, B4). The mean ratio of reagent control was the same across the DNA concentration on day 1 (p=0.254, B1), day 2 (p=0.643, B2), day 3 (p=0.183, B3) and day1-3 (p=0.622, B4).

Table 21 Inter and intra variability of DNA optimization represented by absorbance 450 nm

Sample number	Strepta vidin (μg)	DNA (ng)	Probe (ng)	Antibody dilution	Mean O.D. (SD, %CV)			
					Intra-variability			Inter-variability
					Day 1	Day 2	Day 3	
1	5	440	588	1:400	3.15 (0.01, 0)	1.95 (0.07, 4)	2.15 (0.01, 0)	2.42 (0.58, 24)
2	5	880	588	1:400	2.13 (0.03, 1)	0.91 (0.03, 3)	1.14 (0.07, 6)	1.39 (0.58, 42)
3	5	1,100	588	1:400	1.63 (0.06, 4)	0.61 (0.02, 3)	0.78 (0.07, 9)	1.01 (0.49, 49)
4	5	1,320	588	1:400	1.57 (0.03, 2)	0.75 (0.01, 1)	0.5 (0.01, 2)	0.94 (0.5, 53)
5	5	1,760	588	1:400	0.17 (0.01, 6)	0.39 (0.01, 3)	0.29 (0.01, 3)	0.28 (0.1, 36)

Concentration of CaSki DNA: 440 ng/μl, concentration of probe: 294 ng/μl.

Table 22 Inter and intra variability of DNA optimization represented by ratio

Sample number	Strepta vidin (μg)	DNA (ng)	Probe (ng)	Antibody dilution	Mean Ratio (SD, %CV)			
					Intra-variability			Inter-variability
					Day 1	Day 2	Day 3	
1	5	440	588	1:400	26.21 (2.2, 8)	22.93 (1.3, 6)	23.36 (1.99, 9)	24.17 (2.15, 9)
2	5	880	588	1:400	18.97 (0.3, 2)	12.61 (0.56, 4)	14.19 (1.1, 8)	15.26 (3.02, 20)
3	5	1,100	588	1:400	15.24 (0.47, 3)	8.84 (0.07, 1)	10.17 (0.65, 6)	11.42 (3.04, 27)
4	5	1,320	588	1:400	7.81 (0.58, 7)	11.2 (0.74, 7)	6.62 (0.31, 5)	8.54 (2.17, 25)
5	5	1,760	588	1:400	2.5 (0.2, 8)	5.67 (0.85, 15)	3.97 (0.59, 15)	4.05 (1.49, 37)

Concentration of CaSki DNA: 440 ng/μl, concentration of probe: 294 ng/μl.

5. DIG-labelled probe optimization

   To optimize the concentration of DIG-labelled probe in PCR-ELISA, different concentration of DIG-labelled probe including 73.5 ng, 147 ng, 294 ng, 588 ng were tested. The concentration of DIG-labelled probe was 294 ng/μl. Concentration of streptavidin, DNA concentration and antibody dilution used for DIG-labeled probe optimization were 5 μg/well, 440 ng/well and 1:400, respectively. Reagent control, the PCR master mix reagents without amplified products, was used to evaluate the cross-reaction caused by PCR reagents. The mean absorbance of CaSki was not significantly different across the probe concentration for both Intra (Figure 20. A1-A3) and inter (Figure 20. A4) variability. The mean ratio represents the same results; except for mean ratio of inter- variability (p=0.039) (Figure 21. B4), the probe concentration 294 ng represent the highest ratio when compared to other concentration. Additionally, mean absorbance and mean ratio of reagent control was the same across all probe concentration. Non-specific reaction was not found when testing with reagent control. Moreover, standard deviation and coefficients of variation of intra- and inter-variability were calculated. Intra-variability coefficient of variations of absorbance and ratio was 1-8% (Table 23) and 1-23% (Table 24), respectively. Whereas, Inter-variability coefficient of variations of absorbance and ratio was 18-35% (Table 23) and 10-28% (Table 24), respectively. Inter-variability %CV of ratio in 147 ng and 294 ng probe concentration were 10 and 16, respectively that lower than 20. However, probe concentration 294 ng represent the highest ratio. Thus, DIG-labeled probe 294 ng was chosen for further experiment.
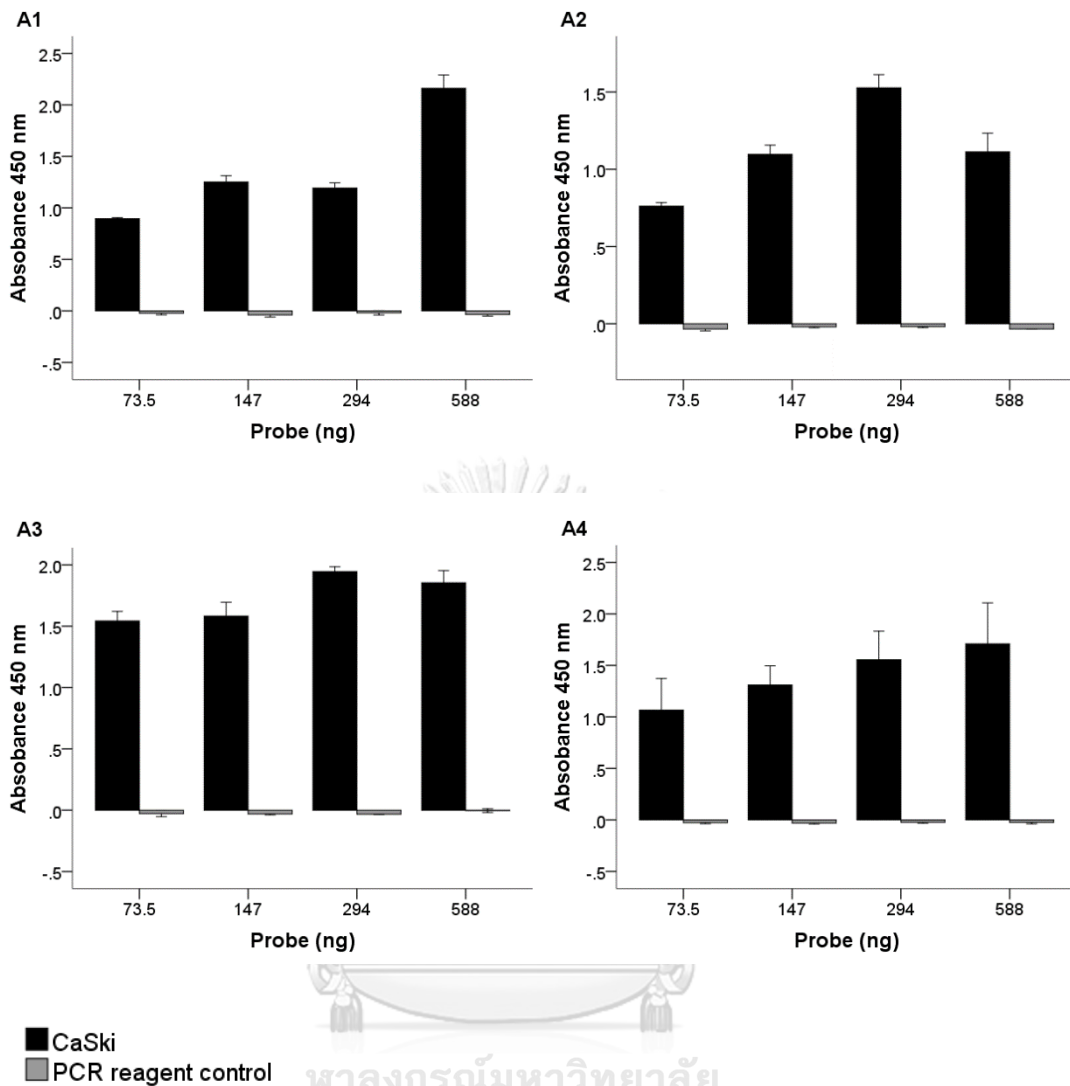
Figure 20 Intra and inter variability of DIG-labelled probe optimization represented by absorbance 450 nm. (A1-A3) Intra-variability obtained duplicate testing on day 1, day 2 and day 3, respectively. (A4) inter-variability tested using data of day 1 to day 3; mean$\pm$2SE are shown. The mean absorbance of CaSki was the same across the probe concentration on day 1 (p=0.083, A1), day 2 (p=0.112, A2), day 3 (p=0.104, A3) and day 1-3 (p=0.078, A4). The mean absorbance of reagent control was the same across the probe concentration on day 1 (p=0.525, A1), day 2 (p=0.139, A2), day 3 (p=0.261, A3) and day1-3 (p=0.832, A4).
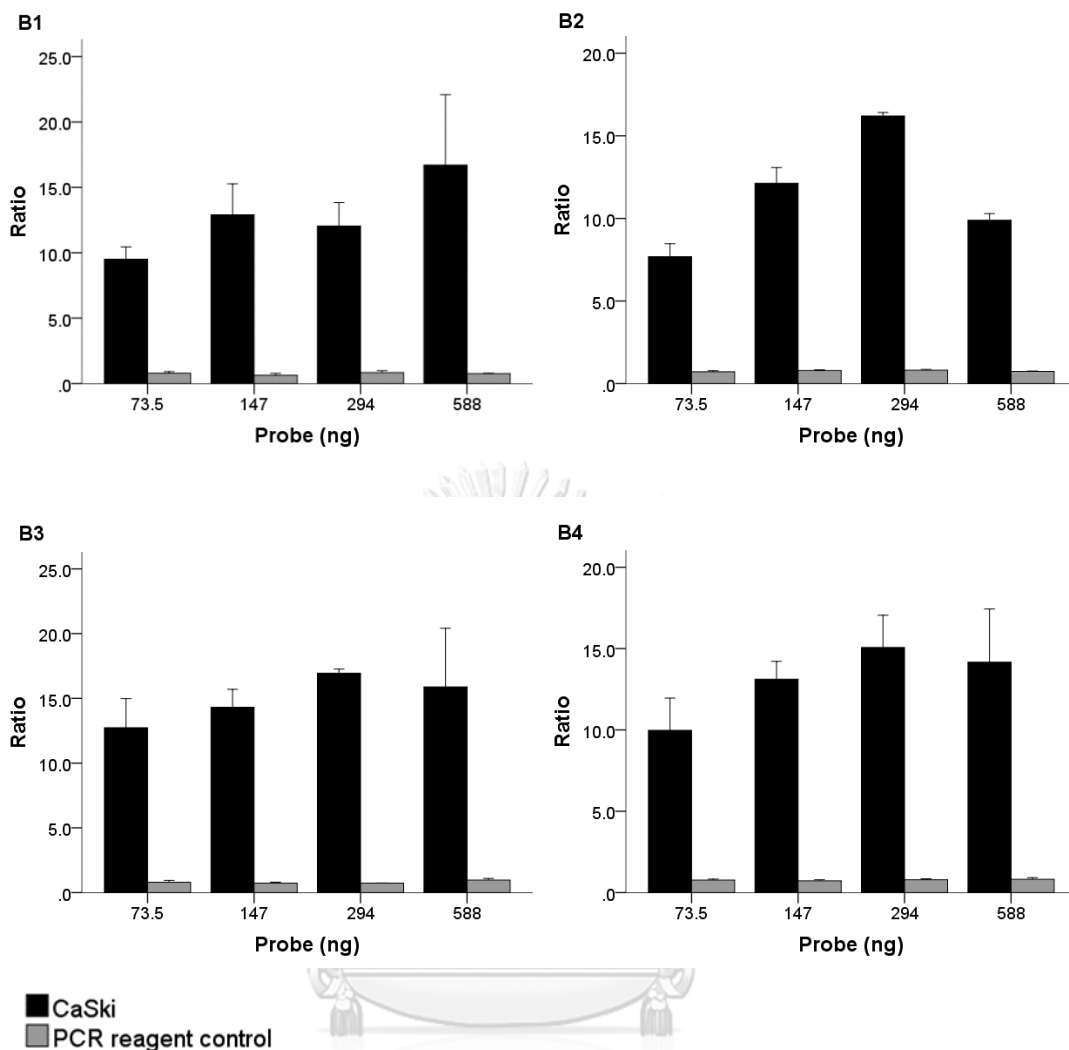
Figure 21 Intra and inter variability of DIG-labelled probe optimization represented by ratio. (B1-B3) Intra-variability obtained duplicate testing on day 1, day 2 and day 3, respectively. (B4) inter-variability tested using data of day 1 to day 3; mean$\pm$2SE are shown. The mean ratio of CaSki was the same across the probe concentration on day 1 (p=0.139, B1), day 2 (p=0.083, B2) and day 3 (p=0.343, B3); except for mean ratio of day1-3 (p=0.039, B4). The mean ratio of reagent control was the same across the probe concentration on day 1 (p=0.212, B1), day 2 (p=0.139, B2), day 3 (p=0.212, B3) and day1-3 (p=0.482, B4).

Table 23 Inter and intra variability of DIG-labelled probe optimization represented by absorbance 450 nm

Sample number	Strept avidin (μg)	DNA (ng)	Probe (ng)	Antibody dilution	Mean O.D. (SD, %CV)			
					Intra-variability			Inter-variability
					Day 1	Day 2	Day 3	
1	5	440	73.5	1:400	0.89 (0.01, 1)	0.76 (0.02, 3)	1.54 (0.06, 4)	1.07 (0.37, 35)
2	5	440	147	1:400	1.25 (0.04, 3)	1.1 (0.04, 4)	1.58 (0.08, 5)	1.31 (0.23, 18)
3	5	440	294	1:400	1.19 (0.04, 3)	1.53 (0.06, 4)	1.95 (0.03, 2)	1.56 (0.34, 22)
4	5	440	588	1:400	2.16 (0.09, 4)	1.11 (0.09, 8)	1.85 (0.07, 4)	1.71 (0.49, 29)

Concentration of CaSki DNA: 440 ng/μl, concentration of probe: 294 ng/μl.

Table 24 Inter and intra variability of DIG-labelled probe optimization represented by ratio

Sample number	Strept avidin (μg)	DNA (ng)	Probe (ng)	Antibody dilution	Mean Ratio (SD, %CV)			
					Intra-variability			Inter-variability
					Day 1	Day 2	Day 3	
1	5	440	73.5	1:400	9.51 (0.67, 7)	7.68 (0.56, 7)	12.74 (1.58, 12)	9.97 (2.43, 24)
2	5	440	147	1:400	12.9 (1.67, 13)	12.13 (0.67, 6)	14.31 (0.98, 7)	13.12 (1.35, 10)
3	5	440	294	1:400	12.04 (1.27, 11)	16.2 (0.15, 1)	16.95 (0.23, 1)	15.06 (2.43, 16)
4	5	440	588	1:400	16.71 (3.8, 23)	9.89 (0.28, 3)	15.89 (3.2, 20)	14.16 (4, 28)

Concentration of CaSki DNA: 440 ng/μl, concentration of probe: 294 ng/μl.

6. Antibody optimization

To optimize the dilution of antibody in PCR-ELISA, different dilution of antibody including 1:400, 1:800, 1:1600, 1:3200, were tested. Concentration of streptavidin, DNA concentration and DIG-labelled probe concentration used for antibody optimization were 5 μg/well, 440 ng/well and 294 ng/well, respectively. Reagent control, the PCR master mix reagents without amplified products, was used to evaluate the cross-reaction caused by PCR reagents. The mean absorbance of CaSki was not significantly different across the antibody dilution for both Intra (Figure 22. A1-A3) and inter (Figure 22. A4) variability. The mean ratio represents the same results; except for mean ratio of inter-variability (p=0.001) (Figure 23. B4), the antibody dilution of 1:3200 represent the highest ratio when compared to other dilution. Additionally, mean absorbance and mean ratio of reagent control was the same across all antibody dilution. Non-specific reaction was not found when testing with reagent control. Moreover, standard deviation and coefficients of variation of intra- and inter-variability were calculated. Intra-variability coefficient of variations of absorbance and ratio was 1-16% (Table 25) and 9-17% (Table 26), respectively. Whereas, Inter-variability coefficient of variations of absorbance and ratio was 1-15% (Table 25) and 7-40% (Table 26), respectively. Antibody dilution of 1:3200 was the only dilution that %CV lower than 20 (%CV=7) for inter-viability calculated using ratio. Thus, antibody dilution of 1:3200 was chosen.

Figure 22 Intra and inter variability of antibody optimization represented by absorbance 450 nm. (A1-A3) Intra-variability obtained duplicate testing on day 1, day 2 and day 3, respectively. (A4) inter-variability using data of day 1 to day 3; mean±2SE are shown. The mean absorbance of CaSki was the same across the antibody dilution on day 1 (p=0.112, A1), day 2 (p=0.801, A2), day 3 (p=0.244, A3) and day 1-3 (p=0.178, A4). The mean absorbance of reagent control was the same across the antibody dilution on day 1 (p=0.119, A1), day 2 (p=0.092, A2), day 3 (p=0.198, A3) and day1-3 (p=0.069, A4).
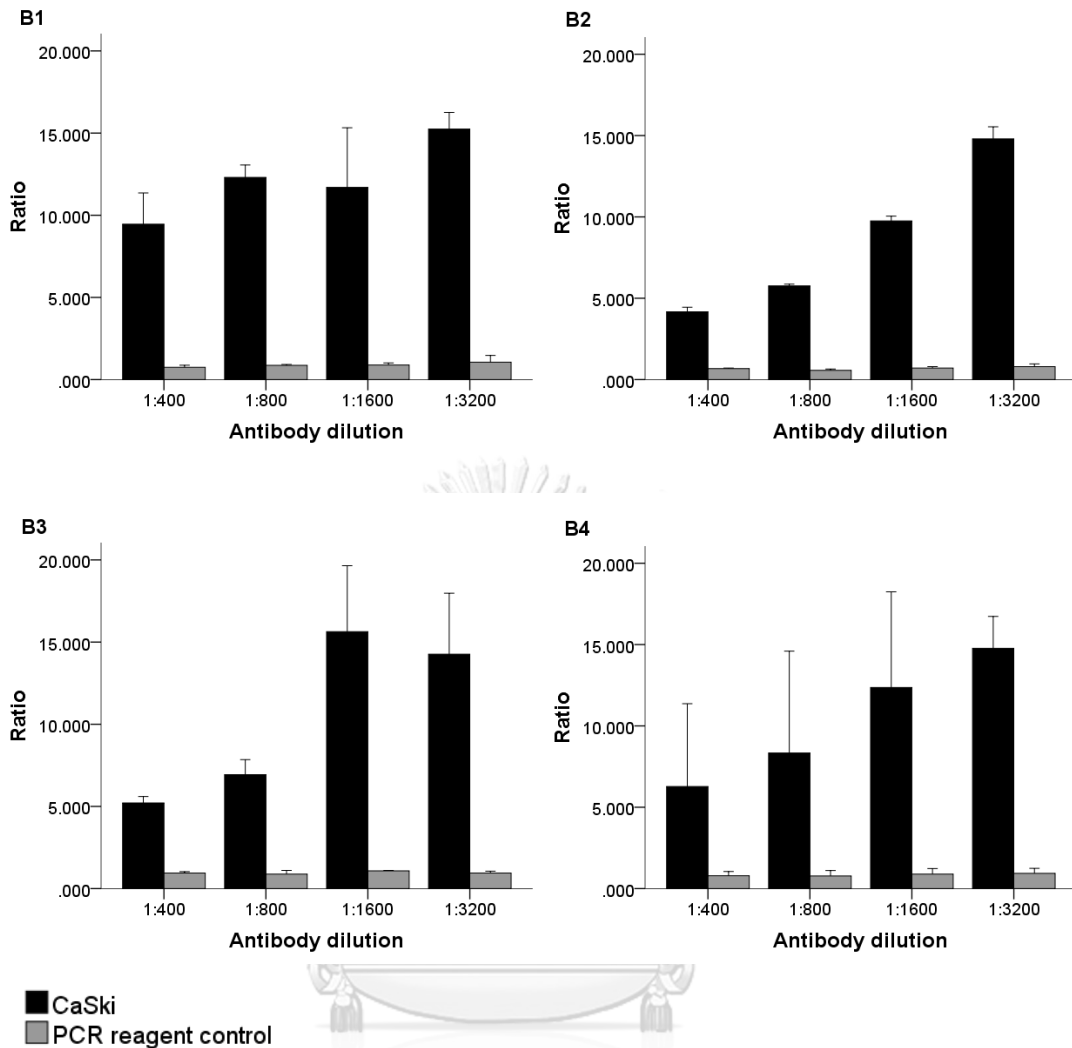
Figure 23 Intra and inter variability of antibody optimization represented by ratio. (B1-B3) Intra-variability obtained duplicate testing on day 1, day 2 and day 3, respectively. (B4) inter-variability tested using data of day 1 to day 3; mean±2SE are shown. The mean ratio of CaSki was the same across the antibody dilution on day 1 (p=0.112, B1), day 2 (p=0.083, B2) and day 3 (p=0.104, B3); except for mean ratio of day1-3 (p=0.001, B4). The mean ratio of reagent control was the same across the antibody dilution on day 1 (p=0.160, B1), day 2 (p=0.139, B2), day 3 (p=0.212, B3) and day1-3 (p=0.310, B4).

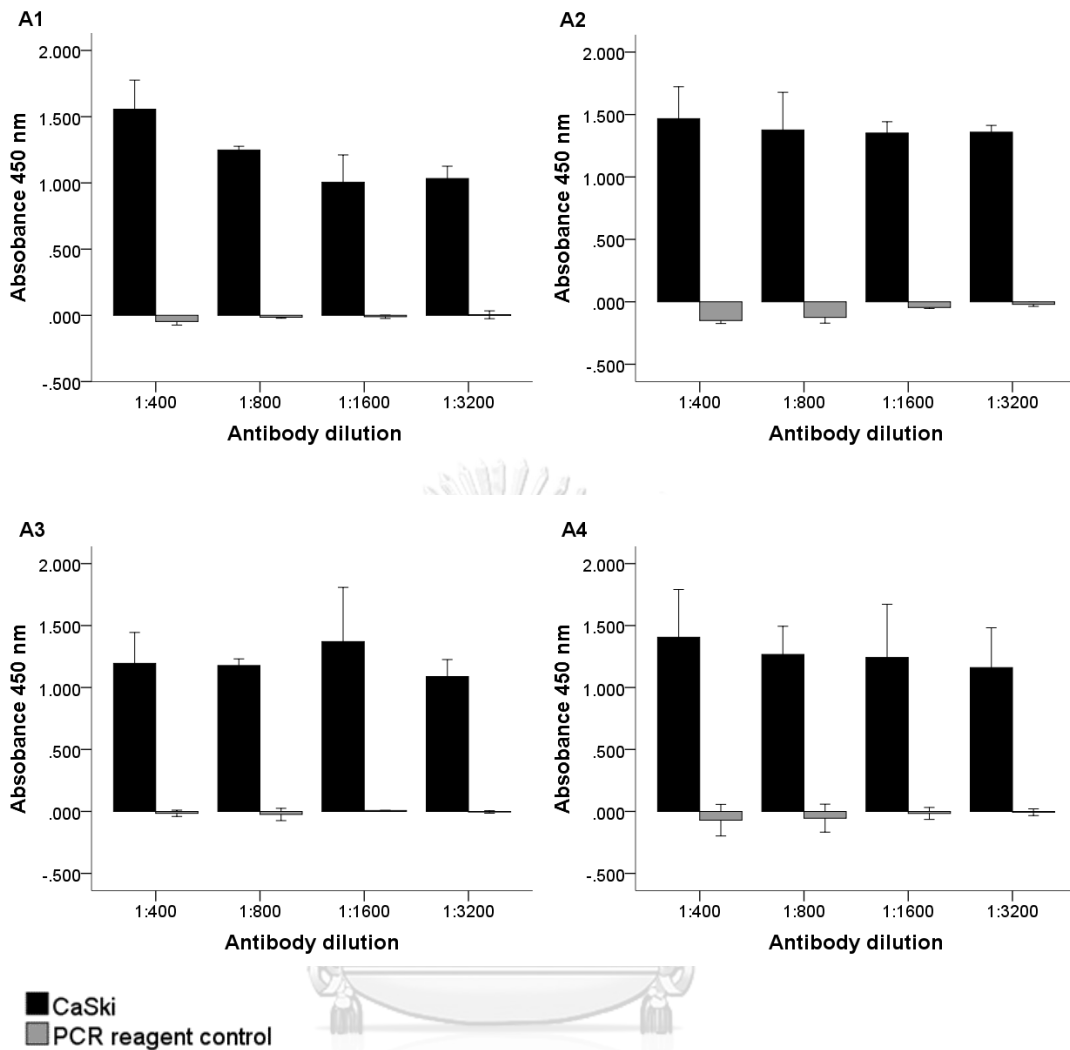**Table 25** Inter and intra variability of antibody optimization represented by absorbance 450 nm

Sample number	Strepta vidin (μg)	DNA (ng)	Probe (ng)	Antibody dilution	Mean O.D. (SD, %CV)			
					Intra-variability			Inter-variability
					Day 1	Day 2	Day 3	
1	5	440	294	1:400	1.56 (0.11, 7)	1.47 (0.13, 9)	1.2 (0.12, 10)	1.41 (0.19, 13)
2	5	440	294	1:800	1.25 (0.01, 1)	1.38 (0.15, 11)	1.18 (0.03, 3)	1.27 (0.11, 9)
3	5	440	294	1:1600	1.01 (0.1, 10)	1.35 (0.05, 4)	1.37 (0.22, 16)	1.24 (0.21, 17)
4	5	440	294	1:3200	1.03 (0.05, 5)	1.36 (0.03, 2)	1.09 (0.07, 6)	1.16 (0.16, 14)

Concentration of CaSki DNA: 440 ng/μl, concentration of probe: 294 ng/μl.

Table 26 Inter and intra variability of antibody optimization represented by ratio

Sample number	Strept avidin (μg)	DNA (ng)	Probe (ng)	Antibody dilution	Mean Ratio (SD, %CV)			
					Intra-variability			Inter-variability
					Day 1	Day 2	Day 3	
1	5	440	294	1:400	9.46 (0.95, 10)	4.17 (0.14, 3)	5.21 (0.2, 4)	6.28 (2.54, 40)
2	5	440	294	1:800	12.3 (0.38, 3)	5.76 (0.06, 1)	6.94 (0.46, 7)	8.33 (3.13, 38)
3	5	440	294	1:1600	11.7 (1.81, 15)	9.75 (0.15, 2)	15.64 (2.01, 13)	12.36 (2.94, 24)
4	5	440	294	1:3200	15.25 (0.5, 3)	14.8 (0.37, 3)	14.27 (1.85, 13)	14.77 (0.98, 7)

Concentration of CaSki DNA: 440 ng/μl, concentration of probe: 294 ng/μl.

7. Streptavidin optimization

To optimize the concentration of streptavidin in PCR-ELISA, different concentration of streptavidin including 0.5, 1, 2, 2.5, 5, 7.5 μg, were tested. DNA concentration, DIG-labelled probe concentration and antibody dilution used for streptavidin optimization were 440 ng/well, 294 ng/well and 1:3200, respectively. Reagent control was used. The mean absorbance of CaSki was not significantly different across the streptavidin concentration for both Intra (Figure 24. A1-A3) and inter (Figure 24. A4) variability. In term of ratio, the same results were found (Figure 25. B1-B4). Non-specific reaction was not found when testing with reagent control. Moreover, standard deviation and coefficients of variation of intra-variability and inter-variability were calculated. Intra-variability coefficient of variations of absorbance and ratio was 1-13% (Table 27) and 1-29% (Table 28), respectively, Whereas, Inter-variability resulted in 6-16% (Table 27) and 7-20% (Table 28). Interestingly, the streptavidin concentration of 2 μg represent the highest ratio with the lowest %CV for inter-viability (Table 28). Thus, streptavidin concentration of 2 μg was chosen.

จุฬาลงกรณ์มหาวิทยาลัย
CHULALONGKORN UNIVERSITY

Figure 24 Intra and inter variability of streptavidin optimization represented by absorbance 450 nm. (A1-A3) Intra-variability obtained duplicate testing on day 1, day 2 and day 3, respectively. (A4) inter-variability tested using data of day 1 to day 3; mean±2SE are shown. The mean absorbance of CaSki was the same across the antibody dilution on day 1 (p=0.161, A1), day 2 (p=0.247, A2), day 3 (p=0.148, A3) and day 1-3 (p=0.429, A4). The mean absorbance of reagent control was the same across the antibody dilution on day 1 (p=0.602, A1), day 2 (p=0.709, A2), day 3 (p=0.119, A3) and day1-3 (p=0.794, A4).
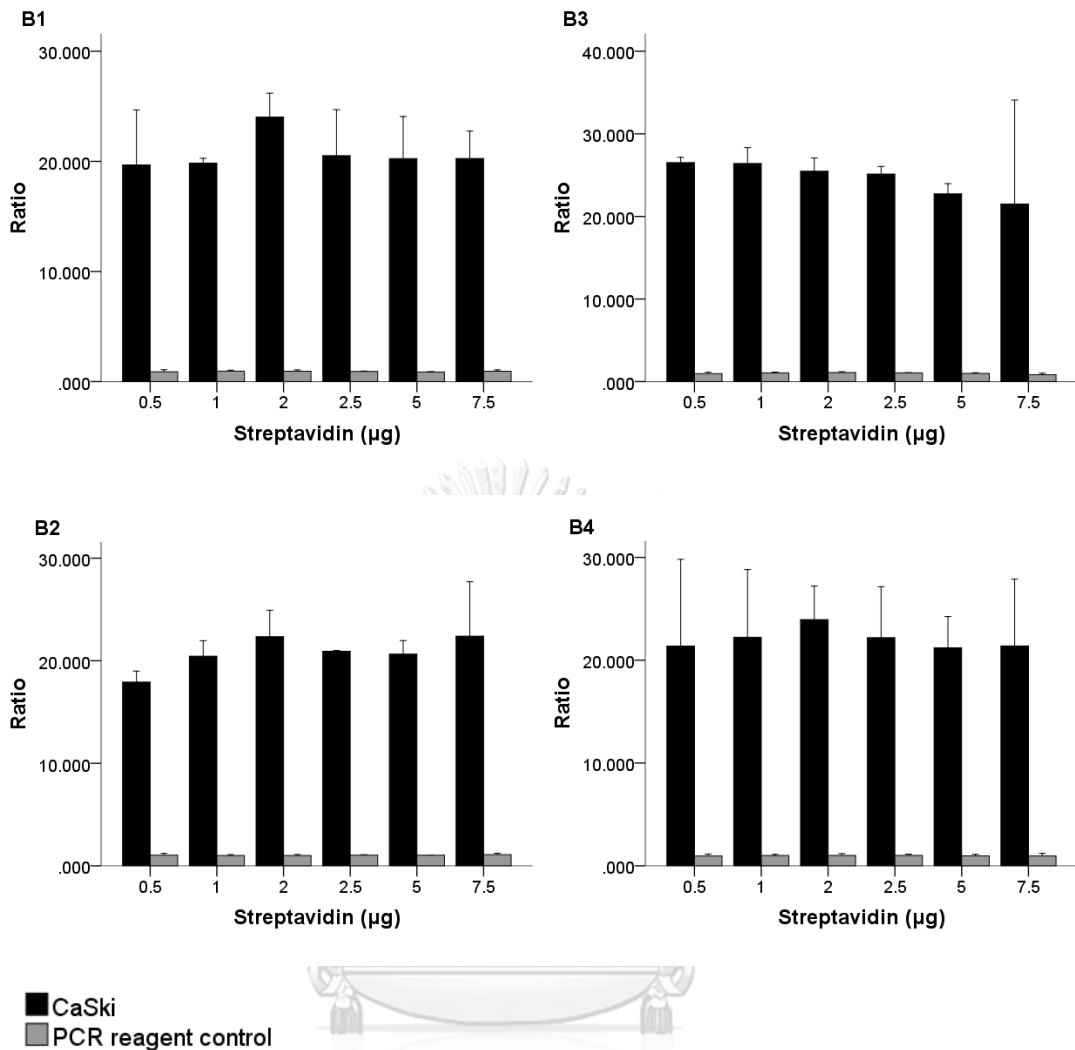
Figure 25 Intra and inter variability of streptavidin optimization represented by ratio. (B1-B3) Intra-variability obtained duplicate testing on day 1, day 2 and day 3, respectively. (B4) inter-variability tested using data of day 1 to day 3; mean$\pm$2SE are shown. The mean ratio of CaSki was the same across the antibody dilution on day 1 (p=0.425, B1), day 2 (p=0.215, B2), day 3 (p=0.199, B3) and day1-3 (p=0.546, B4). The mean ratio of reagent control was the same across the antibody dilution on day 1 (p=0.475, B1), day 2 (p=0.877, B2), day 3 (p=0.119, B3) and day1-3 (p=0.657, B4).

Table 27 Inter and intra variability of streptavidin optimization represented by absorbance 450 nm

Sample number	Strept avidin (μg)	DNA (ng)	Probe (ng)	Antibody dilution	Mean O.D. (SD, %CV)			
					Intra-variability			Inter-variability
					Day 1	Day 2	Day 3	
1	0.5	440	294	1:3200	1.38 (0.07, 5)	1.00 (0.13, 13)	1.31 (0.15, 11)	1.23 (0.20, 16)
2	1	440	294	1:3200	1.24 (0.04, 3)	1.09 (0.01, 1)	1.18 (0.01, 1)	1.17 (0.07, 6)
3	2	440	294	1:3200	1.41 (0.05, 3)	1.14 (0.08, 7)	1.10 (0.07, 6)	1.22 (0.16, 13)
4	2.5	440	294	1:3200	1.23 (0.10, 8)	1.11 (0.01, 1)	1.10 (0.04, 3)	1.14 (0.08, 7)
5	5	440	294	1:3200	1.20 (0.08, 7)	1.10 (0.01, 1)	1.05 (0.01, 1)	1.12 (0.08, 7)
6	7.5	440	294	1:3200	1.22 (0.09, 8)	1.23 (0.08, 7)	1.17 (0.08, 7)	1.20 (0.07, 6)

Concentration of CaSki DNA: 440 ng/μl, concentration of probe: 294 ng/μl.
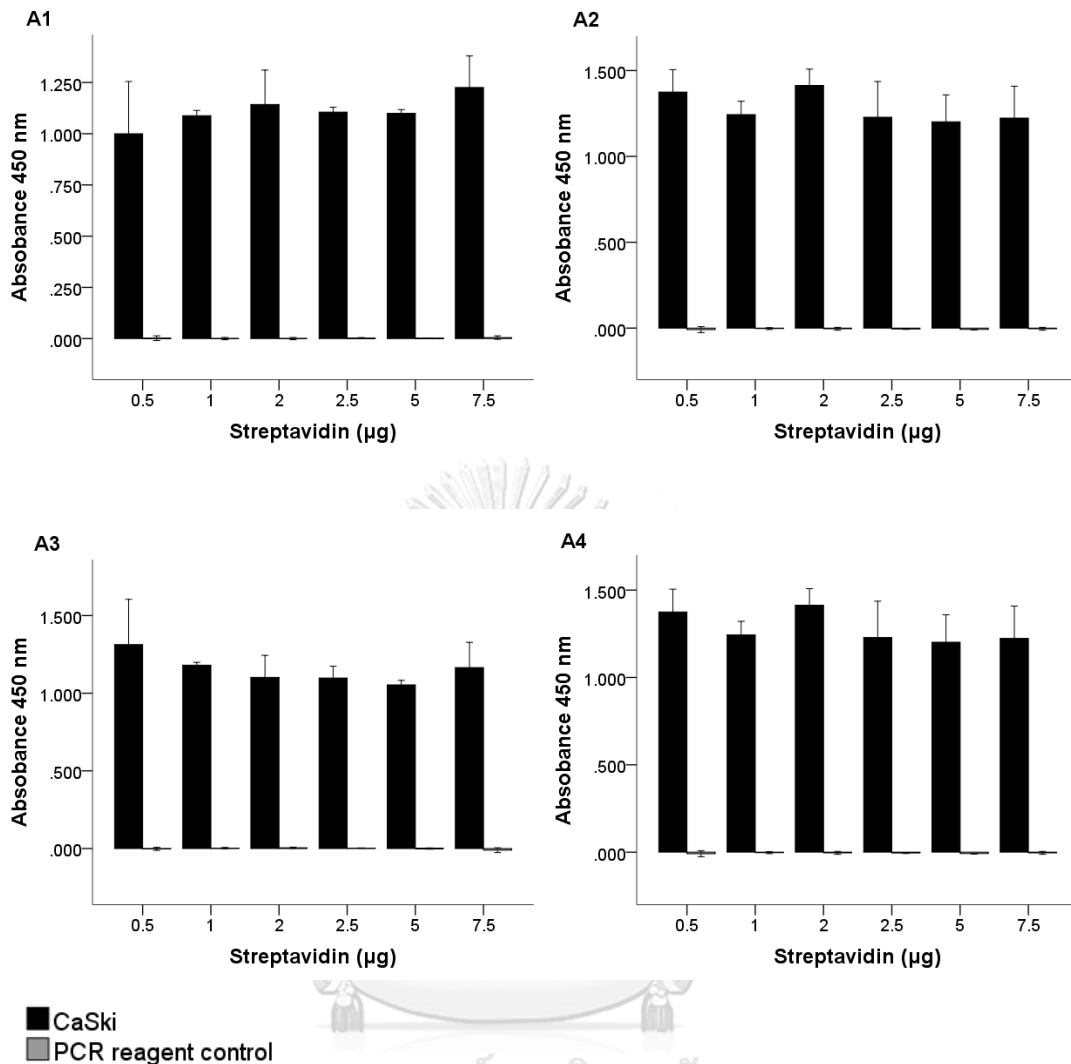
Table 28 Inter and intra variability of streptavidin optimization represented by ratio

Sample number	Strept avidin (μg)	DNA (ng)	Probe (ng)	Antibody dilution	Mean Ratio (SD, %CV)			
					Intra-variability			Inter-variability
					Day 1	Day 2	Day 3	
1	0.5	440	294	1:3200	19.68 (2.50, 13)	17.92 (0.54, 3)	26.52 (0.32, 1)	21.37 (4.22, 20)
2	1	440	294	1:3200	19.85 (0.22, 1)	20.45 (0.75, 4)	26.41 (0.96, 4)	22.23 (3.29, 15)
3	2	440	294	1:3200	24.03 (1.08, 5)	22.35 (1.29, 6)	25.48 (0.08, 3)	23.95 (1.63, 7)
4	2.5	440	294	1:3200	20.52 (2.09, 10)	20.92 (0.04, 0)	25.13 (0.46, 2)	22.19 (2.48, 11)
5	5	440	294	1:3200	20.26 (1.91, 9)	20.64 (0.66, 3)	22.73 (0.62, 3)	21.21 (1.52, 7)
6	7.5	440	294	1:3200	20.26 (1.24, 6)	22.40 (2.66, 12)	21.51 (6.29, 29)	21.39 (3.25, 15)

Concentration of CaSki DNA: 440 ng/μl, concentration of probe: 294 ng/μl.

8. Specificity test

The amplicons of unmethylated L1 that contained four bases different from methylated L1 (A is present in unmethylated sequences (AG) while C is present in methylated sequences (CG)) was used to evaluate the specificity of the developed assay. The hybridization step of DIG labelled probe to PCR amplicons was 60°C, the protocol used in specificity test was as followed: 2 μg/well of streptavidin, 294 ng/well of DIG-labelled probe and 1:3200 of antibody dilution. Standard DNA controls concentration 300 ng/μl including 0%, 25%, 50%, 75% and 100% were used to set the standard curve according to absorbance and pyrosequencing results of standard control DNAs. The example of three standard curves and formulas used to calculate percentage of methylation in samples were shown in Figure 26 and Table 10. The absorbance obtained from different concentrations of unmethylated plasmid PCR product (1000 to 0.001 ng) was used for methylation percentage calculation.

We found that, the protocol using 37 °C at the binding step of DNA-probe hybrids to streptavidin coated plate showed high absorbance (>0.2) when tested with 1000 ng and 100 ng unmethylated plasmid, which resulted in 1.17 and 0.54 respectively. Moreover, percentage of methylation calculated from linear type without intercept standard curve (y=ax) which obtained the highest R-squared (0.739), was also high in 1000 ng and 100 ng unmethylated plasmid (Table 29).

Table 29 Specificity test using 37 °C binding temperature

Unmethylated DNA (ng)	Sample O.D.	%5-mc		
		y = ax+b	y = ax	y = aln(x) + b
1000	1.17	1050.00	42.88	0.01
100	0.54	2621.25	18.24	0.00
10	0.12	3672.50	1.75	0.00
1	0.06	3830.00	-0.73	0.00
0.1	0.05	3843.75	-0.94	0.00
0.01	0.06	3832.50	-0.76	0.00
0.001	0.07	3800.00	-0.25	0.00

* Blank OD = 0.0745

Non-specificity binding was obviously found in specificity test. Therefore, the protocol at streptavidin-hybrids binding step was changed from 37 °C to 60 °C as same as hybridization temperature to prevent non-specific binding. Moreover, the plate was shaking at 300 rpm while incubating. We found that at 60 °C, the absorbances at DNA concentration 1000 ng and 100 ng were slightly decrease but still high (>0.2), which resulted in 1.02 and 0.4, respectively. Moreover, percentage of methylation calculated from linear type without intercept standard curve (y=ax) was also high in 1000 ng and 100 ng unmethylated plasmid (51.74% and 17.46%, respectively). However, the absorbance of unmethylated L1 (unmethylated plasmid PCR product) at 1000, 100 and 10 ng were twice times lower than absorbance obtained from methylated L1 (CaSki PCR product) at the same concentration (Table 30 and Table 31). The absorbance of unmethylated L1 and methylated L1 at concentration lower than 10 ng was as low as blank control's absorbance (<0.1). The protocol at streptavidin-hybrids binding step at 60 °C was used in limit of detection determination, sensitivity test and sample methylation detection.

Table 30 Specificity test using 60 °C binding temperature

Unmethylated DNA (ng)	Sample O.D.	%5-mc		
		y = ax+b	y = ax	y = aln(x) + b
1000	1.02	42.76	51.74	33.39
100	0.40	-36.79	17.46	2.96
10	0.11	-74.29	1.30	0.95
1	0.09	-76.47	0.36	0.89
0.1	0.07	-78.21	-0.39	0.84
0.01	0.07	-78.91	-0.69	0.82
0.001	0.08	-77.44	-0.06	0.86

* Blank OD = 0.0815

(A)
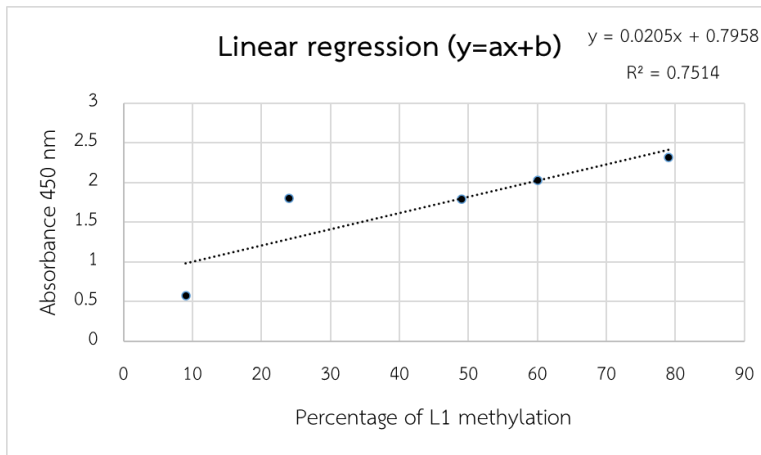
(B)
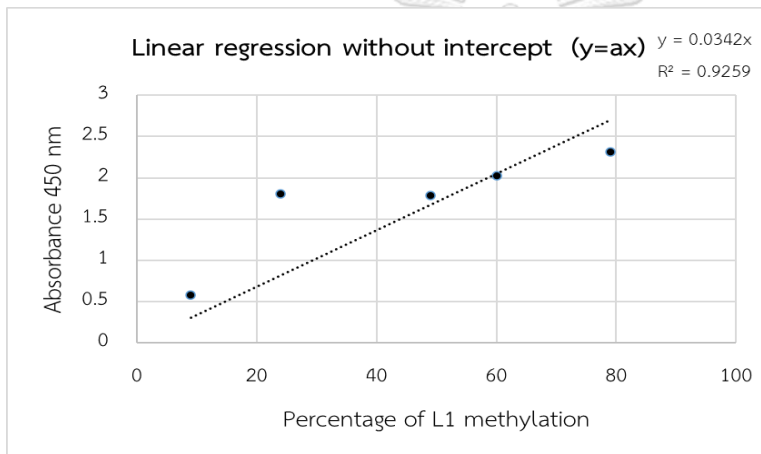
(C)
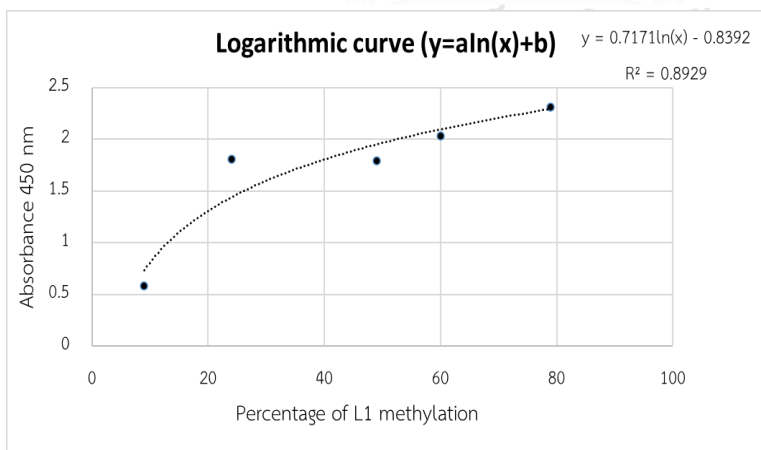
Figure 26 Example of three types of standard curves and formulas used in percentage of L1 methylation calculation (A) Linear type (y=ax+b) (B) Linear type without intercept (y=ax) (C) Logarithmic curve (y=aln(x)+b)

9. Limit of detection

To determine detection limitation of the PCR-ELISA. A ten-fold serial dilution was performed. CaSki DNA was diluted with Milli Q water into 1,000, 100, 10, 1, 0.1, 0.01, 0.001 ng. The protocol used in limit of detection was as followed: 2 μg/well of streptavidin, 294 ng/well of DIG-labelled probe and 1:3200 of antibody dilution. Streptavidin-Probe-DNA hybrids binding step was performed at 60 ℃ with 300 rpm shaking. Three types of standard curves were set Table 10. Percentage of methylation in CaSki DNAs were calculated using formular (y=ax) from linear type without intercept standard curve which obtained the highest R-squared (0.8962).

As we mentioned that the absorbance of unmethylated L1 (unmethylated plasmid) and methylated L1 (CaSki DNA) at concentration <10 ng was the same as blank control, therefore detection limitation in methylated L1 was as low as 10 ng. The methylation percentage was overestimated at DNA concentration 1,000 ng but underestimation at concentration lower than 100 ng (Table 31) when compared with percentage of methylation obtained from pyrosequencing which CaSki DNA resulted in 78-79% (Table 20).

It should be noted that the concentration of standard curve (0%, 25%, 50%, 75% and 100%) used was 300 ng/μl that may be the reason of incorrect methylation percentage of CaSki DNA. Thus, the concentration of samples must be the same as standard curve.

Table 31 Limit of detection

CaSki (ng)	Sample O.D.	%5-mc		
		y = ax+b	y = ax	y = aln(x) + b
1000	1.85	149.62	97.79	863.68
100	0.84	19.62	41.77	16.51
10	0.28	-52.24	10.80	1.85
1	0.13	-70.58	2.90	1.06
0.1	0.09	-75.83	0.64	0.90
0.01	0.09	-76.79	0.22	0.88
0.001	0.10	-75.38	0.83	0.92

* Blank OD = 0.0815

10. Sensitivity test

To determine the sensitivity of the PCR-ELISA. Bisulfite modified CaSki PCR product (100% methylation) was diluted with unmethylated plasmid PCR product (0% methylation) into percentage difference of methylation (Table 32). The concentration of bisulfite modified CaSki PCR product and unmethylated plasmid PCR product was 300 ng/μl. The protocol used in sensitivity test was as followed: 2 μg/well of streptavidin, 294 ng/well of DIG-labelled probe and 1:3200 of antibody dilution. Streptavidin-Probe-DNA hybrids binding step was performed at 60 °C with 300 rpm shaking. Standard DNA controls concentration 300 ng/μl were used to set standard curves according to absorbance and pyrosequencing results (Table 10). Percentage of methylation in diluted samples were calculated using formular (y=ax+b) from linear type standard curve which obtained the highest R-squared (0.96).

The absorbance values obtained from methylation percentage 1.25% to 12.5% were similar to 0% methylation (approximately 0.700-0.800), while absorbance values of methylation percentage >20% was higher than 0% methylation (>0.8) (Table 32).

The absorbance values were used for calculation of methylation percentage using three formula obtained from three standard curves. Percentage of methylation in 1.25%-12.5% samples were not associated with pyrosequencing results, but percentage of methylation in 20%-100% samples were similar to pyrosequencing results. However, percentage of methylation obtained from pyrosequencing were decreased (78% to 10%) as methylation percentage of samples decrease (100% to 1.25%) (Table 32). Percentage of methylation calculated using formular (y=ax+b) in 1.25%-12.5% samples, were 3-20 times lower than results obtained from pyrosequencing, except result of 1.56% sample was as same as pyrosequencing result (percentage of methylation=12%). However, most of results calculated from 1.25% to 12.5% samples were underestimated when compared with pyrosequencing results (Table 32). Whereas, percentage of methylation in 20%-100% samples were ≤2 times lower than results obtained from pyrosequencing. Thus, sensitivity of PCR-ELISA was

as low as 20% which is associated with pyrosequencing result (21%). Since percentage of methylation in 20% sample obtained from PCR-ELISA was 9.5%, clinical sample which represents methylation percentage equal or more than 10% might consider as hypermethylation sample (CIN2 or CIN3).

Table 32 Sensitivity test

Samples (Percentage of methylation)	Absorbance	%5-mc			
		$y = ax+b$	$y = ax$	$y = a\ln(x) + b$	Pyrosequencing
1.25	0.7325	2.7	24.0	8.5	10
1.56	0.89	12.1	29.7	11.7	12
2.5	0.632	-3.4	20.4	6.9	11
3.125	0.7255	2.2	23.8	8.4	12
5	0.6365	-3.1	20.6	7.0	13
6.25	0.718	1.8	23.5	8.2	13
10	0.7005	0.7	22.9	7.9	14
12.5	0.6535	-2.1	21.2	7.2	17
20	0.8455	9.5	28.1	10.7	21
25	0.9395	15.1	31.4	13.0	23
40	1.1275	26.5	38.2	19.2	34
50	1.317	37.9	45.0	28.4	42
80	1.5265	50.5	52.5	43.8	63
100	1.5575	52.4	53.6	46.7	78

* Blank OD = 0.0625

11. Detection of HPV16 L1 gene methylation by using adjusted PCR-ELISA protocol

The protocol used in HPV16 L1 gene methylation detection was as followed: 2 μg/well of streptavidin, 440 ng/well of DNA, 294 ng/well of DIG-labelled probe and 1:3200 of antibody dilution. In streptavidin- probe-DNA hybrids binding step, the plate was incubated at 60 °C for 1 hour with shaking at 300 rpm.

Out of 26 samples, 14 samples represented CIN1, 4 samples represented CIN2, 6 samples represented CIN3, 1 sample represented vaginal intraepithelial neoplasia 3 (VAIN3), and 1 sample represented benign squamous epithelium. All clinical samples' DNA concentration was approximately 600 ng. Thus, standard DNA controls concentration 600 ng/μl were used to set standard curves according to absorbance and pyrosequencing results of standard control DNAs. Percentage of methylation in clinical samples were calculated using formular ($y = a\ln(x) + b$) from logarithmic standard curve which obtained the highest R-squared (0.9647). The percentage of methylation in 26 samples were listed in Table 33.

In CIN1, percentage of methylation in 10 samples were similar to pyrosequencing result (≤2 times difference), which accounted for 71.43% (10/14). Only 4 samples were different from pyrosequencing results (>3 times difference), accounted for 28.57% (4/14). In CIN2/3, percentage of methylation in 8 samples were similar to pyrosequencing result, which accounted for 80% (8/10). Only 2 samples were different from pyrosequencing results, accounted for 20% (2/10). Moreover, percentage of methylation in positive control, negative control, benign squamous epithelium and VIAN3 were associated with pyrosequencing results.

As we mentioned in sensitivity test that clinical sample which represents methylation percentage equal or more than 10% might consider as hypermethylation sample (CIN2 or CIN3). In CIN1, 4 samples represented methylation percentage more than 10%. Thus, overestimated results were found in CIN1, accounted for 28.57% (4/14). In CIN2/3, 5 samples represented methylation percentage more than 10%, which accounted for 50% (5/10). However, 4 samples which obtained percentage of methylation lower than 10% in CIN2/3, also represented low methylation in pyrosequencing (≤10%). When, percentage of methylation at 10% was used as cut-off in this PCR-ELISA method, the accuracy, the precision, the sensitivity and the specificity

would account for 62.5%, 55.56%, 50% and 71.43%, respectively (Table 34 and Table 35).

Table 33 Detection of HPV16 L1 methylation in 26 samples using PCR-ELISA (y=absorbance)

Histology	Sample No.	%5-mc			
		y = ax+b	y =ax	y = aln(x) + b	Pyrosequencing
CIN1	1	-26.6	13.1	4.5	2.5
	2	-13.4	15.3	6.7	4.25
	3	30.4	43.4	23.3	2.75
	4	-5.1	20.2	8.5	0
	5	-15.4	14.0	6.3	1.25
	6	6.5	27.2	11.8	5.25
	7	-12.7	15.6	6.8	4.25
	8	-11.5	16.4	7.0	13
	9	38.8	47.9	29.7	4.5
	10	11.8	30.3	13.7	9.25
	11	-21.9	10.1	5.2	10.25
	12	-10.2	17.2	7.3	10
	13	-17.9	12.5	5.9	4.5
	14	-21.7	10.2	5.2	9.25
CIN2	15	19.6	35.0	17.1	2.5
	16	5.3	30.1	11.3	82.25
	17	7.4	31.1	12.0	62.5
	18	-39.6	6.2	3.1	10.5
CIN3	19	-15.6	13.9	6.3	7.5
	20	34.6	44.0	26.3	15.25
	21	-7.9	23.0	7.8	9.25
	22	-24.7	14.1	4.8	14.5
	23	-9.3	22.3	7.5	16.25
	24	54.7	56.0	46.6	10
VIAN3	25	12.0	30.5	13.8	11.5
Benign squamous epithelium	26	24.9	38.2	19.9	35.25
Positive control		67.0	61.7	65.7	78
Negative control		-17.2	14.2	6.9	10

Table 34 Number of positive and negative samples for CIN2/3 compared with its histology when 10% was used as cut-off

		Histology	
		CIN1	CIN2/3
PCR-ELISA	CIN1	10 (TN)	5 (FN)
	CIN2/3	4 (FP)	5 (TP)

* TP=true positive, TN= true negative, FP=false positive, FN=false negative

Table 35 Accuracy, Precision, Sensitivity and Specificity calculation when 10% was used as cut-off

Test	Formular	Calculation	results
Accuracy	(TP+TN)/(TP+FP+TN+FN)	(5+10)/ (5+4+10+5)	62.5%
Precision	TP/ (TP+FP)	5/ (5+4)	55.56%
Sensitivity	TP/ (TP+FN)	5/ (5+5)	50%
Specificity	TN/ (TN+FP)	10/ (10+4)	71.43%

จุฬาลงกรณ์มหาวิทยาลัย

CHULALONGKORN UNIVERSITY

CHAPTER VI

DISCUSSION

In total, 207 samples were tested for the presence of HPV by Roche Cobas4800 and REBA HPV-ID. Although, HPV positive detection was significantly different between these two methods (McNemar's Test, P value = 0.0005) due to Cobas4800 assay cannot detect LR-HPV types, but there was no significant differences for high-risk HPV detection (McNemar's Test, P value = 0.508). These results were also supported by the concordance rate which was only 0.572 for HPV positive detection and 0.838 for HR-HPV detection.

HPV16 infection is mostly found in CIN2/3 detected by both assays (54.0%-56.7%) but less found in CIN1 (25.95-29.0%) that is consistent with the other studies (99-102). The other HR-HPV types found in CIN2/3 were differentiated by REBA assay, including HPV18, 31, 33, 51, 52, 56, 58, 66 and 59/68. The HR-HPV types distribution in CIN2/3 was similar to the previous studies in which HPV 33, 52 and 58 were found in the third position in East Asian countries (103, 104). However, in CIN3, there were two samples showed single LR-HPV type 42 infections, one sample showed co-infection with HPV16 (Table 14), the results are consistent with several studies, which reported that LR-HPV types and HPV negative could be found in histology equal or more than CIN3 (105-107). Low risk HPV types was mostly found in CIN1, followed by non-CIN.

REBA can detect 32 HPV types including HPV16, HPV18, HPV34, 16 other HR-HPVs, 13 LR-HPVs, while Cobas can detect only 14 HPV types including HPV16, HPV18 and 12 other HR-HPVs. Thus, HPV positive samples detected by REBA (n=174 samples) was higher than HPV positive samples detected by Cobas (n=149 samples) (Table 14). According to HPV typing results, some samples have different results when tested by Cobas and REBA (Table 15). Since REBA can detect more HPV types than Cobas, 2 HPV16 positive samples tested by Cobas resulted in HPV53 (HR-HPV) and LR-HPV positive when tested by REBA, because Cobas cannot detect HPV53 and LR-HPV (Table 15).

However, Cobas HPV test, which is real-time PCR assay, has higher sensitivity than REBA HPV test which is reverse blot hybridization assay. Thus, HPV16 positive samples detected by Cobas (n=70 samples) was higher than HPV16 positive samples

detected by REBA (n=64 samples) (Table 14). There was one HPV16 positive sample detected by Cobas resulted in HPV negative when tested by REBA (Table 15). Since Cobas and REBA detect L1 gene in different region, variation of HPV detection was found. For example, 2 HPV16 positive samples detected by REBA resulted in HPV negative when tested by Cobas (Table 15).

It has been well accepted that persistent infection with HR-HPV types was the majority cause of cervical cancer cases worldwide, in which HPV-16 is the highest prevalence, accounting for 55% of all cervical cancer cases, followed by HPV18 (6). However, minority of HPV infected women progress to cancer and it takes several years to develop malignant transformation (13). Papanicolaou stained (Pap) smear combined with HPV genotyping have been used for screening of cervical cancer since 2012 (14). However, a previous study showed that Pap smear is found to have 20 to 30% of false-negative results (10). Moreover, the study from the National Cancer Institute reported that 50% of HPV positive women referred to colposcopy showed normal cervical lesion (15), which consistent with our study that 63.28% of women referred to colposcopy were CIN1 and only 17.87% were CIN2/3. All aforementioned studies revealed low sensitivity of cytology testing and low specificity of HR-HPV DNA testing, thus, the specific and effective biomarker to be used as triage test is important to reduce the number of women who referred for colposcopy (16-18). Previously, we have reported that HPV16 L1 gene methylation was correlated well with cervical cancer and CIN2/3 (12), which consistent with other studies (80, 108-111). HPV L1 methylation is occurred in host chromosome containing integrated viral genome and is caused by transformation in order to evade host immune. It was reported that the level of average HPV16 L1 gene methylation was higher than host gene methylation (108, 109). In the present study, we have applied methylation test in cervical cells collected from women who were referred for colposcopy. The methylation levels of HPV16 L1 gene were quantitated by using pyrosequencing assay. The methylation results of HPV16 L1 in the control cells which are cervical cancer cell lines containing integrated HPV16 included CaSki (600 copies) and SiHa (1–2 copies) showed high methylation levels (Table 18). The results of cell lines were consistent with previous reports (21, 22). This data indicated that methylation status of the L1 gene is not depending on copy

number of integrated HPV16. Recently, the elevation of HPV16 L1 methylation during carcinogenesis progression has been reported (79, 80, 110, 112-116), suggesting that methylation status could be used as a biomarker for prognostic test of women who have high chance to develop cancer.

In order to evaluate L1 methylation by pyrosequencing, all HPV16 positive DNA obtained from Cobas machine, were used to perform bisulfite treatment and PCR, then only PCR positive samples (130 bps) were used to perform pyrosequencing. Among 70 HPV16 positive samples, only 26 samples represented PCR positive, because DNA obtained from Cobas machine had high volume (approximately 100 μl) and low concentration. Moreover, the process of bisulfite treatment can cause DNA degradation. Thus, DNA should be direct extracted from clinical sample to obtained high concentration sample and to increase the chance of PCR positive.

The study demonstrated that means of methylation of the HPV16 L1 gene was low in CIN1 (<10% of all CpGs), whereas high methylation was statistically significant found in CIN2-3 especially at CpG 5600 and 5609 (>20%) (Table 18, Figure 11). The results were consistent with previous reports (12, 23-25). Both CpGs 5600 and 5609 hypermethylation has been reported to discriminate well between normal and cervical neoplasia (21). The present study also showed high methylation levels of HPV16 5′L1 region in CIN2/3. ROC curve analysis demonstrates that the area under ROC curve (AUC) of CpG 5600 and 5609 were better than CpG positions 5606 and 5615 (Figure 12), suggesting that combination of CpG sites 5600 and 5609 methylation analysis with HR-HPV DNA typing may be useful for clinicians to be used as a biomarker for consideration of the process to manage HR-HPV infected women who are at higher risk of rapid cervical cancer progression.

Molecular techniques for detection of HPV methylation are high cost, need specific equipment and expertise. The cheap and easy to perform assay was developed in the present study. The PCR-ELISA development was first tested with PCR amplicons obtained from CaSki (79% methylation at HPV L1 gene) and PCR reagents control. The highest ratio and coefficients of variation (CV) lower than 20 were used to consider the optimal concentration of each reagents. The %CV used to measure the consistency of

PCR-ELISA optimization of intra and inter-variability of optimal concentration of each reagent, was ranged between 9-16.

The optimized protocol of PCR-ELISA was TBST washing buffer, PBS based reagent, 2 μg/well streptavidin, 440 ng/well DNA, 294 ng/well DIG-labelled probe, 1:3200 antibody dilution. In DNA optimization step, absorbance or ratio was decreased as DNA concentration increased (Figure 18 and Figure 19), because high concentration DNA (≥880 ng) was not balance with probe concentration (588 ng). This might cause DNA-without-probe competitively to bind to streptavidin.

The main challenge of PCR-ELISA optimization is the specificity due to there were only four bases different between methylated L1 amplicons and non-methylated L1 amplicons of probe binding sites, we have first using high temperature at 60℃ in amplicons-probe hybridization, followed by amplicons-streptavidin binding step at 37℃, but non-specific binding was observed. Thus, the protocol at binding step was changed from 37 ℃ to 60 ℃ as the same as hybridization temperature to prevent non-specific binding as reported by other studies (90, 117). These could reduce the OD of unmethylated plasmid at 1,000 ng. We also tested whether the concentration of amplicons has an effect on specificity or not, we found that at low PCR amplicons concentration (100 ng), the OD was lower than high concentration (1,000 ng). The OD obtained from unmethylated L1 was twice times lower than methylated L1 at the same concentration (1,000-10 ng). This indicated that using high temperature at avidin binding step with probe-amplicon hybrids could reduce non-specific binding. However, the absorbance was still high, five to ten times than blank control. Thus, for the present developed PCR-ELISA, according to absorbance, the concentration range 10- 100 ng was considered as suitable concentration of sample used in this PCR-ELISA system.

Sensitivity was performed by diluting CaSki DNA (100% methylation) with unmethylatd plasmid (0% methylation) into several methylation percentage (1.25%-100%). The absorbance values of methylation percentage that higher than 0% methylation was determined as sensitivity value of the PCR-ELISA assay. It was found at 20% methylation; the absorbance value was higher than 0% methylation.

We futher calculated the methylation percentage. Percentage of methylation in 1.25%-12.5% samples were 3-20 times lower than pyrosequencing results, whereas percentage of methylation in 20%-100% samples were ≤2 times lower than results obtained from pyrosequencing. Sensitivity of PCR-ELISA was as low as 20% which is associated with pyrosequencing result (21%). Since percentage of methylation in 20% sample obtained from PCR-ELISA was 9.5%, clinical sample which represents methylation percentage equal or more than 10% might consider as hypermethylation sample (CIN2 or CIN3). Surprisingly, this cut-off is consistent with L1 methylation detection by pyrosequencing (Table 18) in the present study and previous study of our research group (63).

Limit of detection was performed by diluting CaSki DNA using ten-fold dilution. The detection limit of methylated L1 was as low as 10 ng to obtain absorbance two-three times higher than 10 ng of unmethylated L1 and blank control. The lower concentration of methylated and unmethylated L1 (1 ng to 0.001 ng) revealed similar absorbance to blank control. According to the results of methylation percentage of CaSki (methylation L1) calculated by three different formulas obtained from standard curve (0%, 25%, 50%, 75% and 100% at 300 ng each), the methylation values were overestimated and underestimated at 1,000 ng and 100 ng, respectively. Therefore, we can also conclude that in the quantitative PCR-ELISA, the concentration of standard curve and sample must be the same or similar to obtain the accurate methylation percentage as shown when we used 300 ng of standard controls but 1000 ng of samples, the absorbance of samples were higher than 100% methylation of standard control. Therefore, the concentration of standard controls was changed from 300 to 600 ng, as same as the concentration of PCR amplicons of each sample (approximately 600 ng).

The present study used formamide and denhardt solution-based hybridization buffer that worked well with probe and 100% methylated amplicons hybridization. However, the high absorbance was observed in 0% methylation, even though, high temperature was used in both hybridization and binding step. Other reagents-based

hybridization buffer is recommended for further development of PCR-ELISA. Salmon sperm DNA was one component that can be added in hybridization buffer.

26 clinical samples which were already evaluated L1 methylation by pyrosequencing, were used to perform PCR-ELISA. Percentage of methylation which similar to pyrosequencing results in CIN1 and CIN2/3 was 71.43% and 80%, respectively. Percentage of methylation in positive control, negative control, benign squamous epithelium and VIAN3 were associated with pyrosequencing results. The ability of CIN2/3 detection was also considered as sensitivity of PCR-ELISA assay. As well as, the ability to discriminate CIN1 from CIN2/3 was considered as specificity. When, percentage of methylation at 10% was used as cut-off in this PCR-ELISA method, the sensitivity and the specificity would account for 50% and 71.43%, respectively. However, clinical samples used in present study is limited. Thus, the larger sample size is needed to achieve more accurate specificity and sensitivity.
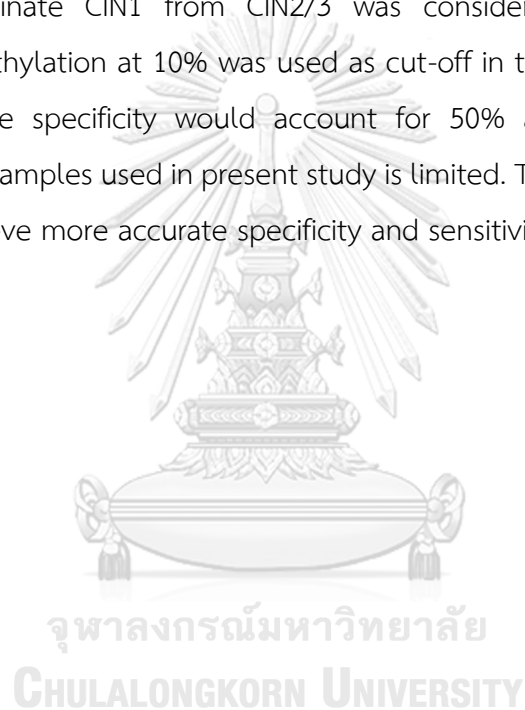
APPENDIX A

REAGENTS, MATERIALS, AND INSTRUMENT

Media and Reagents

Absolute ethanol	(Merck, Germany)
Agarose	(USB, USA)
Bovine Serum Albumin Fraction V	(Bio Basic, Canada)
Denhardt's solution (50X)	(Thermo Fisher Scientific, USA)
Digoxigenin-labelled probe	(Sigma Aldrich, USA)
Dulbecco's Modified Eagle's Medium (DMEM)	(GIBCO, USA)
ELISA Coating Buffer 1X	(Abcam, UK)
Ethyl alcohol 70%	(Defence Pharmaceutical Factory, Thailand)
Ethylenediaminetetraacetic acid (C10H16N2O8; EDTA)	(Bio Basic, Canada)
EZ DNA Methylation-Gold™ Kit	(Zymo Research, USA)
Fetal bovine serum (FBS)	(GIBCO, USA)
Formamide deionized	(Life Sciences, USA)
GeneRuler 1 kb	(Thermo Fisher Scientific, USA)
GpC Methylase kit	(Zymo Research, USA)
Hydrochloric acid	(Sigma Aldrich, USA)
Leupeptin	(Sigma Aldrich, USA)
Mouse monoclonal antibody to Digoxigenin (HRP)	(Abcam, UK)

Native Streptavidin (5mg/ml)	(Abcam, UK)
Penicillin G	(Bio Basic, Canada)
Pepstatin A	(Sigma Aldrich, USA)
Phosphate-buffered saline 10X (PBS)	(Apsalagen, Thailand)
PMSF	(Sigma Aldrich, USA)
QIAamp® genomic DNA kits	(Qiagen, Germany)
Saline Sodium Citrate Buffer 20X (SSC)	(Invitrogen, USA)
Sepharose beads	(GE Healthcare, USA)
Sodium chloride	(Merck, Germany)
Sodium dodecyl sulfate (SDS)	(Bio Basic, Canada)
Sodium hydroxide	(Sigma Aldrich, USA)
Sodium phosphate, dibasic	(Bio Basic, Canada)
Sodium phosphate, monobasic	(Bio Basic, Canada)
Streptomycin	(Sigma Aldrich, USA)
Sulfuric acid 95-97%	(Merck, Germany)
TaKaRa EpiTaq HS for bisulfite-treated DNA	(Takara Bio, USA)
TMB ELISA substrate	(Abcam, UK)
Tris Buffered saline 20X (TBS)	(AMRESCO, USA)
Trypsin	(Bio Basic, Canada)
Tween20	(USB, USA)

Materials

10, 200, 1,000 μl Tip	(Accumax, India)
15- and 50-ml Centrifuge tube	(JetBioFil, China)
1.5- and 0.2-ml Microcentrifuge tube	(Axygen, USA)
Nunc MaxiSorp flat-bottom 96 well plates	(Thermo, China)
pH indicator strips	(Johnson, UK)
Tissue culture flask (T25 and T75)	(Thermo, China)
Syringe-driven filters	(JetBioFil, China)

Instruments

Autoclave	(Hirayama, Japan)
Biohazard safety cabinet	(Flufrance, France)
Block heater	(Life Sciences, USA)
Centrifuge 5430 R	(Eppendorf, Germany)
ChemiDoc	(Bio-rad, UK)
Cobas® 4800 system	(Roche, Australia)
CO_2 incubator	(Thermo Fisher Scientific, USA)
Hot air oven	(Gallenkamp, UK)
Incubator	(Memmert, Germany)
Inverted microscope	(Leica, Germany)
Microcentrifuge	(Eppendorf, Germany)
Micromixer	(FINEPCR, Korea)

Microplate reader	(Perkin Elmer, USA)
Microwave	(Electrolux, Sweden)
Mixer-vortex	(SARSTEDT, Germany)
Nanodrop spectrophotometer	(Eppendorf, Germany)
PyroMark™ Q96 machine	(Qiagen, Germany)
REBA HPV-ID®	(Molecules and Diagnostics, Korea)
Refrigerator	(Sanyo, Japan)
Safety cabinet	(Augustin, Thailand)
Scales	(Precisa, Switzerland)
Spindown	(Hercuvan, Malaysia)
Thermal cycler	(Thermo Fisher Scientific, USA)
Water bath	(Julabo, Germany)

APPENDIX B

REAGENTS PREPARATION

Reagent for sample collection

1. **5mM Phosphate buffer pH 8.0 (50X)**

   Sodium monophosphate (NaH_2PO_4) 0.164 g

   Sodium diphosphate (Na_2HPO_4) 2.645 g

   DDW 80 ml

   Adjust pH with HCl or NaOH to reach pH 8.0

   Stored at -20 °C

2. **5mM Phosphate buffer pH 8.0 (1X)**

   5mM Phosphate buffer pH 8.0 (50X) 800 μl

   DDW 39.2 ml

   Stored at 4 °C

3. **10% NaCl**

   Sodium chloride 2 g

   DDW 20 ml

   Stored at 4 °C

4. **10% Bovine serum albumin**

   Bovine serum albumin 4 g

   5mM Phosphate buffer pH 8.0 40 ml

   Stored at -20 °C

5. **Lysis buffer**

   10% BSA 5 ml

   Tween20 2.5 ml

Leupeptin	500	μl
Pepstatin A	500	μl
PMSF	500	μl
10% NaCl	250	μl
5mM Phosphate buffer pH 8.0	41	ml

Stored at 4 °C

Reagents for cells cultivation

1. **1X Phosphate-buffered saline**

| 10X PBS (steriled) | 50 | ml |
| DDW (steriled) | 450 | ml |

Stored at room temperature

2. **Pen/Strep antibiotic (10^5 units/ml)**

Penicillin G	0.6	g
Streptomycin	1.5	g
DDW (steriled)	200	ml

Sterilized by filtration (0.2 μm) and stored at -20 °C

3. **10% DMEM (Growth medium)**

DMEM	180	ml
Fetal bovine serum	20	ml
Pen/Strep Antibiotic (10^5 units/ml)	2	ml

Stored at 4 °C

4. 10X Trypsin-EDTA

Trypsin	0.25	g
EDTA	0.1	g
NaCl	4.5	g
DDW	500	ml

Sterilized by filtration (0.2 μm) and stored at -20 ℃

5. 1X Trypsin-EDTA

10X Trypsin-EDTA	1	ml
DDW (steriled)	9	ml

Stored at 4 ℃

Reagents for Polymerase Chain Reaction-Enzyme-Linked-Immunosorbent Assay

1. 10% Sodium dodecyl sulfate

Sodium dodecyl sulfate	2	g
DDW	40	ml

Stored at room temperature

2. Washing buffer (1X TBST)

20X TBS	2	ml
Tween20	20	μl
DDW	38	ml

Stored at 4 ℃

3. **Blocking buffer (3% Bovine serum albumin)**

Bovine serum albumin	1.2	g
1X PBS	40	ml

Stored at -20 ℃

4. **Hybridization buffer (6X SCC/50%Formamode/0.5%SDS/5XDenhardt)**

20X SCC	6	ml
Formamide deionized	10	ml
10% SDS	1	ml
50X Denhardt	2	ml
DDW	1	ml

Stored at -20 ℃

5. **Post-hybridization washing buffer (2X SCC/0.1% Sodium dodecyl sulfate)**

20X SCC	4	ml
10% Sodium dodecyl sulfate	400	µl
DDW	36	ml

Stored at room temperature

6. **Dilution buffer (0.5% Bovine serum albumin)**

Bovine serum albumin	0.2	g
1X PBS	40	ml
Tween20	20	µl

Stored at -20 ℃

7. **Stop solution (0.5 M Sulfuric acid)**

Sulfuric acid 95-97%   2.805   ml

DDW   97.195 ml

Stored at room temperature

REFERENCES

1.   Van Doorslaer K, Tan Q, Xirasagar S, et al. The Papillomavirus Episteme: a central resource for papillomavirus sequence data and analysis. Nucleic Acids Research. 2012;41(D1):D571-D8.

2.   Van Doorslaer K, Li Z, Xirasagar S, et al. The Papillomavirus Episteme: a major update to the papillomavirus sequence database. Nucleic Acids Research. 2017;45(D1):D499-D506.

3.   Tommasino M. The human papillomavirus family and its role in carcinogenesis. Seminars in Cancer Biology. 2014;26:13-21.

4.   Bernard H-U. Regulatory elements in the viral genome. Virology. 2013;445(1-2):197-204.

5.   Graham SV. Human papillomavirus: gene expression, regulation and prospects for novel diagnostic methods and antiviral therapies. Future Microbiology. 2010;5(10):1493-506.

6.   Stanley M. Pathology and epidemiology of HPV infection in females. Gynecologic Oncology. 2010;117(2):S5-S10.

7.   Burd EM. Human Papillomavirus and Cervical Cancer. Clinical Microbiology Reviews. 2003;16(1):1-17.

8.   Pretorius RG, Peterson P, Novak S, et al. Comparison of two signal-amplification DNA tests for high-risk HPV as an aid to colposcopy. J Reprod Med. 2002;47(4):290-6.

9.   Solomon D, Schiffman M, Tarone R, et al. Comparison of three management strategies for patients with atypical squamous cells of undetermined significance: baseline results from a randomized trial. J Natl Cancer Inst. 2001;93(4):293-9.

10.   Clarke MA, Wentzensen N, Mirabello L, et al. Human papillomavirus DNA methylation as a potential biomarker for cervical cancer. Cancer Epidemiol Biomarkers Prev. 2012;21(12):2125-37.

11.   Petros PINIDIS PT, Georgios IATRAKIS, Stefanos ZERVOUDIS, Zacharoula KOUKOULI, Anastasia BOTHOU, Georgios GALAZIOS, Simona VLADAREANU. Human Papilloma Virus' Life Cycle and Carcinogenesis. Journal of Clinical Medicine. 2016;11(5): 48-54.

12. Kocjan BJ, Bzhalava D, Forslund O, et al. Molecular methods for identification and characterization of novel papillomaviruses. Clinical Microbiology and Infection. 2015;21(9):808-16.

13. Doorbar J. The papillomavirus life cycle. Journal of Clinical Virology. 2005;32:7-15.

14. Herfs M, Yamamoto Y, Laury A, et al. A discrete population of squamocolumnar junction cells implicated in the pathogenesis of cervical cancer. Proceedings of the National Academy of Sciences. 2012;109(26):10516-21.

15. Day PM, Kines RC, Thompson CD, et al. In Vivo Mechanisms of Vaccine-Induced Protection against HPV Infection. Cell Host Microbe. 2010;8(3):260-70.

16. Lambert PF, Bienkowska-Haba M, Patel HD, et al. Target Cell Cyclophilins Facilitate Human Papillomavirus Type 16 Infection. PLoS Pathogens. 2009;5(7).

17. Kines RC, Thompson CD, Lowy DR, et al. The initial steps leading to papillomavirus infection occur on the basement membrane prior to cell surface binding. P Natl Acad Sci USA. 2009;106(48):20458-63.

18. Surviladze Z, Dziduszko A, Ozbun MA. Essential Roles for Soluble Virion-Associated Heparan Sulfonated Proteoglycans and Growth Factors in Human Papillomavirus Infections. Plos Pathogens. 2012;8(2).

19. Digiuseppe S, Bienkowska-Haba M, Guion LG, et al. Cruising the cellular highways: How human papillomavirus travels from the surface to the nucleus. Virus Res. 2017;231:1-9.

20. DiGiuseppe S, Luszczek W, Keiffer TR, et al. Incoming human papillomavirus type 16 genome resides in a vesicular compartment throughout mitosis. Proceedings of the National Academy of Sciences. 2016;113(22):6289-94.

21. Thompson DA, Zacny V, Belinsky GS, et al. The HPV E7 oncoprotein inhibits tumor necrosis factor alpha-mediated apoptosis in normal human fibroblasts. Oncogene. 2001;20(28):3629-40.

22. Yoo GH, Washington J, Oliver J, et al. The effects of exogenous p53 overexpression on HPV-immortalized and carcinogen transformed oral keratinocytes. Cancer. 2002;94(1):159-66.

23. Ozbun MA. Infectious human papillomavirus type 31b: purification and infection of an immortalized human keratinocyte cell line. J Gen Virol. 2002;83:2753-63.

24. Gadducci A, Guerrieri ME, Greco C. Tissue biomarkers as prognostic variables of cervical cancer. Critical Reviews in Oncology/Hematology. 2013;86(2):104-29.

25. Munger K, Baldwin A, Edwards KM, et al. Mechanisms of Human Papillomavirus-Induced Oncogenesis. Journal of Virology. 2004;78(21):11451-60.

26. Siddiqa A, Broniarczyk J, Banks L. Papillomaviruses and Endocytic Trafficking. International Journal of Molecular Sciences. 2018;19(9).

27. Ljubojevic S, Skerlev M. HPV-associated diseases. Clinics in Dermatology. 2014;32(2):227-34.

28. Sanclemente G, Gill DK. Human papillomavirus molecular biology and pathogenesis. J Eur Acad Dermatol. 2002;16(3):231-40.

29. Dunne EF, Park IU. HPV and HPV-Associated Diseases. Infectious Disease Clinics of North America. 2013;27(4):765-78.

30. Anic GM, Lee JH, Stockwell H, et al. Incidence and Human Papillomavirus (HPV) Type Distribution of Genital Warts in a Multinational Cohort of Men: The HPV in Men Study. J Infect Dis. 2011;204(12):1886-92.

31. Jacobs MV, Snijders PJF, Voorhorst FJ, et al. Reliable high risk HPV DNA testing by polymerase chain reaction: an intermethod and intramethod comparison (vol 52, pg 498, 1999). J Clin Pathol. 1999;52(10):790-.

32. Armstrong LR, Preston EJD, Reichert M, et al. Incidence and prevalence of recurrent respiratory papillomatosis among children in Atlanta and Seattle. Clin Infect Dis. 2000;31(1):107-+.

33. Harwood CA, McGregor JM, Proby CM, et al. Human papillomavirus and the development of non-melanoma skin cancer. J Clin Pathol. 1999;52(4):249-53.

34. Harwood CA, Proby CM. Human papillomaviruses and non-melanoma skin cancer. Curr Opin Infect Dis. 2002;15(2):101-14.

35. Clifford G, Franceschi S, Diaz M, et al. HPV type-distribution in women with and without cervical neoplastic diseases. Vaccine. 2006;24:26-34.

36. Ostor AG. Natural-History of Cervical Intraepithelial Neoplasia - a Critical-Review. Int J Gynecol Pathol. 1993;12(2):186-92.

37. Narisawa-Saito M, Kiyono T. Basic mechanisms of high-risk human papillomavirus-induced carcinogenesis: roles of E6 and E7 proteins. Cancer Sci. 2007;98(10):1505-11.

38.   Munger K, Basile JR, Duensing S, et al. Biological activities and molecular targets of the human papillomavirus E7 oncoprotein. Oncogene. 2001;20(54):7888-98.

39.   Howley PM. Warts, cancer and ubiquitylation: lessons from the papillomaviruses. Trans Am Clin Climatol Assoc. 2006;117:113-26; discussion 26-7.

40.   de Freitas AC, de Oliveira THA, Barros MR, Jr., et al. hrHPV E5 oncoprotein: immune evasion and related immunotherapies. J Exp Clin Cancer Res. 2017;36(1):71.

41.   Arbyn M, Tommasino M, Depuydt C, et al. Are 20 human papillomavirus types causing cervical cancer? J Pathol. 2014;234(4):431-5.

42.   Hutchinson ML, Isenstein LM, Goodman A, et al. Homogeneous Sampling Accounts for the Increased Diagnostic-Accuracy Using the Thinprep(Tm) Processor. Am J Clin Pathol. 1994;101(2):215-9.

43.   Sheets EE, Constantine, Natalie M., Dinisco, Sheryl, Dean, Barbara, Cibas, Edmund S. Colposcopically Directed Biopsies Provide a Basis for Comparing the Accuracy of ThinPrep and Papanicolaou Smears. Obstetrical & Gynecological Survey. 1995;50(9):p659-61.

44.   Hwang SJ, Suh MJ, Yoon JH, et al. Identification of characteristic molecular signature of Mullerian inhibiting substance in human HPV-related cervical cancer cells. Int J Oncol. 2011;39(4):811-20.

45.   Abreu ALP, Souza RP, Gimenes F, et al. A review of methods for detect human Papillomavirus infection. Virol J. 2012;9.

46.   Wentzensen N, Doeberitz MV. Biomarkers in cervical cancer screening. Dis Markers. 2007;23(4):315-30.

47.   Cuschieri K, Wentzensen N. Human papillomavirus mRNA and p16 detection as biomarkers for the improved diagnosis of cervical neoplasia. Cancer Epidem Biomar. 2008;17(10):2536-45.

48.   Dockter J, Schroder A, Hill C, et al. Clinical performance of the APTIMA (R) HPV Assay for the detection of high-risk HPV and high-grade cervical lesions. Journal of Clinical Virology. 2009;45:S55-S61.

49.   Usha Rani Poli PDB, and Swarnalata Gowrishankar. Visual Inspection with Acetic Acid (VIA) Screening Program: 7 Years Experience in Early Detection of Cervical Cancer and Pre-Cancers in Rural South India. Indian J Community Med. 2015;40(3): 203–7.

50.   Sahasrabuddhe VV, Luhn P, Wentzensen N. Human papillomavirus and cervical cancer: biomarkers for improved prevention efforts. Future Microbiology. 2011;6(9):1083-98.

51.   Sano T, Oyama T, Kashiwabara K, et al. Expression status of p16 protein is associated with human papillomavirus oncogenic potential in cervical and genital lesions. Am J Pathol. 1998;153(6):1741-8.

52.   Ikenberg H, Bergeron C, Schmidt D, et al. Screening for cervical cancer precursors with p16/Ki-67 dual-stained cytology: results of the PALMS study. J Natl Cancer Inst. 2013;105(20):1550-7.

53.   Mehlhorn G, Obermann E, Negri G, et al. HPV L1 detection discriminates cervical precancer from transient HPV infection: a prospective international multicenter study. Modern Pathol. 2013;26(7):967-74.

54.   Melsheimer P, Kaul S, Dobeck S, et al. Immunocytochemical detection of HPV high-risk type L1 capsid proteins in LSIL and HSIL as compared with detection of HPV L1 DNA. Acta Cytol. 2003;47(2):124-8.

55.   Griesser H, Sander H, Hilfrich R, et al. Correlation of immunochemical detection of HPV L1 capsid protein in Pap smears with regression of high-risk HPV positive mild/moderate dysplasia. Anal Quant Cytol. 2004;26(5):241-5.

56.   Rauber D, Mehlhorn G, Fasching PA, et al. Prognostic significance of the detection of human papilloma virus L1 protein in smears of mild to moderate cervical intraepithelial lesions. Eur J Obstet Gyn R B. 2008;140(2):258-62.

57.   Scheidemantel T, Simmerman K, Ji X, et al. Expression Pattern of HPV L1 Capsid Protein in PAP Tests: A Potential Biomarker in Risk Assessment for High Grade SIL Lesion. Cancer Cytopathol. 2008;114(5):349-.

58.   Stein RA. DNA methylation profiling: a promising tool and a long road ahead for clinical applications. Int J Clin Pract. 2011;65(12):1212-3.

59.   Deaton AM, Webb S, Kerr ARW, et al. Cell type-specific DNA methylation at intragenic CpG islands in the immune system. Genome Res. 2011;21(7):1074-86.

60.   Illingworth RS, Bird AP. CpG islands - 'A rough guide'. Febs Lett. 2009;583(11):1713-20.

61.   Mirabello L, Sun C, Ghosh A, et al. Methylation of the HPV16 L1 gene is associated with disease progression in a prospective population-based cohort. Cancer Res. 2011;71.

62.   Kalantari M, Calleja-Macias IE, Tewari D, et al. Conserved methylation patterns of human papillomavirus type 16 DNA in asymptomatic infection and cervical neoplasia. Journal of Virology. 2004;78(23):12762-72.

63.   Chaiwongkot A, Niruthisard S, Kitkumthorn N, et al. Quantitative methylation analysis of human papillomavirus 16L1 gene reveals potential biomarker for cervical cancer progression. Diagn Microbiol Infect Dis. 2017;89(4):265-70.

64.   Denton KJ, Bergeron C, Klement P, et al. The sensitivity and specificity of p16(INK4a) cytology vs HPV testing for detecting high-grade cervical disease in the triage of ASC-US and LSIL pap cytology results. Am J Clin Pathol. 2010;134(1):12-21.

65.   Jin B, Li Y, Robertson KD. DNA methylation: superior or subordinate in the epigenetic hierarchy? Genes Cancer. 2011;2(6):607-17.

66.   Jaenisch R, Bird A. Epigenetic regulation of gene expression: how the genome integrates intrinsic and environmental signals. Nat Genet. 2003;33 Suppl:245-54.

67.   Paulsen M, Ferguson-Smith AC. DNA methylation in genomic imprinting, development, and disease. J Pathol. 2001;195(1):97-110.

68.   Robertson KD. The role of DNA methylation in modulating Epstein-Barr virus gene expression. Curr Top Microbiol Immunol. 2000;249:21-34.

69.   Badal V, Chuang LS, Tan EH, et al. CpG methylation of human papillomavirus type 16 DNA in cervical cancer cell lines and in clinical specimens: genomic hypomethylation correlates with carcinogenic progression. J Virol. 2003;77(11):6227-34.

70.   Kim K, Garner-Hamrick PA, Fisher C, et al. Methylation patterns of papillomavirus DNA, its influence on E2 function, and implications in viral infection. J Virol. 2003;77(23):12450-9.

71.   Vinokurova S, Wentzensen N, Kraus I, et al. Type-dependent integration frequency of human papillomavirus genomes in cervical lesions. Cancer Res. 2008;68(1):307-13.

72.   Chaiwongkot A, Vinokurova S, Pientong C, et al. Differential methylation of E2 binding sites in episomal and integrated HPV 16 genomes in preinvasive and invasive cervical lesions. Int J Cancer. 2013;132(9):2087-94.

73.   Burgers WA, Blanchon L, Pradhan S, et al. Viral oncoproteins target the DNA methyltransferases. Oncogene. 2007;26(11):1650-5.

74.   De-Castro Arce J, Gockel-Krzikalla E, Rosl F. Silencing of multi-copy HPV16 by viral self-methylation and chromatin occlusion: a model for epigenetic virus-host interaction. Hum Mol Genet. 2012;21(8):1693-705.

75.   Bernard HU. Gene expression of genital human papillomaviruses and considerations on potential antiviral approaches. Antivir Ther. 2002;7(4):219-37.

76.   Kajitani N, Satsuka A, Kawate A, et al. Productive Lifecycle of Human Papillomaviruses that Depends Upon Squamous Epithelial Differentiation. Frontiers in Microbiology. 2012;3.

77.   Norman I, Hjerpe A, Andersson S. High-risk HPV L1 capsid protein as a marker of cervical intraepithelial neoplasia in high-risk HPV-positive women with minor cytological abnormalities. Oncol Rep. 2013;30(2):695-700.

78.   Sirinart Aromseree AC, Tipaya Ekalaksananan, Bunkerd Kongyingyoes, Natcha Patarapadungkit, and Chamsai Pientong. The Three Most Common Human PapillomavirusOncogenic Types and Their Integration State inThai Women with Cervical Precancerous Lesionsand Carcinomas. Journal of Medical Virology. 2014;86:1911–9.

79.   Bryant D, Tristram A, Liloglou T, et al. Quantitative measurement of Human Papillomavirus type 16 L1/L2 DNA methylation correlates with cervical disease grade. J Clin Virol. 2014;59(1):24-9.

80.   Mirabello L, Frimer M, Harari A, et al. HPV16 methyl-haplotypes determined by a novel next-generation sequencing method are associated with cervical precancer. Int J Cancer. 2015;136(4):E146-53.

81.   Fraga MF, Esteller M. DNA methylation: a profile of methods and applications. Biotechniques. 2002;33(3):632, 4, 6-49.

82.   Herman JG, Graff JR, Myohanen S, et al. Methylation-specific PCR: a novel PCR assay for methylation status of CpG islands. Proc Natl Acad Sci U S A. 1996;93(18):9821-6.

83.   Palmisano WA, Divine KK, Saccomanno G, et al. Predicting lung cancer by detecting aberrant promoter methylation in sputum. Cancer Res. 2000;60(21):5954-8.

84.   Thomassin H, Kress C, Grange T. MethylQuant: a sensitive method for quantifying methylation of specific cytosines within the genome. Nucleic Acids Res. 2004;32(21):e168.

85.   Kristensen LS, Nielsen HM, Hager H, et al. Methylation of MGMT in malignant pleural mesothelioma occurs in a subset of patients and is associated with the T allele of the rs16906252 MGMT promoter SNP. Lung Cancer. 2011;71(2):130-6.

86.   Tost J, Gut IG. DNA methylation analysis by pyrosequencing. Nat Protoc. 2007;2(9):2265-75.

87.   Dupont JM, Tost J, Jammes H, et al. De novo quantitative bisulfite sequencing using the pyrosequencing technology. Anal Biochem. 2004;333(1):119-27.

88.   Al Dahouk S, Tomaso H, Nockler K, et al. The detection of Brucella spp. using PCR-ELISA and real-time PCR assays. Clin Lab. 2004;50(7-8):387-94.

89.   Godfroid J, Nielsen K, Saegerman C. Diagnosis of brucellosis in livestock and wildlife. Croat Med J. 2010;51(4):296-305.

90.   Musiani M, Venturoli S, Gallinella G, et al. Qualitative PCR-ELISA protocol for the detection and typing of viral genomes. Nat Protoc. 2007;2(10):2502-10.

91.   Mohammad Hasani S, Mirnejad R, Amani J, et al. Comparing Rapid and Specific Detection of Brucella in Clinical Samples by PCR-ELISA and Multiplex-PCR Method. Iran J Pathol. 2016;11(2):144-50.

92.   Gomes LI, Dos Santos Marques LH, Enk MJ, et al. Development and evaluation of a sensitive PCR-ELISA system for detection of schistosoma infection in feces. PLoS Negl Trop Dis. 2010;4(4):e664.

93.   Cabrera L, De Witte J, Victor B, et al. Specific detection and identification of African trypanosomes in bovine peripheral blood by means of a PCR-ELISA assay. Vet Parasitol. 2009;164(2-4):111-7.

94.   Tahk H, Lee MH, Lee KB, et al. Development of duplex RT-PCR-ELISA for the simultaneous detection of hepatitis A virus and hepatitis E virus. J Virol Methods. 2011;175(1):137-40.

95.   Raji N, Sadeghizadeh M, Tafreshi KN, et al. Detection of human Papillomavirus 18 in cervical cancer samples using PCR-ELISA (DIAPOPS). Iran J Microbiol. 2011;3(4):177-82.

96.   Bagheri R, Rabbani B, Mahdieh N, et al. PCR-ELISA: a diagnostic assay for identifying Iranian HIV seropositives. Mol Gen Mikrobiol Virusol. 2013(3):36-9.

97.   Puppe W, Weigl J, Grondahl B, et al. Validation of a multiplex reverse transcriptase PCR ELISA for the detection of 19 respiratory tract pathogens. Infection. 2013;41(1):77-91.

98.   Fatemeh Tayebeh SN, Seyed Ali Mirhosseini, Jafar Amani. Novel PCR-ELISA Technique as a Good Substitute in Molecular Assay. Journal of Applied Biotechnology Reports. 2017;4(2):567-72.

99.   Siriaunkgul S, Suwiwat S, Settakorn J, et al. HPV genotyping in cervical cancer in Northern Thailand: adapting the linear array HPV assay for use on paraffin-embedded tissue. Gynecol Oncol. 2008;108(3):555-60.

100.   Sriamporn S, Snijders PJ, Pientong C, et al. Human papillomavirus and cervical cancer from a prospective study in Khon Kaen, Northeast Thailand. Int J Gynecol Cancer. 2006;16(1):266-9.

101.   Thomas DB, Qin Q, Kuypers J, et al. Human papillomaviruses and cervical cancer in Bangkok. II. Risk factors for in situ and invasive squamous cell cervical carcinomas. Am J Epidemiol. 2001;153(8):732-9.

102.   Sukasem C, Pairoj W, Saekang N, et al. Molecular epidemiology of human papillomavirus genotype in women with high-grade squamous intraepithelial lesion and cervical cancer: will a quadrivalent vaccine be necessary in Thailand? J Med Virol. 2011;83(1):119-26.

103.   Lin H, Ma YY, Moh JS, et al. High prevalence of genital human papillomavirus type 52 and 58 infection in women attending gynecologic practitioners in South Taiwan. Gynecol Oncol. 2006;101(1):40-5.

104.   Bhatla N, Lal N, Bao YP, et al. A meta-analysis of human papillomavirus type-distribution in women from South Asia: implications for vaccination. Vaccine. 2008;26(23):2811-7.

105.   Wheeler CM, Hunt WC, Schiffman M, et al. Human papillomavirus genotypes and the cumulative 2-year risk of cervical precancer. J Infect Dis. 2006;194(9):1291-9.

106.   Kim S, Lee D, Park S, et al. REBA HPV-ID(R) for efficient genotyping of human papillomavirus in clinical samples from Korean patients. J Med Virol. 2012;84(8):1248-53.

107.   Lee YS, Gong G, Sohn JH, et al. Cytological Evaluation and REBA HPV-ID HPV Testing of Newly Developed Liquid-Based Cytology, EASYPREP: Comparison with SurePath. Korean Journal of Pathology. 2013;47(3).

108.   Lorincz AT, Brentnall AR, Scibior-Bentkowska D, et al. Validation of a DNA methylation HPV triage classifier in a screening sample. Int J Cancer. 2016;138(11):2745-51.

109.   Louvanto K, Franco EL, Ramanakumar AV, et al. Methylation of viral and host genes and severity of cervical lesions associated with human papillomavirus type 16. Int J Cancer. 2015;136(6):E638-45.

110.   Mirabello L, Schiffman M, Ghosh A, et al. Elevated methylation of HPV16 DNA is associated with the development of high grade cervical intraepithelial neoplasia. Int J Cancer. 2013;132(6):1412-22.

111.   Wentzensen N, Sun C, Ghosh A, et al. Methylation of HPV18, HPV31, and HPV45 genomes and cervical intraepithelial neoplasia grade 3. J Natl Cancer Inst. 2012;104(22):1738-49.

112.   Badal S, Badal V, Calleja-Macias IE, et al. The human papillomavirus-18 genome is efficiently targeted by cellular DNA methylation. Virology. 2004;324(2):483-92.

113.   Fernandez AF, Rosales C, Lopez-Nieva P, et al. The dynamic DNA methylomes of double-stranded DNA viruses associated with human cancer. Genome Res. 2009;19(3):438-51.

114.   Mirabello L, Sun C, Ghosh A, et al. Methylation of human papillomavirus type 16 genome and risk of cervical precancer in a Costa Rican population. J Natl Cancer Inst. 2012;104(7):556-65.

115.   Sun C, Reimers LL, Burk RD. Methylation of HPV16 genome CpG sites is associated with cervix precancer and cancer. Gynecol Oncol. 2011;121(1):59-63.

116.   Turan T, Kalantari M, Calleja-Macias IE, et al. Methylation of the human papillomavirus-18 L1 gene: a biomarker of neoplastic progression? Virology. 2006;349(1):175-83.

117.   Musiani M, Gallinella G, Venturoli S, et al. Competitive PCR-ELISA protocols for the quantitative and the standardized detection of viral genomes. Nat Protoc. 2007;2(10):2511-9.

VITA

NAME   Sasiprapa Liewchalermwong

DATE OF BIRTH   22 December 1994

PLACE OF BIRTH   Bangkok

INSTITUTIONS ATTENDED   Chiang Mai University

HOME ADDRESS   30 Soi Sriaksorn, Thung Maha Mek, Sathon, Bangkok 10120

PUBLICATION   -

AWARD RECEIVED   -